Neural Network based Modeling, Characterization and Identification of Chaotic Systems in Nature

Thesis submitted in partial fulfilment of the requirements
for the award of the degree of
Doctor of Philosophy

by

Archana R

Reg. No: 3829

Under the guidance of

Dr. R Gopikakumari &**Dr. A Unnikrishnan**

Division of Electronics Engineering
School of Engineering
Cochin University of Science and Technology
Kochi- 682022
India

March 2015

Neural Network based Modeling, Characterization and Identification of Chaotic Systems in Nature

Ph. D thesis under the Faculty of Engineering

Author

Archana R
Research Scholar
School of Engineering
Cochin University of Science and Technology
archanasreenivasan@rediffmail.com

Supervising Guide

Dr. R Gopikakumari
Professor
Division of Electronics Engineering
Cochin University of Science and Technology
Kochi - 682022
gopika@cusat.ac.in, gopikakumari@gmail.com

Co-Guide

Dr. A Unnikrishnan
Outstanding scientist (Rtd), NPOL, DRDO, Kochi 682021 &
Principal
Rajagiri School of Engineering & Technology
Kochi 682039
unnikrishanan_a@live.com

Division of Electronics Engineering
School of Engineering
Cochin University of Science and Technology
Kochi- 682022
India

Certificate

This is to certify that the work presented in the thesis entitled **"Neural Network based Modeling, Characterization and Identification of Chaotic Systems in Nature"** is a bonafide record of the research work carried out by Mrs. Archana R under our supervision and guidance in the Division of Electronics Engineering, School of Engineering, Cochin University of Science and Technology and that no part thereof has been presented for the award of any other degree.

Dr. R Gopikakumari
Supervising Guide

Dr. A Unnikrishnan
Co-guide

Declaration

I hereby declare that the work presented in the thesis entitled **"Neural Network based Modeling, Characterization and Identification of Chaotic Systems in Nature"** is based on the original work done by me under the supervision and guidance of Dr. R Gopikakumari, Professor, Division of Electronics Engineering, School of Engineering, Cochin University of Science and Technology, Kochi-21 and Dr. A Unnikrishnan, Outstanding Scientist (Rtd.), NPOL, DRDO, Kochi-21 & Principal, Rajagiri School of Engineering & Technology Kochi-39 and that no part thereof has been presented for the award of any other degree.

Thrikkakkara Archana R

Acknowledgements

The guidance and support of many people have enlightened me in this tough period of life, especially the following personalities.

First and foremost I would like to express my profound gratitude to my research guides, Dr. R.Gopikakumari, Professor, Division of Electronics, School of Engineering, Cochin University of Science and Technology and Dr.A Unnikrishnan, Principal, Rajagiri School of Engineering and Technology, Kakkanad, Kochi under whose patient supervision and guidance I have been able to complete my research. The unconditional support and sincere help from them have made this work a reality.

I express deep sense of gratitude for the valuable suggestions and support given by Dr. V. P. N Nampoori, Professor Emeritus, International School of Photonics, Cochin University of Science and Technology

I wish to thank the Vice Chancellor and Registrar, Cochin University of Science and Technology for the opportunity to complete the research work and submit the thesis. I also thank Dr. K Madhu, Principal, School of Engineering, Dr. Binu Paul, member, Doctoral committee and members of the Research Committee for guidance and help at various stages of the period of research. I wish to express gratitude to the office staff of various sections of Cochin University of Science and Technology for help and assistance. Thanks are also due to the faculty, Division of Electronics, School of Engineering, and office staff at School of Engineering for all help and assistance provided in relation with the research work.

Sincere thanks are due to Mr. P.S Sreejith, Associate Professor, Division of Mechanical Engineering, Cochin University of Science and Technology for

the timely help related to the research. Sincere thanks are expressed to Mrs. Jaya V L for the timely help in the implementation of MRT and SMRT concepts. Thanks are also due to Dr. Bindhya Varghese for the help in finalizing structure of the thesis.

I am indebted to my friends Mrs. Leena N, Mrs. Parvathy R, Dr. Bindu V, Mrs. Bindu C J and Dr. Binimol Punnoose for their constant encouragement throughout the research. I gratefully acknowledge the support and encouragement from Chairman and Management, Dr. K S M Panicker-, Principal, Dr. C Sheela-Vice Principal, Dr. Pailo Paul-Dean, Engineering sciences, all my colleagues and well wishers at Federal Institute of Science and Technology, Angamaly over the years of the research work.

I am deeply indebted for the consistent support given by my loving and caring husband Mr. P Sreenivas, without whom I would not have been able to complete the research. I have deep sense of gratitude to my daughter Aparna and son Chandrasekhar who had been understanding and patient for the whole period of my research. Thanks are also due to my grandmother, brothers, sisters, uncles, aunts, cousins and in-laws for their sincere well wishes and prayers.

I am truly grateful for the blessings, of my late parents K K Sadanandan, H Revathi and mother- in- law P P Saraswathi Ammal, which had guided me through the difficult path. When times were tough the loving memories about them kept me going.

No work will become fruitful without the blessing of the Almighty- the creator, preserver and destroyer of the universe who himself is knowledge, power and truth. I submit my work on the lotus feet of the God.

Abstract

Modeling of chaotic systems, based on the output time series, is quite promising since the output often represents the characteristic behaviour of the total system. It has been an interesting topic for researchers over the past few years. So far, some methods are developed for the identification of chaotic systems. Because of the intense complexity of chaotic systems, the performance of existing algorithms is not always satisfactory. Application of chaotic system theory to socially relevant problems like environmental studies is the need of the hour.

Neural networks have the required self-learning capability to tune the network parameters (i.e. weights) for identifying highly non-linear and chaotic systems. In the present work, effectiveness of modeling a chaotic system using dynamic neural networks has been demonstrated. From the rich literature available for non-linear modeling with neural networks, the Recurrent Neural Network (RNN) structure is selected. The Extended Kalman Filter (EKF) algorithm is used to train the RNN. Further, the Expectation Maximization algorithm is used to effectively arrive at the initial states and the state covariance. Particle filter algorithm with its two important variants namely Sampling Importance Resampling (SIR) and Rao Blackwellised algorithms are also used for training the given RNN. Four standard chaotic systems, Lorenz, Rossler, Chua and Chen, are modelled with the three algorithms. The best algorithm is found to be EKF-EM based on the least mean square error criterion. Validation of RNN model with EKF-EM algorithm is done in time domain by Estimation of embedding dimension, Phase plots, Lyapunov Exponents, Kaplan -Yorke dimension and Bifurcation diagrams. Analysis of the chaotic systems is also performed in the transform domain using Fourier, Wavelet and Mapped Real Transforms.

Natural chaotic systems are analyzed based on the selected model structure and training algorithm, taken for analysis. Sunspot, Venice Lagoon and North Atlantic oscillations are the three of the natural chaotic systems modelled with the selected RNN model structure and EKF-EM algorithm.

Important contributions of the thesis are:

1. Successfully demonstrated that given the output of any chaotic system, it is possible to build a stable model by the proposed RNN structure trained with EKF-EM algorithm.
2. A successful method for online computation of Lyapunov exponent, from a noisy chaotic dataset, along with the bifurcation diagram is developed.
3. Proved that RNN model is capable to characterize the invariant properties of chaotic systems that are Phase plots, Lyapunov Exponents, Kaplan – Yorke dimension and Embedding dimension.
4. Transform domain analysis of chaotic systems demonstrated that MRT transformation is capable of retaining the properties of chaotic system.
5. Use of MRT enables the chosen window to be represented by any one of the MRT coefficients through which the computation time can also be considerably reduced.
6. Three important natural chaotic systems considered for study, namely Sunspot, Venice Lagoon, and North Atlantic oscillation, are modelled with considerably low error and computation time.
7. Characteristics of the natural systems like phase plots, embedding dimension, Lyapunov exponents and MRT coefficients are computed and analysed.

Contents

List of Figures

List of Tables

List of Algorithms

Nomenclature

f, g & h	Non-linear functions
x	State vector
u	Input vector
y	Output vector
A, B, C & D	Constant matrices defining the system parameters
σ	Ratio of fluid viscosity of a substance to its thermal conductivity called (Prandtl number)
β	Difference in temperature between top and bottom of the gaseous system
γ	Width to height ratio of the box used to hold the gas
NARX	Non-linear Auto-Regressive with eXogeneous inputs
w_k	Process noise
v_k	Measurement noise
EKF	Extended Kalman Filter
EM	Expectation Maximization
RNN	Recurrent Neural Network

SIS	Sequential Importance Sampling
SIR	Sampling Importance Resampling
SMC	Sequential Monte Carlo
RBPF	Rao- Blackwellised Particle Filter
MRT	Mapped Real Transform
UMRT	Unique MRT
SMRT	Sequency based unique MRT
Θ_1& Θ_2	Parameters of the modeling functions f and g.
MSE	Mean square error
λ	Lyapunov Exponent
KYD	Kaplan – Yorke Dimension
D_{KY}	Kaplan – Yorke Dimension
d_e	Embedding dimension
d	Correlation dimension
T	Time lag
x_k	State vector at instant k
Z_k	Measurement vector at instant k

$\hat{x}_k$	Posteriori estimate of state
$\tilde{x}_k$	Approximate state vector
$P_{k/k-1}$	Estimate of covariance at k^{th} instant upto k-1 measurements
Q	Process noise covariance
R	Measurement noise covariance
DFT	Discrete Fourier Transform
H	Jacobian matrix of partial derivatives of x with respect to h
V	Jacobian matrix of partial derivatives of with respect to v.

Chapter 1

Introduction

1. Introduction

The subject of system theory plays a significant role in the field of engineering.A system is a group of ordered, focused arrangement that involves of interconnected and codependent elements. The elements of the systems can be modules, units, features, members, fragments etc. These elements repeatedly influence one, another directly or indirectly, to maintain their activity and the existence of the system, in order to achieve the goal of the system [26].The universe itself is a large system which is subjected to constant changes. The galaxies, solar system and other possible celestial systems are all subsystems of the universe. On a relatively smaller scale, the earth itself is a system with many elements like water, land, atmosphere etc. influencing the growth and sustenance of every living and non-living organisms like animals, plants, ocean and mountains, all being its subsystems. The systems theory encompasses the study of the behaviour of a system in response to changes in the inputs and parameters that govern the behaviour.

The research and development of system theory began in the mid-1600s, when Newton proposed the differential equations, discovered his laws of motion and universal gravitation, and combined them to explain Kepler's laws of planetary motion. Later on, the system theory was extended to all engineering fields and analysis of industries, products and processes. The basic procedure in the system theoretical frame work always includes mathematical modelling, development of efficient algorithms for analysis and subsequently simulation and validation of the model, with a view to predict the behaviour at any instance. Almost all real world systems are by and large non-linear. In restricted cases these systems could be modelled by differential equations. As the complexity of the system increases, the order

and number of differential equations required to represent the system increase and the analysis become more and more complex. It is also an accepted fact that with advent of efficient computers, the complexity in analysis is meaningfully handled to a great extent. On the other hand, with the development of intelligent computational techniques, like neural networks, a more effective representation of non-linear systems has been possible, thus giving an effective thrust in the development of modelling techniques and algorithms for non-linear systems. Among the non-linear systems, systems with sensitive dependence on initial conditions are referred to as Chaotic Systems. Many natural phenomena like solar radiations, oceanic waves, changes in whether all exhibit chaotic behaviour very often. The modelling and analysis of such systems have become very topical in the field of system theory. The present thesis addresses the topic of modelling the chaotic systems from the available output in the form of time series, with a view develop techniques to characterise the systems and predict the behaviour subsequently.

1.1 Linear and non-linear systems

The systems are classified broadly into two: linear and non-linear.Linear systems satisfy the properties of superposition and homogeneity. The principle of superposition states that for two different inputs, x_1 and x_2, in the domain of the function *f*,

$$f(\alpha_1 x_1 + \alpha_2 x_2) = \alpha_1 f(x_1) + \alpha_2 f(x_2) \qquad (1.1)$$

The property of homogeneity states that for a given input, x, in the domain of the function *f*, and for any real number *k*,

$$f(kx_1) = kf(x_1) \qquad (1.2)$$

any system that does not satisfy these properties is non-linear. Linear Time Invariant (LTI) systems are commonly described by the equations

$$\frac{dx}{dt} = Ax(t) + Bu(t) \tag{1.3}$$

$$\mathrm{y(t)} = Cx(t) + Du(t) \tag{1.4}$$

where ***x*** is the system state vector, ***u*** is the input vector, and ***y*** is the output vector. A, B, C and D are constant matrices defining the system parameters. A non-linear system on the other hand may be defined by the following non-linear equations

$$\frac{dx}{dt} = f\left(x(t), u(t)\right) \tag{1.5}$$

$$\mathrm{y(t)} = g\left(x(t), u(t)\right) \tag{1.6}$$

where f and g are non-linear functions.

1.2 Dynamical systems

Dynamical system is a system that changes over time according to its functional characterisation. It deals with the analysis of processes that are continuously undergoing changes in system states. Study of dynamical systems involves the determination of how a given state of the system moves to another state [26]. This process is called state transition. The state transition is represented by state transition diagrams. A non-linear dynamical system has two parts:

a) a state vector, which describes exactly the state of some real or hypothetical system

b) a set of parameterized functions, which describes the state transition in time.

State vector can be described by

$$\vec{x}(t) = [x_1(t), x_2(t), ..., x_n(t)] \tag{1.7}$$

The set of functions can be described by

$$f_1(x_1, x_2, ..., x_n),\ f_2(x_1, x_2, ..., x_n), ...,\ f_n(x_1, x_2, ..., x_n) \tag{1.8}$$

Entire system can be then described by a set of differential equations.

$$\begin{aligned}
\frac{dx_1}{dt} &= x = f_1(x_1, x_2, ..., x_n) \\
\frac{dx_2}{dt} &= \dot{x}_2 = f_2(x_1, x_2, ..., x_n) \\
&\vdots \\
\frac{dx_n}{dt} &= \dot{x}_n = f_n(x_1, x_2, ..., x_n)
\end{aligned} \tag{1.9}$$

where $x_1, x_2, ..., x_n$ are the state variables. For example, the state variables of a single particle moving in one dimension are position and velocity. In a dynamical system, the present state is completely determined by the previous states of the system [26].

A *phase space* is an n-dimensional space in which all possible states of a system are represented with each possible state of the system corresponding to one unique point. A *phase plot* is a plot of different states of a system in the phase plane. Phase plots depend on initial conditions. In a phase plot, the axes will be system states.

The phase plots of a non-linear system for stable, marginally stable or unstable [54], systems are shown in Figure 1-1.

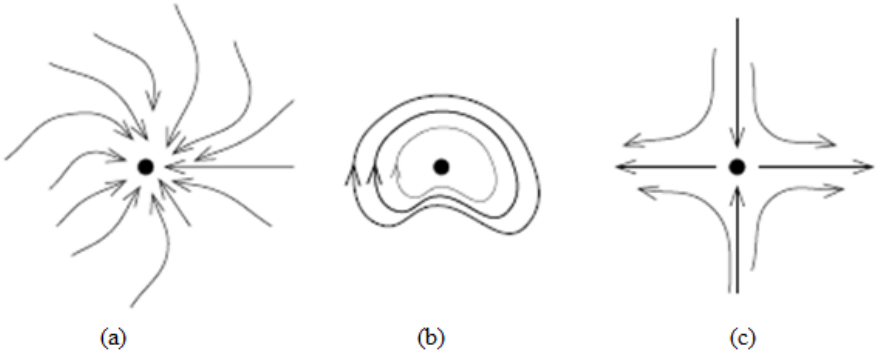

Figure 1-1 (a) stable, (b) marginally stable and (c) unstable phase plots

Initial conditions and external inputs can affect stability of the systems and shape of phase plots as depicted in Figure 1-1 (image courtesy www.sovietencyclopedia.org). A limit cycle is a type of phase plot similar to a unique, self-excited oscillation. It is also a closed trajectory in the state space. Non-linear systems with high dependency on initial conditions are called chaotic systems. The phase plots of chaotic systems show distinct properties, as discussed in the section to follow.

1.3 Chaotic Systems

Chaos theory is the qualitative study of unstable aperiodic behaviour in non-linear dynamical systems. The chaotic systems have been of interest to many researchers over years. Chaos is a complex and unpredictable phenomena, which occur in non-linear systems, which are sensitive to their initial conditions. The theory has origins back to around 1900, but advanced more swiftly after mid-century. Currently, chaos theory continues to be a very active area of research.

The modern theoretical analysis of chaotic systems started with the meteorologist Edward Lorenz. In 1963, while simulating atmospheric convection using a simple non-linear model, he observed extreme sensitivity to changes in initial conditions [2]. He compared these results with earlier observations of Henry Poincare and concluded that this particular system behaviour is chaotic in nature. He repeated the experiment with different initial conditions and verified the observation. Each experiment was found to be validating the extreme sensitivity of the system to initial conditions. The corresponding observations were published in 1965 and the scientific world received these results with enthusiasm. The system of equations were later on known as Lorenz system. The strange attractors of Lorenz system evolved as the wings of a butterfly. The system is represented by the following three non-linear differential equations with variables x, y, and z

$$\dot{x} = \sigma(y - x) \tag{1.10}$$

$$\dot{y} = -xz + \gamma x - y \tag{1.11}$$

$$\dot{z} = xy - \beta z \tag{1.12}$$

σ represents the ratio of fluid viscosity of a substance to its thermal conductivity called, "Prandtl number". The constants γ and β represent difference in temperature between top and bottom of the gaseous system, width to height ratio of the box used to hold the gas in the gaseous system respectively. The variable “x” represents rate of rotation of the cylinder, "y" represents the difference in temperature at opposite sides of the cylinder, and "z" represents the deviation of the gaseous system temperature from atmospheric temperature. Variables x, y and z are the three states of the system that can be separately plotted as three time series. Figure 1-2 shows the time series x of the Lorenz system simulated in Matlab for parameter

values $\sigma = 1,\ \gamma = 26.5\ ,\ \beta = \frac{8}{3}$ and initial conditions x_0=0, y_0=0.1, z_0=0 for which the system will be chaotic. The behaviour of the system is controlled by three parameters σ, γ and β. x, y and z are system states. According to the observation of Lorenz, the change in any one parameter caused an abrupt change in system behaviour. In the following illustrations; Figure 1-2 to 1-5, variable x is represented as state1, y as state 2 and z as state 3.

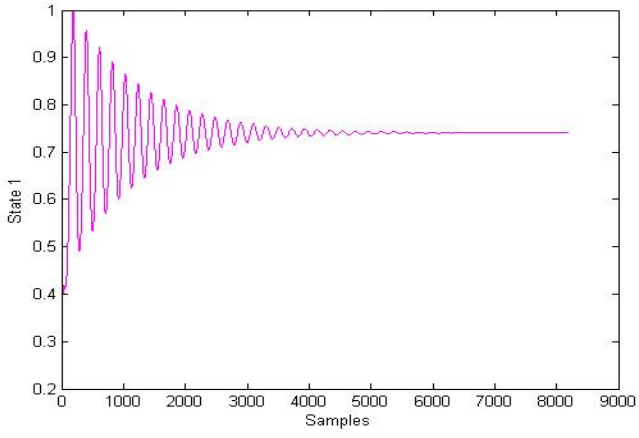

Figure 1-2Lorenz time series state1 for σ=1

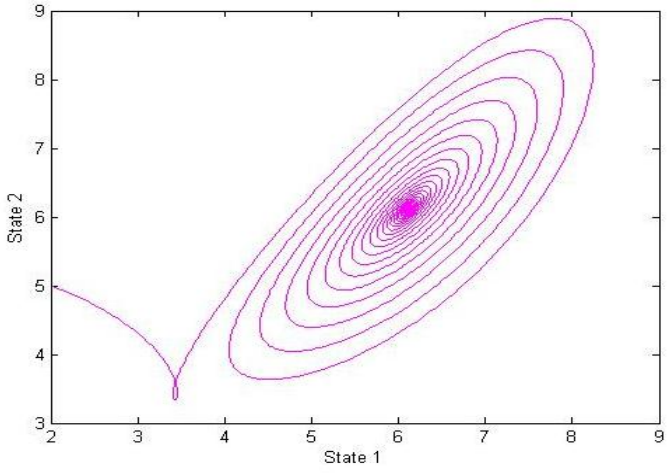

Figure 1-3Lorenz phase plot states 1 &2 for σ=1

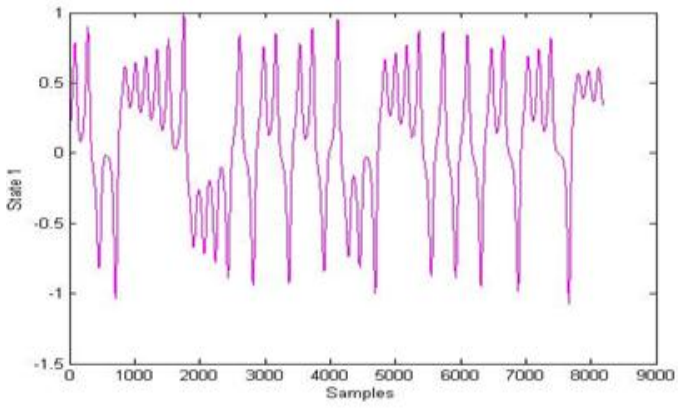

Figure 1-4Lorenz time series state1 for σ=10

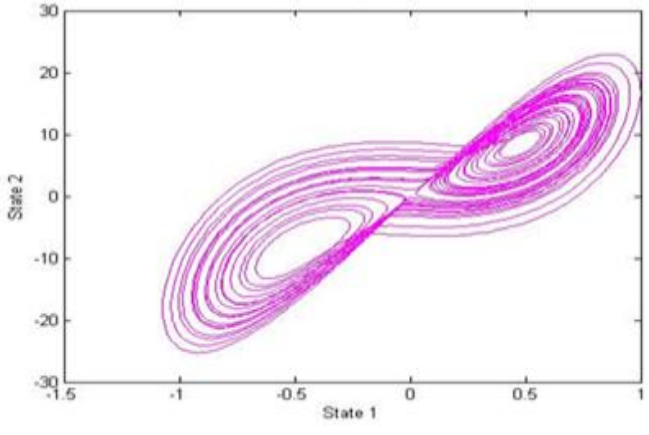

Figure 1-5 Lorenz phase plot state1 & state2 for σ=10

Figure 1-2 and 1-3 shows time series and phase plot of Lorenz system for the parameter σ =1. But when the parameter σ is changed to 10, the properties of time series and phase plot undergoes a significant transition as in Figure 1-4 and 1-5. The shape of the phase plot in Figure 1-5 is called the famous "Lorenz butterfly". This type of phase plots, which have two equilibrium points and the solution of the state space travels from one to another is called a strange attractor, which is considered as the signature of chaotic systems. In chaotic systems, there exists unstable aperiodic behavior that depends sensitively on initial conditions. The aperiodic behavior occurs when none

of the variables describing the state of the system undergoes a regular repetition of values. Such a behavior never repeats and it continues to manifest the effects of any small perturbation. Hence, any prediction of a future state in an aperiodic chaotic system is practically impossible. Though prediction of chaotic systems is in general difficult, a well-established parameterized model often helps to characterize the system and even predict the system, thus getting an insight into the dynamic behaviour of the system [100]. A comparatively smaller change in a system parameter may cause very large change in the total behaviour. Lorenz used this result to state the "Butterfly effect" which states that "sometimes the flapping of a tiny butterfly may cause hurricanes in the nature". Lorenz system was followed by many other chaotic systems like Rossler, Chen, Chua, Lu, Henon etc. some of which are analysed in this work.

Chaos theory helps one to understand patterns in nature. Chaotic patterns show up everywhere around the world, including cloud formations, the currents in the ocean, the flow of blood through fractal blood vessels, the formation of branches of trees, astronomy, epidemiology, air turbulence etc. The Earth's atmospheric behaviour is an extremely complex system that can be described by physics in the form of thermodynamics, fluid mechanics, radiation, etc. However, the equations derived from these laws that are used for weather forecasting are very sensitive to initial conditions. This chaotic nature means that long-term weather forecasting is inherently problematic. The work of Lorenz in chaotic weather systems made the modeling and analysis of chaotic weather systems an interesting topic for research. Modeling and analysis of real-world chaotic systems has thus become a necessity, in view of the large scale impact of these systems and the topical interest they have generated.

1.4 Chaotic systems in Nature

Chaotic behaviour in systems has been very natural and many manifestations of chaotic behaviour have been observed in nature. The solar radiation, Earth's atmospheric system, oceanic currents, storms, etc. are a few to mention. Some of the typical systems are summarised in the sections to follow. The present thesis also analyses these natural systems using the models developed here.

1.4.1 Chaotic weather systems

Weather systems are of different types like winds, rainfall, earthquake, ocean waves etc. Most of these weather systems are highly non-linear or chaotic in nature. There are different forms of chaotic weather systems in nature. Tornados, hurricanes, oceanic oscillations, sea clutters, sunspots, tides, water level variations in lagoons are all examples of such systems. The final outcome of these systems are of different nature, such as tornados and hurricanes are harmful for human kind, whereas oceanic oscillations, sunspots etc. are helpful in revealing many important atmospheric effects.

1.4.2 Sunspot time series

Sunspots appear as dark spots on the surface of the Sun (Figure1-6 courtesy NASA). Sunspots are magnetic regions on the Sun with thousands of times stronger magnetic field than Earth's magnetic field. They develop and persist for periods ranging from hours to months, and are carried around the surface of the Sun by its rotation. Sunspots themselves produce only minor effects on solar emissions even though the magnetic activity that accompanies the sunspots can produce dramatic changes in the ultraviolet and soft x-ray emission levels. These changes over solar cycle have important consequences in Earth's upper atmosphere.

Figure 1-6 Sunspot

One striking feature that emerges from the long-term data is that the number of sunspots observed in a given year varies in a dramatic and highly predictable way. Sunspots usually come in groups with two sets of spots. One set will have positive or north magnetic field while the other set will have negative or south magnetic field. Often, sunspot area is represented as a physical index of solar activity [113].

As was mentioned in the previous paragraph, the sunspots themselves produce only minor effects on solar emissions. These changes over solar cycle have important consequences in Earth's upper atmosphere. The number of sunspots visible on the sun shines and diminishes with an approximate 11-year cycle. The connection between solar activity and terrestrial climate is an area of on-going research.

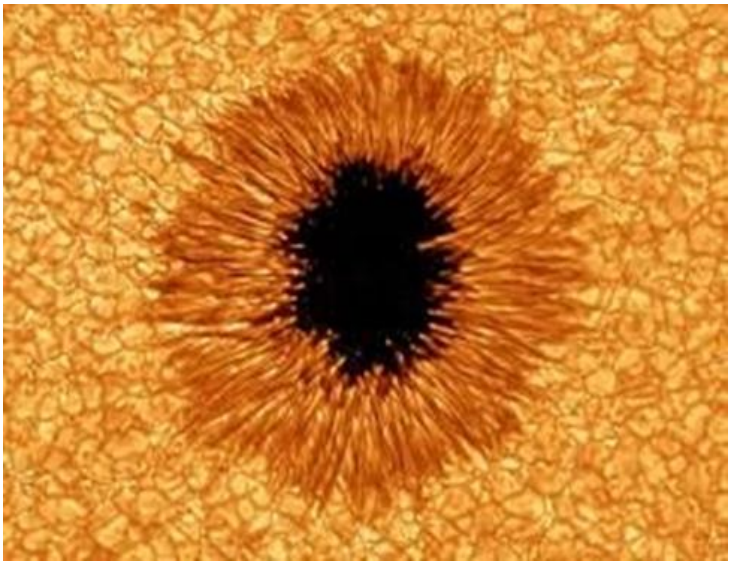

Figure 1-7 Enlarged picture of sunspot

The sunspot can be divided into two parts:

- The central umbra, the darkest part, where the magnetic field is approximately normal to the Sun's surface.

- The surrounding penumbra, lighter, where the magnetic field is more inclined. (Figure. 1-7image courtesy: New Jersey Institute of Technology, Big Bear Solar Observatory)

Early records of sunspots indicate that the Sun went through a period of inactivity in the late 17th century. Very few sunspots were seen on the Sun from about 1645 to 1715. This period of solar inactivity corresponds to a climatic period called the "Little Ice Age" when rivers that are normally ice-free froze and snow fields remained year-round at lower altitudes. There is evidence that the Sun has had similar periods of inactivity in the more distant past.

Sunspots have been monitored since the time of Galileo. The number of sunspots visible from a particular area is systematically counted and recorded in many parts of the world. There is a striking variation in the number of sunspots that is cyclic, with a period of approximately 11 years. This 11 year periodicity is called the sunspot cycle [66].

1.4.3 Venice Lagoon Time series

The Lagoon of Venice is the most important survivor of a set of lagoons that existed in Roman times extended from Ravenna north to Trieste [117]. In the sixth century, the Lagoon gave security to Roman people from invaders. Later, it provided naturally protected conditions for the growth of the Venetian Republic and its maritime empire. It still provides a base for a seaport, the Venetian Arsenal, and for fishing, as well as a limited amount of hunting and fish farming ..

Figure 1-8 Venice lagoon

Venetian Lagoon stretches from River Sile in the north to Brenta in the south, with a surface area of around 550 square kilometres. The land area is around 8% including Venice itself and many smaller islands. About 11% is permanently covered by network of dredged channels while around 80%

consists of mud flats, tidal shallows and salt marshes. Figure 1-8(image courtesy, Earth Observatory system-NASA). The lagoon is the largest wetland in Mediterranean BasinIt is connected to the Adriatic Sea by three inlets. Sited at the end of a largely enclosed sea, the lagoon is subjected to high variations in water level. The most extreme variations occur by spring tides, known as the "Acqua Alta" (Italian word for "high water"), that regularly flood much of Venice. The Venetian lagoon is an important natural wetland which is home to one of world's most beautiful cities 'Venice'. Modeling and analysis of Venice lagoon water level is a highlight of this thesis, explained in Section 6.2.

1.4.4 North Atlantic Oscillation Index.

North Atlantic Oscillation (NAO) is a climatic phenomenon in the North Atlantic Ocean due to the difference in atmospheric pressure at sea level between the Icelandic low and the Azores high [50]. It controls the strength and direction of westerly winds and storm tracks across the North Atlantic through fluctuations in the strength of Icelandic low and Azores high. It is part of the Arctic oscillation, and varies over time with no particular periodicity. NAO was discovered in 1920s by Sir Gilbert Walker. Unlike the El Niño-Southern Oscillation phenomenon in the Pacific Ocean, NAO is a largely atmospheric mode. It is one of the most important manifestations of climatic fluctuations in the North Atlantic and surrounding humid climates.

A large difference in pressure at the two stations, positive NAO, leads to increased westerlies and consequently cool summers & mild wet winters in Central Europe. If the pressure difference is low, negative NAO, westerlies are suppressed (Figure 1-9, image courtesy; NOAA). As a result Northern Europe suffers from cold dry winter and storms track towards

the Mediterranean Sea. This brings increased storm activity and rainfall in Southern Europe and North Africa, especially during the months of November to April. The NAO is responsible for much of the variability in weather in the North Atlantic region, affecting wind speed & direction, temperature, moisture distribution & intensity, number & track of storms [109]. A very significant time series called NAO index is given by continuous measurement of pressure difference in the above mentioned stations

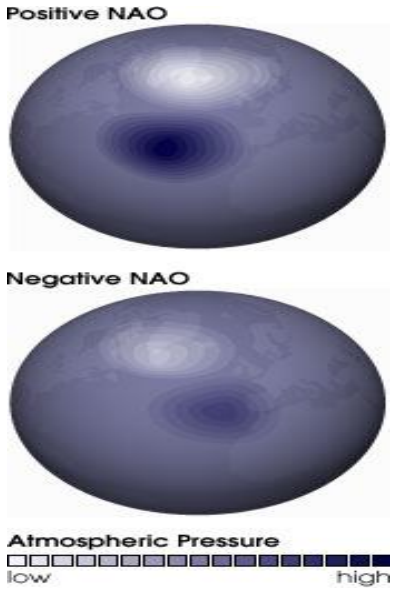

Figure 1-9 Positive and negative NAO

The modeling and analysis of NAO index will be helpful for better weather forecasts. A detailed study of NAO index is presented in Section 6.3. After the chaotic weather systems are modelled, the outputs are also analysed time and frequency domains.

1.5 System modeling

Simulation and analysis of mathematical models are important for understanding physical and biological phenomena. The knowledge created

from modeling, simulation, analysis and visualization contributes to reveal the secrets they embody. Linear systems can be uniquely described by their impulse, step or frequency response. Transfer functions, root locus, bode plot, frequency spectrum are all tools for analysis of linear systems. Graphical representations of these responses are widely employed for analysis.

On the other hand, for the non-linear system analysis, a mathematical representation of the relationship of all the state variables of the system is required. The model parameters bring out the system behaviour in a telling and easy to assimilate manner [15]. It is most essential that the model parameters are derived from the measured systems output, especially when one is trying to characterize unknown systems. The procedure of system modeling adopts the following factors:

- Prior knowledge
- Data collection
- Choice of model parameters
- Selection of the best model
- Validation of selected model

Figure 1-10 shows the block schematic of system modeling approach. The mathematical model usually consists of many differential equations and the solutions of such equations by classical methods are often difficult. Hence, analysis of the models was considered to be quite involved in the early times. Later on, with the development of fast computers and simulation software, the analysis of even complex mathematical models became quite easy. [15].

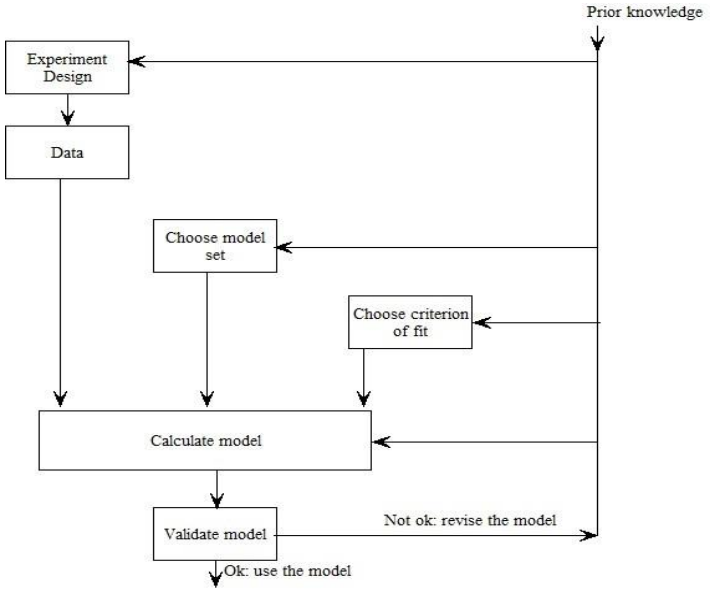

Figure 1-10 System modeling: a block diagram

With the advancement in the field of Soft Computing, modeling of highly non-linear and chaotic systems took a new turn. Fuzzy logic and neural networks are two important branches in artificial intelligence, which support soft computing. Artificial Neural Networks (ANN) mimics the human brain. They are highly parallel and distributed interconnection of processing units. The neural networks with non-linear activation function helps in precise modeling of highly non-linear and chaotic systems [22]. They can be effectively used in non-linear and chaotic system modeling and analysis.

1.6 Neural networks for chaotic system modeling.

The basic computational element of an ANN is often called a neuron or simply a node. It receives input from some other units, or perhaps from an external source. Each input has an associated weight w, which can be modified so as to model synaptic learning. The unit computes some

activation function *f* of the weighted sum of its inputs [45]. Figure 1-11 shows the architecture of a single artificial neuron with inputs, weights, summing point, activation function and output.

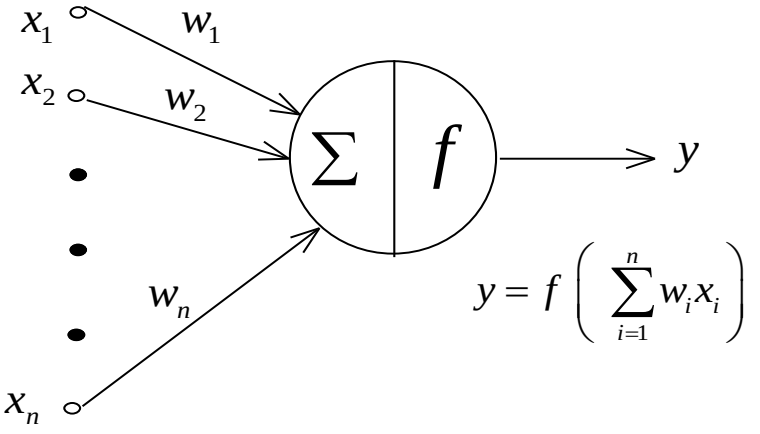

Figure 1-11 Artificial neuron

Neural Network types can be classified based on various factors as illustrated in Figure 1-12.

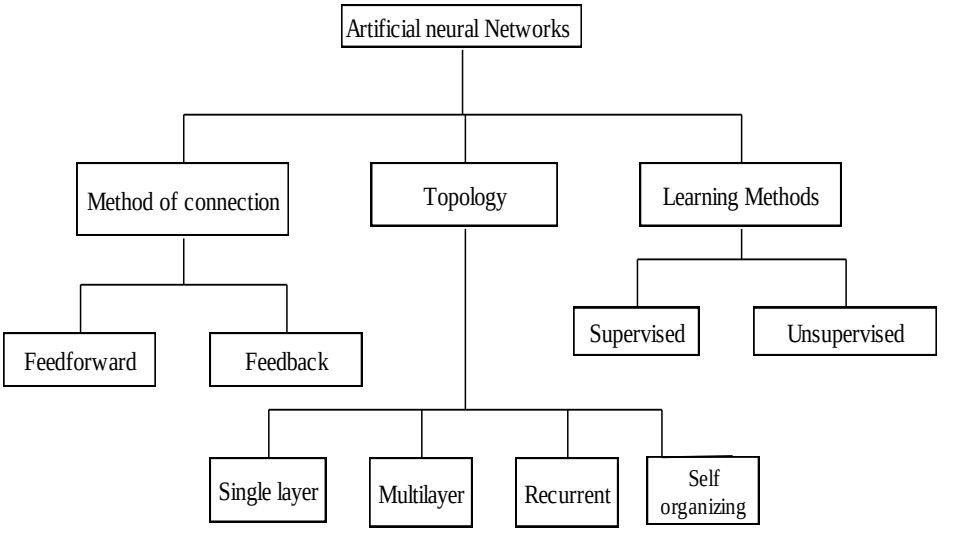

Figure 1-12 Classification of neural network

Application of neural network in modeling non-linear systems has been addressed by many researchers in the past few years. Among the different architectural formation of the artificial neural Networks, Recurrent Neural Networks come out to be most effective in handling the evolutionary nature of the Chaotic Systems. Built with multi-layer networks, with feedback in their hidden layer, the information flow in Recurrent Neural Networks is multidirectional. Such networks inherently possess sense of time and memory. Hence recurrent neural networks could be used in creating models of highly non-linear and chaotic systems [77]

1.6.1 Recurrent neural networks

The fundamental feature of a Recurrent Neural Network (RNN) is the feed-back connection. Learning can be achieved by similar gradient descent procedures as that used in back-propagation algorithm. The presence of feedback loops has a profound impact on the learning capability of the network and its performance. An effective model reported in literature [45] has a single output, regressing on the past output values as shown in Figure 1-13 and 1-14. It is realized using a delay line on the inputs, known as Non-linear Auto-Regressive with eXogeneous inputs (***NARX***) model:

$$y(t+1) = f[(y(t), y(t-1), \ldots y(t-p), x(k), x(k-1), \ldots x(k-q), \Omega)] \qquad (1.13)$$

where x(k) = v(k) account for the noise driving the system and Ω is the parameter set of the model. This type of neural network is particularly effective for time series modeling. The present thesis therefore addresses the issues of modeling chaotic systems from output series using recurrent neural networks.

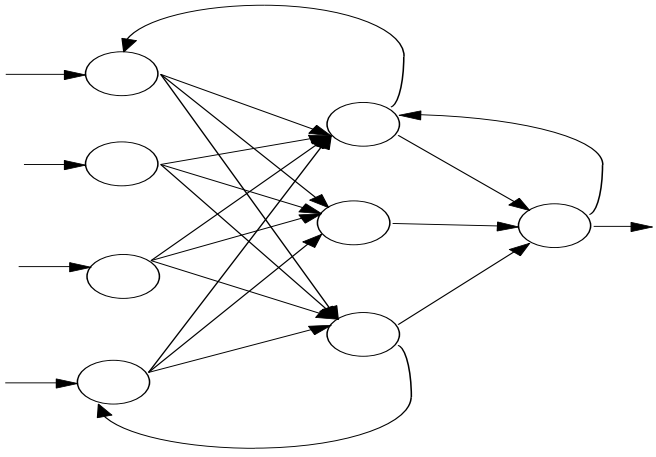

Figure 1-13 Recurrent neural network

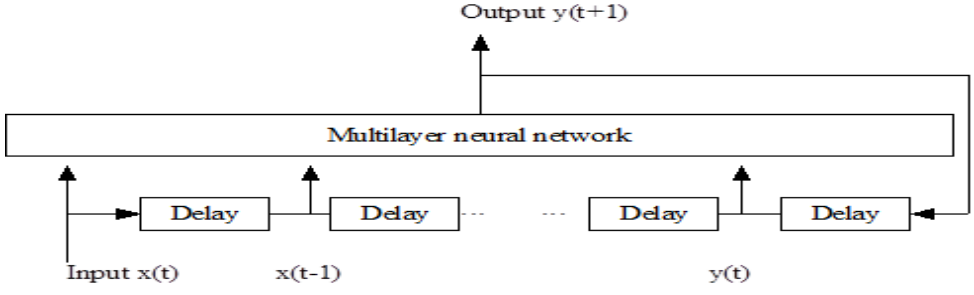

Figure 1-14 RNN-NARX model

There are many training algorithms, both supervised and unsupervised, for neural networks. Starting from perceptron learning rule, the list is large with delta learning rule, Widrow Hoff learning rule, gradient descent rule, etc. [45] the invention of error back propagation learning for multilayer neural networks has made the non-linear modeling much easier. However, it is well known that the any algorithm that depends on the gradient suffers from the problem of local minima, since the objective function to be optimized to derive the model parameters is not always convex. In attempting to derive alternative algorithms in order to overcome the problem of the local minima, the Extended Kalman filter (EKF) was proposed [56], for estimating the model parameter through training from the measured data. Since the

assumptions on the Guassianity, as required in the EKF are not promised as the output goes through the non-linearity, other approaches like the Particle filtering algorithms came up as effective choice in training the recurrent neural networks. These algorithms are utilized to create an efficient model structure for chaotic modeling [77] [98].

1.6.1.1 Kalman filter algorithm

The Kalman filter algorithm has been in existence over more than 50 years; but is still one of the most sought out techniques for target tracking and parameter estimation. Named after Rudolf E. Kalman, the great success of Kalman filter algorithm is due to its relatively small computational requirement, elegant recursive properties, and its status as the optimal estimator for one-dimensional linear systems with Gaussian error statistics [57]. Typical applications include smoothing noisy data and providing estimates for parameters of interest. From a theoretical stand point, the Kalman filter deals with linear dynamic system, described by a vector difference equation with additive white Gaussian noise, which models unpredictable disturbances. Generally in the context of the Linear System modeling, the Kalman filter can be used to estimate the state, x $\in \Re^n$, of a discrete-time controlled process governed by the linear stochastic difference equation, along with the model parameters.

$$x_k = Ax_{k-1} + Bu_k + w_{k-1} \tag{1.13}$$

with a measurement z $\in \Re^m$ that is

$$z_k = Hx_k + v_k \tag{1.14}$$

where u is the input vector, A, B and H are parameter matrices of the system. Process & measurement noises w_k & v_k are independent (of each other),

white, and with normal probability distribution $p(v) \sim N(0,R),\ p(w) \sim N(0,Q)$ where Q is the process noise covariance and R the measurement noise covariance. The true state x_k of the system cannot be directly observed and can be estimated using Kalman filter algorithm from the models of the system. In the case of non-linear systems the Kalman filter algorithm needs modifications [57].

1.6.1.2 Extended Kalman Filter algorithm (EKF)

The Kalman filtering process has been designed to estimate the unknown states in a linear stochastic system with apriory knowledge of known states and noise statistics. The Kalman filter can be extended for non-linear systems along a linearization procedure. The resulting filter is referred to as Extended Kalman Filter (EKF).

Let the system is described by the non-linear functions

$$x_k = f(x_{k-1}, w_{k-1}) \tag{1.15}$$

$$z_k = h(x_k, v_k) \tag{1.16}$$

EKF recursively estimates the state x_k from the previous time step k-1, using the error between the estimated input and the measured input and the Kalman Gain. The algorithm also estimates the covariance matrix of the parameters and the states computed. The algorithm thus attempts to reduce the variance in the estimate, while trying to minimize the modeling error. EKF algorithm gives a systematic procedure for estimation of process and measurement state updates, as explained in Appendix A.

One of the basic problems in implementation of the EKF algorithm is the choice of initial values of state and state co-variance. Since arbitrary choices can lead to divergence of the filter, the EM algorithm has been effectively

employed to calculate the initial values for an initial set of measurements [74].

With all its attractive features as an effective estimator, the estimates of EKF algorithm could be less accurate, since the Guassianity assumed by the algorithm is not satisfied, when the output of the model under goes the non-linear transformation. Computing the pdf of the states, (called particles) generated using an Importance function, the particle filtering algorithm alleviates the limitation of non-Guassianity in the modeling.

1.6.1.3 Particle filter algorithm

The objective of a particle filter is to estimate the posterior density of state variables, given the observation variables. The particle filter is designed for a Hidden Markov Model (HMM), where the system consists of hidden and observable variables [60]. The observable variables are related to the hidden variables by some known function. Similarly, the probabilistic dynamic system describing evolution of the state variables should also be known. A generic particle filter estimates posterior distribution of the hidden states using observation and measurement. Optimal filtering problem involves estimation of the state vector at the instant k with all the measurements up to and including k, denoted by $z_{1:\,k}$. This problem can be formulized, in a Bayesian set up, as a two-step recursive computation of distribution $p(x_k|z_{1:k})$[97].The new measurement z_k is used to update the distribution $p(x_{k-1} \mid z_{1:k-1})$, from Bayes' rule, to obtain the posterior distribution over $x_{k:}$ as

$$p(x_k \mid z_{1:k}) \propto p(z_k \mid x_k)\, p(x_k \mid z_{1:k-1}) \tag{1.17}$$

the prediction step involves

$$p(x_k \mid z_{1:k-1}) = \int p(x_k \mid x_{k-1})\, p(x_{k-1} \mid z_{1:k-1}) dx_{k-1} \tag{1.18}$$

The $p(x_k \mid z_{1:k-1})$ is to be evaluated from the integral in Equation 1.18 where $p(x_k \mid x_{k-1})$ is known from the probabilistic origin of equation (1.3). Before receiving the most recent measurement z_k, the distribution $p(x_{k-1} \mid z_{1:k-1})$ is known prior to x_k.

In general, the computations in prediction and update steps cannot be carried out analytically [60]. Hence approximate methods such as Monte Carlo sampling are required. Particle filters are suboptimal filters, which perform Sequential Monte Carlo (SMC) estimation based on point mass or "particle" representation of probability densities. The SMC ideas, in the form of sequential importance sampling, had been introduced in statistics back in 1950s. Although these ideas continued to be explored during 1960s and 1970s, they were largely overlooked and ignored. Most likely the reason for this was the modest computational power available at that time. In addition, all these early implementations were based on plain sequential importance sampling that degenerates over time.

Inclusion of re-sampling step in the development of SMC method, coupled with ever faster computers, made particle filters useful in practice for the first time. Research activity in the field has dramatically increased since then, with many improvements of particle filters and their numerous applications. A detailed derivation of particle filter and its variants are presented in Appendix A.

Model validation has to be performed after the selection of a proper model structure like the NARX and implementation structure like the RNN and an efficient training algorithm to estimate the model (or network) parameters from known input. The availability of a stable model to represent the chaotic

system can be a useful for analyzing wide variety of physical phenomena, including turbulence, vibrations of buckled elastic structures, behavior of certain atmospheric changes etc.

1.7 Time domain characterization of chaotic systems

The change in the qualitative character of chaotic systems can be analyzed from phase plots, bifurcation diagram and Lyapunov exponents [14]. Phase plots illustrate the state space evolution of the chaotic system. Lyapunov Exponents and Kaplan- Yorke dimensions are sets of invariant geometric measures that describe the dynamical content of a system. The embedding dimension of a dynamic system is the smallest integer for which the system states can be embedded into, without intersecting itself. Bifurcation diagram is characterized by growth rate of a perturbation [14]. In the present work all these characteristics of chaotic systems are studied using the models developed and presented in Section 4.1.

1.8 Frequency analysis of chaotic systems

Representing a periodic function as a linear combination of sines and cosines decomposes the function into its components of various frequencies, much as a prism resolves a light beam into its constituent colours. Resulting coefficients of the trigonometric basis functions tell what frequencies are present in the function in what amounts. Moreover, this representation of the function in frequency domain enables some of the manipulations required in many applications, such as signal processing or solving differential equations, to be performed efficiently than in time domain. There are many frequency domain analysis tools like Fourier transform and its variants. The discrete time Fourier transform has got wide application in signal analysis and is most effective when the signal is stationary. Time-frequency analysis is helpful to study the time-frequency pattern of non-stationary signals from

non-linear dynamics, when data are sampled at fixed rate. The most explored algorithms of time-frequency analysis are Wavelet Transform and Wigner Ville Distribution [18]. Mapped Real Transform (MRT) is an alternate form of signal representation in the frequency domain, which makes use of operations in real domain only [42]. In the present thesis, the behaviour of the chaotic systems are also examined in the frequency domain using Fourier Transform, Wavelet Transform and MRT in Sections 5.1 to 5.3.

1.9 Motivation

The mathematical modeling of linear and simple non-linear systems is straightforward and many efficient techniques have been developed for the analysis of such systems. The modeling and analysis of highly non-linear and chaotic systems is still considered to be a difficult task because of the complex nature of the systems itself. Complexity in analysis of such systems were reduced with the development of soft computing techniques, such as neural networks and fuzzy logic. The availability of good number of estimation techniques to estimate the parameters of the model from the time series of the chaotic systems was a major motivation in evolving state space models, which can fully characterize the chaotic system. Among the different approaches proposed for modeling and analysis of chaotic systems, the artificial neural networks appear to be quite promising. Availability of rich literature in neural network training methods also was a motivating factor to explore the modeling of chaotic systems. Accordingly, the thesis focused on the modeling and analysis of chaotic systems using soft computing techniques. Though the frequency domain analysis of chaotic systems is limited because of their broad banded nature of such systems, the analysis using new transforms like MRT appears to be quite promising. Having modeled mathematically described chaotic systems, it was felt that study of different types of natural chaotic systems is in order. Typical systems like

the weather systems which have high impact on the environment were considered in the study noting that such an analysis is a need of the day. The amazing challenges in the modeling and analysis of chaotic systems, along with an opportunity to suggest new techniques and methodologies in the analysis motivated the work reported in the thesis. Developing stable and accurate methods to estimate the time varying parameters of computable mathematical models of chaotic systems is a major objective of the proposed work. Building the models from time series of observations underscores the methodology adopted in this work. The thesis has been organized as follows.

1.10 Outline of the thesis

- Chapter 1 introduces the concept of systems and reviews different types of systems like linear, non-linear and chaotic systems. It also introduces different techniques of system modelling. The idea of representing systems using NARX models and the utilisation of neural networks, with emphasis on RNN to model the chaotic systems, is also introduced in the chapter. Different types of chaotic systems and their characteristics are discussed concisely. Important chaotic weather systems and some important frequency domain concepts are discussed briefly.
- A comprehensive review of the literature available on system modelling, analysis and characterization of chaotic systems along with frequency domain concepts used in this work are reviewed in Chapter 2.
- Chapter 3 explores the selection of a best model structure for chaotic systems. Four important chaotic systems-Lorenz, Rossler, Chen and Chua – are thus modelled with RNN, using the NARX model. Three versatile algorithms are used to train the RNN:
  (i) EKF algorithm with EM to initialise the error covariance

(ii) SIR particle filter algorithm

(iii) RB particle filter algorithm

- In Chapter 4 the RNN model is extended to the estimation of important time domain characteristics of chaotic systems like strange attractors, Lyapunov exponents, Kaplan - Yorke dimensions, bifurcation diagrams and embedding dimensions.
- Some important frequency domain characteristics of chaotic systems using Fourier transform (FT), wavelet transform (WT) and Mapped real transform (MRT) are presented in Chapter 5.
- Modeling and analysis of some important chaotic systems in nature like Sunspot time series, Venice Lagoon time series and North Atlantic Oscillations is presented in Chapter 6.
- Chapter 7 concludes the work with scope for future work
- Some of the topics available in literature, relevant to the work presented in the thesis, such as EKF, SIRPF and RBPF algorithms are briefly discussed in Appendix A. The Fourier, wavelet and Mapped Real transforms are discussed briefly in Appendix B.

Chapter 2

Literature Review

2. Literature Review

Literature review is a critical discussion and summary of collected works relevant to the topic of research problem. The chapter reviews literature associated with the main areas of interest in this work. The survey on past works describes how the proposed problem is related to prior research in system modeling.

2.1 System theory

System theory is a branch of engineering which deals with study of linear and non-linear dynamic systems. Non-linear dynamics has a long history in the branch of mathematics. Kepler started explaining planetary motion with circular orbits. In the mid-1600s Newton invented differential equations, which later became a major tool to describe the behaviour of dynamic systems. Further, he discovered laws of motion and universal gravitation. Combining these, he was able to accurately calculate the elliptical orbit of planetary motion. Driven by the propositions of Laplace, Fourier, Nyquist and Lyapunov, the theory of linear systems grew up on strong footings. Later on dynamic system theory moved over to address non-linear systems leading to the studies of non-linear oscillators and their applications in physics and engineering. Many problems in fluid mechanics, electrical circuits, structural analysis etc. were analysed using well established techniques in non-linear systems.

2.2 Chaotic systems

The behaviour of a dynamic system sometimes depends sensitively on the initial conditions. Such systems are referred to as chaotic systems. The first major development in the branch of chaotic systems was occurred in 1890 with the work of Henry Poincare [26]. He proved that the knowledge of all

possible behaviour of the system states was essential in solving non-linear problems. He concluded that the solution to non-linear equations may sometimes behave in a much complicated or 'chaotic' fashion than anyone has previously imagined.

The scientific world had to wait around 70 years for another significant development in the field of chaotic system. It was in 1963 Edward Lorenz [2], an American meteorologist, discovered the sensitive dependence on initial conditions on his differential equation model of weather. These equations are henceforth called Lorenz equations and are still explored with the same enthusiasm as its launching period. A detailed analysis and simulation of Lorenz system is found in the book by F. C. Hoppensteadt [54].

Later on, many chaotic systems were evolved, out of which three of them are extremely relevant and are analyzed in detail in the work reported here. Otto Rössler designed the Rössler system in 1976 [5]. It consists of three non-linear ordinary differential equations. These differential equations define a continuous-time dynamical system that exhibits chaotic dynamics. The original Rössler paper says the Rössler system was designed with some similarities to the Lorenz system. But the equations are simpler than Lorenz system and hence are easy to analyze. Chen found a new chaotic system in 1999 [47]. Chen systems are most suited for generating hyper chaos. The analysis of Chen system contributed to a better understanding of a whole family of similar and closely related chaotic systems. T Matsumoto [11] reported that a chaotic attractor has been observed with an extremely simple autonomous circuit suggested by Leon Chua of the University of California, Berkeley [7]. The system was named Chua chaotic system and is analyzed in detail in the present work.

There are a number of new chaotic and hyper chaotic systems which are derived from the classical Lorenz, Rossler, Chen and Chua systems [80] [102]. Guoyuan Qi presents an independent and new chaotic system with four differential equations [96].

2.3 Chaotic weather systems

Chaotic dynamical systems are present in the nature in various forms such as the weather, activities in human brain, variation in stock market, flows and turbulence. The Sunspot time series, the Venice lagoon time series and the North Atlantic Oscillations- are some weather systems analyzed in the present work.

Naked eye observations of sunspots are known from different cultures as noticed by Bray &Longhead [1]. In particular, the ancient Chinese have kept detailed although very incomplete records going back over 2000 years which is effectively summarized by Wittmann &Wu [16]. Nevertheless, it was the rediscovery of sunspots by Galilei, Scheiner and others around 1611, with the help of the then newly invented telescope that marked the beginning of the systematic study of the Sun in the western world and heralded the dawn of research into the Sun's physical character. Over the ages the view on the nature of sunspots has undergone major revisions. Overviews of the structure and physics of sunspots are given by Thomas [23] and Solanki [66]. Theoretical models of sunspot structure and dynamics is explained in detail by John H Thomas [23]. A frequency domain analysis of sunspot is presented in a paper of P Chen [32].

Sunspot areas are available since 1818 in the Greenwich series obtained from daily photographic images of the sun. Although sunspots themselves produce only minor effects on solar emissions, the magnetic activity that accompanies

the sunspots can produce dramatic changes in the ultraviolet and soft x-ray emission levels. These changes over the solar cycle have important consequences for the Earth's upper atmosphere. The sunspot number is calculated by first counting the number of sunspot groups and then the number of individual sunspots. This method is suggested by Wolf [10]. The sunspot index has a physical meaning related to the solar magnetic flux emerging at sunspots [35].

The NAO is characterized by an oscillation of atmospheric mass between the Arctic and the subtropical Atlantic. According to R. J. Greatbatch [50] it is usually defined through changes in surface pressure. He also points out that permanent low-pressure system over Iceland (the Icelandic Low) and a permanent high-pressure system over the Azores (the Azores High) control the direction and strength of westerly winds into Europe. The relative strengths and positions of these systems vary from year to year and this variation is known as the NAO. It measures the strength of the westerly winds blowing across the North Atlantic Ocean between 40^{o}N and 60^{o}N. Studies of C. Collette and M. Ausloos [73] reveal that the NAO accounts for 31% of the variance in hemispheric winter surface air temperature north of 20^{o}N.

NASA has accepted an index for the NAO as the difference between normalized mean winter (December to February) sea level pressure (SLP) anomalies at Ponta Delgadas, Azores and Akureyri, Iceland [88].The studies of R. J. Greatbatch also reveals that large difference in the pressure at the two stations (denoted NAO+) leads to increased westerlies and, consequently, cool summers and mild and wet winters in Central Europe and Atlantic areas. In contrast, if the index is low (NAO-), westerlies are suppressed, these areas suffer cold winters and storms. The detailed studies

of NAO also points out that it strongly affects the Atlantic ocean by inducing substantial changes in surface wind patterns. According to Greatbatch [50], changes in NAO have a wide range of effects on marine and terrestrial ecosystems, including distribution and population of fish, flowering dates of plants, growth, reproduction and demography of many land animals. The modeling and analysis of NAO index considered as a time series is an important problem. The chaotic origins of NAO are investigated by S. M. Osprey.et. al [109] and R Washington[51].

2.4 System modeling

Box and Jenkins in [4] gives an introductory idea about system modeling and introduces the Box-Jenkins model. Lennart Ljung explains the key concepts of modeling and identification of linear and non-linear system in [15]. According to Ljung the construction and estimation of models on non-linear dynamic systems relies upon many different disciplines like physical modeling, mathematical statistics, neural network techniques, learning theory, support vector machines, and automatic control. Yakov Bar-Shalom and Xiao-Rong propose that non-linear models play important roles in many different application fields, and many specific areas have developed their own techniques [28].

2.5 Neural network for modeling non-linear systems

Simon Haykin [45] presents extensive materials on neural network architectures, learning methods etc. and finds that neural networks can be successfully used for system modeling and identification. V Gorlovka in his paper demonstrates that multilayer neural networks with back propagation algorithm can be effectively used for modeling of non-linear systems [55]. The extended Kalman Filter algorithm is a variant of the basic linear Kalman filter. Both these are well explained by Greg Welch and Garry Bishop [57].

Shu hi Li gives a comparative study of back propagation and EKF algorithm for neural network training and suggests that EKF is more convergent [56].

Peter Trebaticky suggests that RNN are suitable for non-linear modeling when trained with EKF algorithm [77]. The application of RNN in online modeling and identification of non-linear system is underlined in the work of L Palma et. al. Puskorius and Feldcamp [31] also highlight the fact that RNN trained with EKF algorithm performs well in non-linear modeling. In addition, Si-Zhao Quin Hong [24] gives a comparison of four Neural network learning methods for dynamic system modeling and suggest EKF algorithm.Meanwhile Wu Xue-Dong and Song Zhi-Hua gives an important observation that some variants of Kalman filter are suitable for modeling of chaotic system [93]. This result is in line with the earlier method suggested by R G Hutchins [38] and H Leung [75] for the identification of chaotic systems with neural networks. One of the well-known issues in the Kalman Filter is the proper assumption of the initial conditions, since arbitrary choices can lead to divergence of the filter. J F G De Freitas et.al [44] proposes a method to calculate the initial values of the state variable and its covariance (along with other properties like the measurement and plant variance) by maximizing the expectation of the state estimate from the given measurement.

Particle filtering methods are a novel area for neural network modeling which results in very low error. Afonso [98] suggested particle filter training algorithms for RNN for various applications. Arnauld Doucet gives a detailed study of Particle filters and its variants like SIRPF, Auxiliary PF, RBPF etc. with detailed algorithm, examples and explanations [97]. Q. Wen and P. Qicoiig [84] proves that particle filters can be successfully used for neural network training. M. Sanjeev Arulampalam, Simon Maskell, Neil

Gordon, and Tim Clapp[60] [71] in their paper demonstrates that particle filters and all its variants can be suitably used for training all types of neural networks with non-linear activation functions. The RBPF is an efficient algorithm with an adaptation of Kalman filter and best suited for training neural networks as suggested by Daucet et al [53]. Dong and Hua in their research paper validates that [93] EKF and particle filter are suited for reconstruction of chaotic signals.

2.6 Time Domain Characterization of Chaotic systems

The change in the qualitative character of chaotic systems can be depicted by phase plots, strange attractors, Lyapunov exponents, Kaplan -Yorke dimension, bifurcation diagrams and embedding dimension. Phase plots and strange attractors illustrate the state space evolution of the chaotic system. A detailed explanation of strange attractors can be seen in J C Sprotts paper [49]. The Lyapunov Exponents and Kaplan –Yorke dimension describe the dynamical content of the system. A. Wolf describes a practical method to calculate the Lyapunov exponent from a noisy time series [12]. M Ateae [67] and CE Meador [110] in two separate studies reveal important methods to calculate the same.J Kaplan and J A Yorke [6] have conjectured that the dimension of a strange attractor can be approximated from the spectrum of Lyapunov exponents. Such a dimension has been called the Kaplan-Yorke (or Lyapunov) dimension, and it has been shown that this dimension is also helpful in the analysis of typical strange attractors.

An equivalent dynamical system can be developed by assuming proper dimension which is able to embed all the properties of the actual dynamical system. If the selected dimension is not optimum the reconstruction may preserve only some of the properties of the dynamical system. A set has

embedding dimension n if n is the smallest integer for which it can be embedded into without intersecting itself. Taken's theorem states that the original dynamic properties of the attractor can be retained as long as the embedding dimension is accurately estimated [8]. Choice of the minimum embedding dimension can be done by the method of false nearest neighbours as explained by Takens in [9]. H. Ma and C. Han [82] also give valuable suggestion for selecting suitable embedding dimension and delay time. Liangyue Cao established with proof that the method of false nearest neighbours is actually the most suitable method for estimating the minimum embedding dimension [40].

A bifurcation diagram is a plot that shows the value of the changing parameter, on one axis and the solution to the system on the other axis. H. Broer et al [61] explains bifurcation in other words as change in the qualitative character of a solution as a control parameter is varied is known as a bifurcation. E. J. Doedel [85] explains that bifurcation causes the solution of a system to change from a stable fixed point to a chaotic attractor.In yet another research paper, E. J. Doedel [85], explains in detail the bifurcations of Lorenz systems whereas J. Lü et al. does the same of Chen system [62]. Specific applications of bifurcation analysis can be seen in studies of S. Grillo [105].Bifurcation analysis is extended to hyper chaotic systems by H. Jia [102].

2.7 Frequency analysis of chaotic systems

The introduction of Fourier and fast Fourier transforms is considered as a turning point in frequency domain analysis of signals as observed by Cooley and Tukey[3]. From the notes of D. Batenkov[76]a detailed information of Fourier analysis was initiated. Even though the broad band spectrum of chaotic signals limits the use of Fourier analysis, P. Cvitanovi and M. J.

Feigenbaum [63] gives a very useful Fourier analysis of chaotic systems which is also verified by D. Kugiumtzis and A. Tsimpiris [106] .In her dissertation, S. H. Isabelle [36] gives a very useful time series analysis of non-linear systems in the Fourier aspect. This work is supported by the findings of Aberbanel,et al [30].

The first literature that relates to the wavelet transform is Haar wavelet. It was proposed by the mathematician Alfred Haar in 1909. However, the concept of the wavelet did not exist at that time, until 1981, the concept was proposed by the geophysicist Jean Morlet [48]. Afterward, Morlet and the physicist Alex Grossman invented the term wavelet in 1984. Before 1985, Haar wavelet was the only orthogonal wavelet people know. A lot of researchers even thought that there was no orthogonal wavelet except Haar wavelet. Fortunately, the mathematician Yves Meyer constructed the second orthogonal wavelet called Meyer wavelet in 1985 [25]. In 1988, Stephan Mallat [18] and Meyer proposed the concept of multiresolution. In the same year, Ingrid Daubechies [17] found a systematical method to construct the compact support orthogonal wavelet. In 1989, Mallat proposed the fast wavelet transform. With the appearance of this fast algorithm, the wavelet transform had numerous applications in the signal processing field. In the study report of Alfred Mertins[48] the concepts of wavelet transforms are summarized.

The thesis of Vela Arevalo gives a broad idea about the time frequency analysis of non-linear systems with stress on wavelet transform [64]. C. Lamarque and J. Malasoma gives an interesting study of wavelet transforms applied for non-linear oscillations [37]. The basic functions of the wavelet transform have the key property of localization in time(or space) and in frequency as suggested by P Chen[32]. The initial approaches of chaotic

systems analysis using wavelet is seen in the work of Carlo Cattani [90]. J. S. Murgu particularly used the Daubechies wavelet for analysis of chaotic systems which inspired the present work [89]. Wavelet analysis of Lorenz system by Kaiyan Zliu [69] was of significant importance to the present area of interest. S. Azad and S. K. Sett of IIT Bombay has proved that wavelet can be used for detecting chaotic transitions in Logistic map [65]. Another important contribution in this area was from C. Chandré and T. Uzer [78]. They have proved that instantaneous frequencies of chaotic system can be identified from the ridge plot of wavelet coefficients. Based the on work of X. Jiang and S. Mahadevan [107] the wavelet coefficient level of decomposition suited for chaotic applications was selected.

R Gopikakumari in her dissertation in 1998 [42] modified 2-D DFT definition in terms of real additions, derived a visual representation of the DFT coefficient in terms of 2 x 2 DFT and developed a parallel distributed architecture for the hardware implementation of N x N DFT for any even N. Rajesh Cherian Roy, together with R Gopikakumari, extended this idea to develop a new real transform in 2004 named MRT (Mapped Real Transform, originally M-dimensional Real Transform) [70] which can represent signals using real additions and without complex arithmetic, and which offers a different way of signal analysis. MRT is an evolving transform that can be used for the frequency domain analysis of 2-D signals. MRT mapping is highly redundant [103]. Different placement schemed were proposed by Bhadran and Rajesh Cherian Roy to remove the redundancy and placing the unique MRT coefficients [104]. A computationally efficient algorithm for placing these coefficients called Unique MRT (UMRT) was developed for the forward and inverse transforms by Preetha [111]. Exploiting the visual representation of unique MRT coefficients, a new placement named Sequency based Unique MRT(SMRT) was developed by

Jaya [112]. Considering the fact that chaotic systems always consist of a large array of data samples, it seems that SMRT with its Sequency based placement techniques may prove to be a suitable tool for analysis of such systems.

2.8 Conclusion

The availability of rich literature as portrayed above is a major motivation in taking up the topics addressed in the thesis. Some of the papers on Extended Kalman Filter, Expectation maximization and Frequency domain analysis are very seminal and furnished valuable information in developing some of the techniques reported in the thesis.

Chapter 3

Selection of Model Structure

3. Selection of Model Structure

It is well known that many natural systems exhibit chaotic behaviour at some time or other. Magnetic radiations from sun, climatologic systems, and fluid flow are a few typical occurrences in nature, producing occasional manifestations of chaotic behaviour. Though chaotic phenomena described by well-established mathematical equations are completely defined in terms of initial values and parametric sets, what is interesting in natural systems is the lack of complete knowledge of the forcing functions of the dynamic systems. Such chaotic phenomena are often manifest as output time series only. It therefore becomes imperative to use the output time series alone to develop a model for the chaotic system. Such a modeling exercise is quite challenging in view of the requirement of blind identification from given output series. Literature has reported the use of the NARX [75] model to represent time series emanating out of non-linear systems. Fortunately, artificial neural networks configured as Recurrent Neural Networks directly map the NARX model and are shown to possess the required self-learning capability to tune the network parameters (i.e. weights) to identify highly non-linear and chaotic systems [22] [24]. Non-linear dynamical systems can be approximated to any accuracy by a recurrent neural network, with no restrictions on the compactness of the state space according to the Universal approximation theorem [45]. The following section deals with the choice of best neural network model structure for representing chaotic system.

3.1 Recurrent Neural Networks

The fundamental feature of a Recurrent Neural Network (RNN) is the presence of at least one feed-back connection, so that activation can flow round in a loop [44]. The architectures of recurrent neural networks exploit the powerful non-linear mapping capabilities of the Multi-Layer Perceptron

with some form of memory. The simplest form of fully recurrent neural network has the previous set of hidden unit activations fed back along with the inputs. These networks have the potential to be used in unison with dynamic elements and feedback [55]. In effect, the recurrent neural networks, used for modeling or model based predictive control, are multi-layer neural networks with a delay element in their feedback loop. Figure 3-1 below illustrates the architecture of the RNN used in this work for modeling chaotic system.

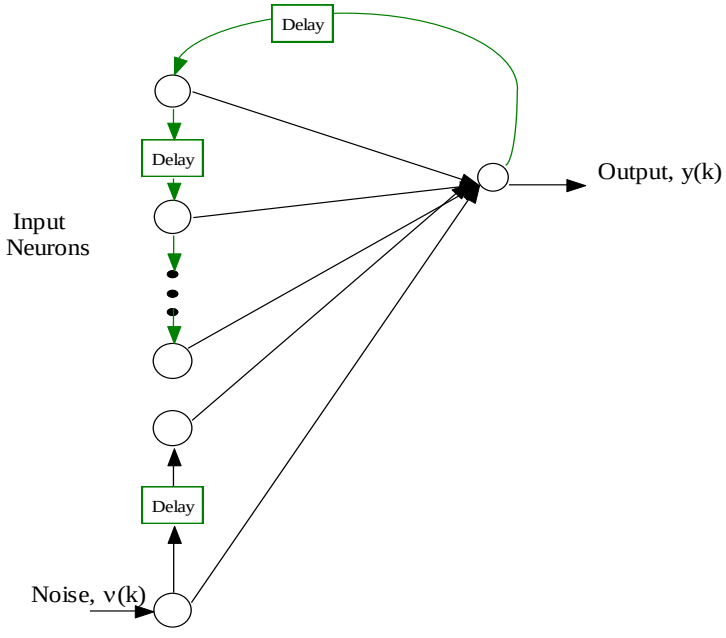

Figure 3-1 Recurrent neural network for time series modeling

While the representational capability of RNN to describe evolutionary phenomena like time series is well understood, the learning of the neural network parameters requires a competent and effective learning algorithm. There are many efficient training algorithms reported in literature for training RNN. Back propagation, Least mean square algorithm, conjugate gradient

algorithm [45], different types of competitive learning algorithms etc. are a few to mention.

Earlier studies on non-linear modeling have explored some training algorithms and a comparative study to select the best algorithm for non-linear modeling has been reported[22][24].

Since the problem of local minima is a well known issue in the objective fucntion to be minimised, grdient based tachniuqes generaly do not promise comprehensive solution to the paraneter estimation problem in RNN. On the other hand, the results reported in [24] highlights the Extended Kalman Filter (EKF) as a promising for non-linear modeling. Accordingly, in the work reported here the EKF algorithmis and their variannts have been used forestimating the weights of the RNN modelin the time seriesof chaotic system. Expectation Maximization technique is incorporated to compute the intial values of the states and co-variance matirces. The complete algorithm is described in Appendix A.The thesis also examines the efficacy of using particle filter algorithm, with its two variants to train the RNN for chaotic system modeling.

3.2 RNN training with EKF algorithm

The chaotic system with a single output can be represented by the NARX model equation below:

$$y_{k+1} = g(y_k, y_{k-1}, ..., y_{k-p}, \upsilon_1, \upsilon_2, ..., \upsilon_q, \Theta) \qquad (3.1)$$

where υ account for the noise driving the system, Θ represents the parameters of the modeling functions. Given the time series measurements y_k , the parameters Θ are estimated optimally for known functional representations. In the present work, neural networks are used to represent

the non-linearity. Given the output time series of the chaotic system to be modeled, the weights of neural networks are estimated using the EKF algorithm. When recurrent neural networks are used, Equation (3.1) becomes

$$y_{k+1} = h(\sum_{i=0}^{p-1} \mathrm{w}_i^m \mathrm{y}_{k-i} + \sum_{i=0}^{q} w_i^n \upsilon_i) \tag{3.2}$$

where w^m & w^n are the forward and recurrent weights of the RNN and $h(x) = \frac{1-\tanh(x)}{1+\tanh(x)}$ is the non-linearity corresponding to the measurement function in the EKF model. The state equation is given by the identity transformation,

$$W_{k+1} = W_k + \omega_k \tag{3.3}$$

$$W_k = [w^m \quad w^n]^T \tag{3.4}$$

ω_k is the process noise with covariance $Q = \omega\omega^T$ and υ is the measurement noise with covariance $R = \upsilon\upsilon^T$. The EKF equations are given by projecting the states ahead

$$W_{k+1} = h\left(W_k\right) \tag{3.5}$$

and the error covariance ahead

$$P_k = P_{k-1} + Q \tag{3.6}$$

The Kalman gain is computed using

$$K_k = P_{k-1} H_k^T (H_k P_{k-1} H_k^T + R_k)^{-1} \tag{3.7}$$

H is the Jacobean of partial derivatives of h with respect to W. The estimate of W is updated from the given measurement

$$W_{k+1} = W_k + K_k(y_k - h(W_k, \ ( )) \tag{3.8}$$

where $h( )$ is as given in Equation 3.2. Now update error covariance

$$(\mathrm{P}_k = I - K_k H_k \ \mathrm{P}_k^{-}) \tag{3.9}$$

Starting with some reasonable assumptions on W[0], P[0], Q and R the estimate y_{k+1} is obtained from Equation 3.2. It is compared with given time series and the weights are updated by (3.8). The process is repeated for every *k*. The EKF often converges with sufficient number of samples, the exact number being decided by the accuracy in the choice of the parameters and initial conditions as described above. One of the basic problems in the implementation of the EKF is the choice of the initial values of W[0] and P[0]. Since arbitrary choices can often lead to divergence of the filter, EM algorithm [44] is used considering its capability in computing the initial values of W[0] and P[0].The outline of the algorithm is given below.

3.2.1 EM Algorithm

As has been indicated earlier, the EKF Algorithm [57] for training Multi-Layer Perceptron suffers from some shortcomings, namely choosing the initial states and covariance W [0], P[0], along with the process error covariance Q and measurement error covariance R. It is proposed to alleviate the problem by using the EM algorithm [44]. Using the Expectation maximization approach, the algorithm maximizes the likelihood p(**W** , Y $|$ Θ), where Θ = { Q,R, π , μ} - the set of parameters governing the likelihood function. Assuming that the measurements are independent,

$$p(W, Y \mid \Theta) = p(W_1)\prod_{k=2}^{N} p(w_k \mid w_{k-1})\prod_{k=1}^{N} p(y_k \mid w_k)) \tag{3.10}$$

The first term $p(W_1)$ is parameterized with π &μ, whereas the other terms

have Q and R as parameters. In the E step, the algorithm computes the likelihood using the known parameters Θ and in the M step maximizes the expected likelihood of data known thus far. The maximization is done by differentiating W w.r.t. Θ and equating to zero. It has been shown [44] that the estimates $\mu = W_{1|N}$ and $\pi = P_{1|N}$. Starting with $W_{N|N}$, $P_{N|N,}$ obtained after computing the forward estimates in EKF over N measurements, the "Rauch-Tung- Striebel smoother" [44] is executed on the same data series in the reverse order to do the following backward recursions. For the time series modeling problem, A = I. The recursion converges to $W_{1|N}$ and $P_{1|N}$

$$J_{k-1} = P_k H^T P_{k-1}^{-1} \tag{3.11}$$

$$J_{k-1} = P_{k-1} I P_{k/k-1}^{-1} \tag{3.12}$$

$$\hat{W}_{k-1} = W_{k-1} J_{k-1} \left(W_{k-1} - A W_k \right) \tag{3.13}$$

$$\hat{P}_{k-1} = \bar{P}_{k-1} + J_{k-1} \left(\bar{P}_k - \bar{P}_{k-1} \right) J_{k-1}^T \tag{3.14}$$

The EKF algorithm for RNN training is given below:

EKF Algorithm for RNN Training

1. *All the weights are initialized to small random values. The state covariance matrix P(0|-1) is initialized to a diagonal matrix with relatively small values.*

2. *The EKF algorithm is executed for the first N measurements using equations 3.5 to 3.9.*

3. *Starting with* $W_{1|N}$ and $P_{1|N}$ *the equations (*3.10) *to* (3.13) *are executed to obtain* W_N and P_N

4. *The initial values obtained are used again to correctly estimate the weights* W using *the* EKF, *until the modeling error comes down to acceptable limits.*
5. *Driven by noise, the time series corresponding to the chaotic system to be modelled is regenerated using W.*

Algorithm 3.1

Other algorithms are to be explored to select the best training method for RNN. Particle filter algorithm and some of its variants [53] [60] [71] seems to be worth testing.

3.3 RNN training with Particle Filter algorithm

The particle filters attempts to find the posterior distribution of the hidden states in general using observation and measurement as discussed in Section 1.6.1.3. This problem has been formulated, in a Bayesian set up, as a two-step prediction and update computation of distribution $p(x_k|z_{1:k})$[97]. In general, the computations in prediction and update steps cannot be carried out analytically [60]. Accordingly a set of particles are generated by sampling from a known probability density function, called importance sampling function. Each of this particles undergo state transformation and are combined using weights which are updated for every measurement. Following [97], the weights are calculated using the likelihood ratio of the measurement with respect to each particle. In order to avoid degeneracy of the weights a resampling step is included [60]. Inclusion of re-sampling step coupled with ever faster computers, made particle filters a versatile algorithm. The proposed RNN is trained with particle filter algorithm. A detailed explanation of particle filters is given in appendix A.3 Two important variants of particle filter algorithm Sampling Importance

Resampling Particle Filter (SIRPF) and Rao Blackwellised Particle Filter (RBPF) are explored in this section.

3.3.1 RNN training with SIRPF

The inclusion of resampling step in the generic particle filter algorithm resulted in one of the best variant, the SIRPF algorithm. Here the weights of RNN correspond to the states of particle filter and each data sample of the time series produces the weight from likelihood function.

SIRPF Algorithm for RNN Training

1. *The RNN weights are to be initialized to random values in the range 0 :1 for i=1:N*
2. *Each of the selected RNN weights are sampled to finite number of particles,* $W_1^i, W_2^i \ . \ . \ . \ W_N^i$
3. *The importance weights* $w_1(W_1^i), w_2(W_2^i) \ . \ . \ . \ w_N(W_N^i)$ *are calculated using likelihood function*
4. *The weights are resampled back to N particles*
6. *The importance weights are normalized*
7. *The RNN weights are updated by combining the particles along with the importance weights.*
8. *The model output is recalculated and compared with the given data to calculate the error*
9. *If the MSE is within limits, the process is terminated*
9. *Else, go to step 1.*

Algorithm 3.2

3.3.2 RNN training with RBPF

One of the important constraints of SIRPF algorithm is the requirement of large number of particles, to converge to an optimum solution. Calculation of importance weights, sampling and resampling steps are to be repeated for all the particles. Complexity of the algorithm increases with increase in number of particles. Kalman filter is combined with a particle filter to reduce the number of particles required to obtain a given level of performance. This variant of particle filter is called RBPF and algorithm is as follows

RBPF algorithm for RNN Training

1. The weights W_i *are partitioned into* R_i *and* X_i *such that* $p(R_{1:i} | Y_{1:i})$ *can be predicted with Particle Filter (PF) and* $p(X_i \mid R_{1:i}, Y_{1:i})$ *can be updated analytically using a Kalman filter.*

2. The RNN weights in the hidden layer are partitioned by using linear and using nonlinear activation functions.

3. The weights of linear neurons are updated with Kalman Filter.

4. The particle filter algorithm 3.2 is used for non-linear neurons

Algorithm 3.3

The above steps 1 to 4 are detailed in Algorithm A.3. All the RNN weights are updated with the help of RBPF algorithm in each iteration and the results are obtained.

3.4 Performance evaluation of the training algorithms

Time series output from four standard chaotic systems, viz. Lorenz, Rossler, Chua and Chen, are modeled using RNN neural network architecture and

trained by the above three algorithms. The weight vector W is estimated for an initial set of data. Thereafter, driven by the noise, the RNN free wheels to produce the output time series and compared with the target time series. Performance of each training algorithm is evaluated based on least mean square error between the target time series and the modelled output.

3.4.1 Lorenz system

The Lorenz system, represented by the Equations (1.10) to (1.12), discussed in Section 1.3 is modelled using RNN architecture. It is assumed that the time series of state *x* alone is known. The state x is estimated using RNN with the three algorithms EKF, SIRPF & RBPF. the modeling results of EKF is given in Figure 3-2.

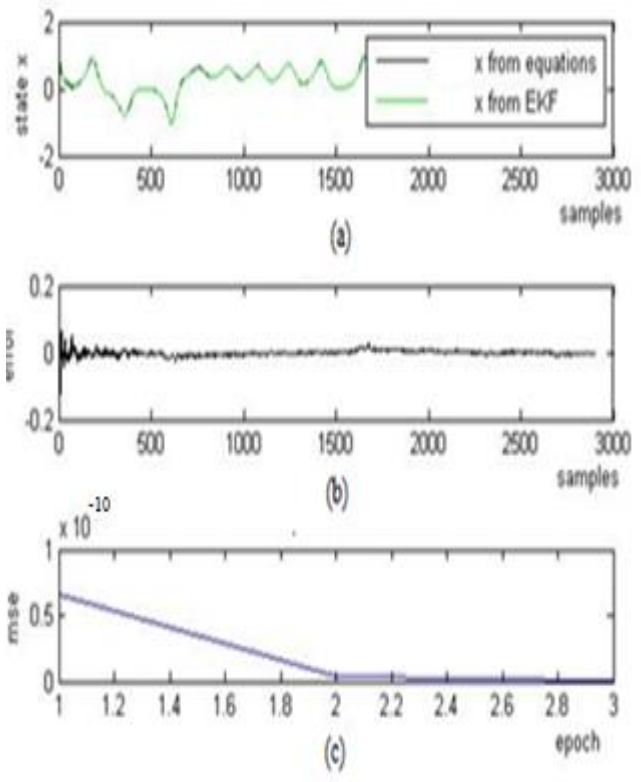

Figure 3-2 Lorenz model with EKF

Similarly the results of SIRPF and RBPF are plotted in Figure 3-3& 3-4. In all the three figures there are three subplots

(a) Time series of state x, generated from dynamic equations superimposed on the time series generated from RNN model structure

(b) Modeling error of each sample

(c) Mean square error

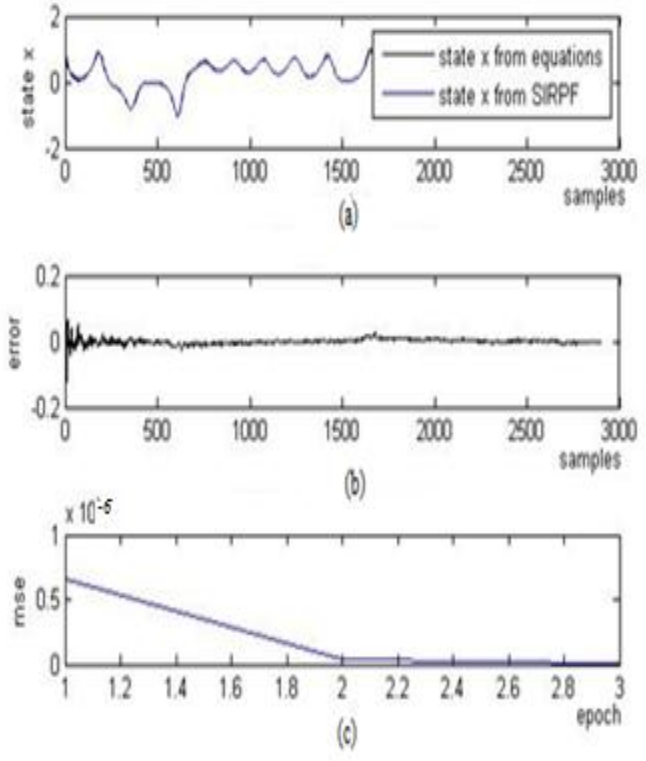

Figure 3-3Lorenz model with SIRPF

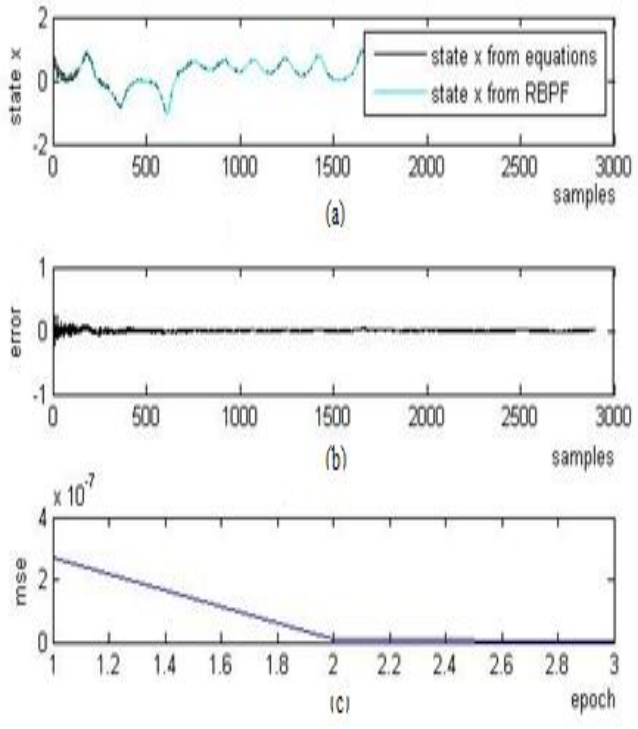

Figure 3-4Lorenz model with RBPF

The modeling error of Lorenz system calculated over 3000 samples is given in Table 3.1. It shows superiority of the EKF algorithm with EM technique over the others.

Table 3.1 Comparison of Mean Square Error (MSE) - Lorenz system

Data	**MSE with EKF**	MSE with SIRPF	MSE with RBPF
Lorenz	**6.052×10^{-10}**	6.003×10^{-6}	2.803×10^{-7}

Further the RNN is trained with three algorithms and tested on other standard chaotic systems, Rossler, Chen & Chua as follows.

3.4.2 Rössler system

Otto Rössler designed the Rössler system in 1976 [5]. It consists of three non-linear ordinary differential equations. These differential equations define a continuous-time system that exhibits chaotic dynamics. It was the second significant improvement in chaos theory after Lorenz. The research in chaotic theory was further motivated other researchers to come up with similar systems. The original Rössler system was designed with some similarities to the Lorenz system. But the equations are simpler than Lorenz system and hence are easy to analyze. The system is described by the non-linear equations

$$\dot{x} = -y - z \tag{3.15}$$

$$\dot{y} = x + ay \tag{3.16}$$

$$\dot{z} = bx - cz + xz \tag{3.17}$$

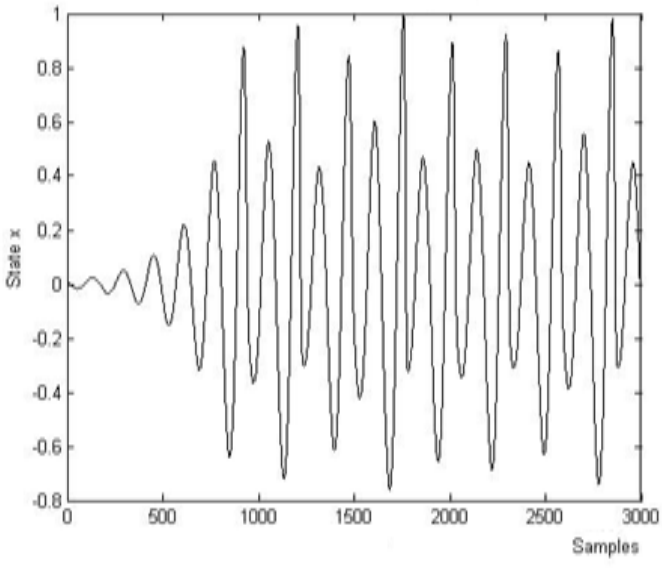

Figure 3-5 Time series 'x' of Rossler system

The system is simulated in MATLAB, with a= 2, b=0.2, c=5.7 and initial conditions $x_0 = y_0 = z_0 = 0.1$ for which the system will be chaotic.

Figures 3-6 to 3-8 show the plot of time series, modeling error and mean square error of Rossler system with EKF, SIRPF and RBPF respectively.

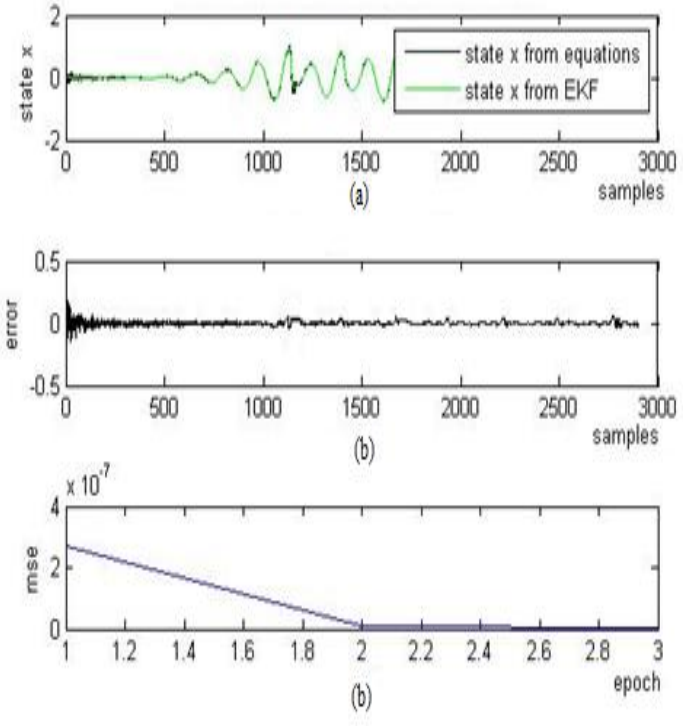

Figure 3-6 Rossler model with EKF

The Rossler system time series is reconstructed accurately which verifies the efficiency of RNN. The plots show a very low modeling error for EKF algorithm. Following Figures explore the efficiency of SIRPF and RBPF algorithms for Rossler system. The Rossler system dynamic equations were found to be useful in modeling equilibrium in chemical reactions.

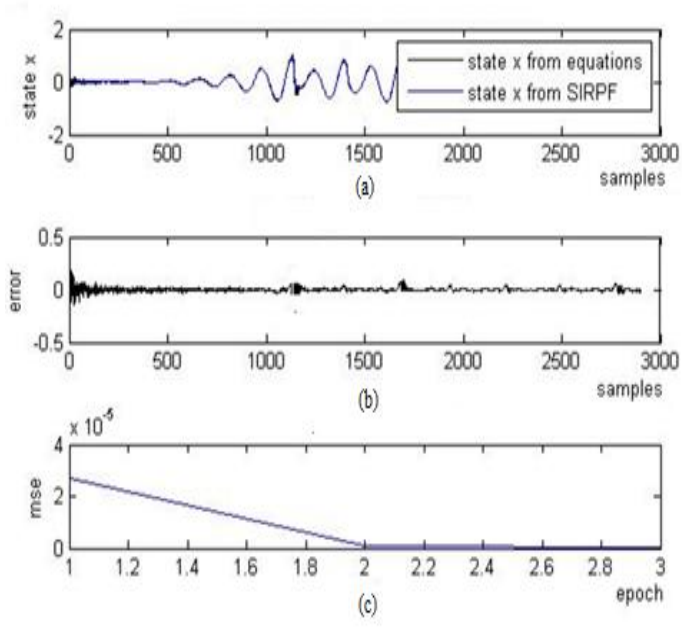

Figure 3-7 Rossler model with SIRPF

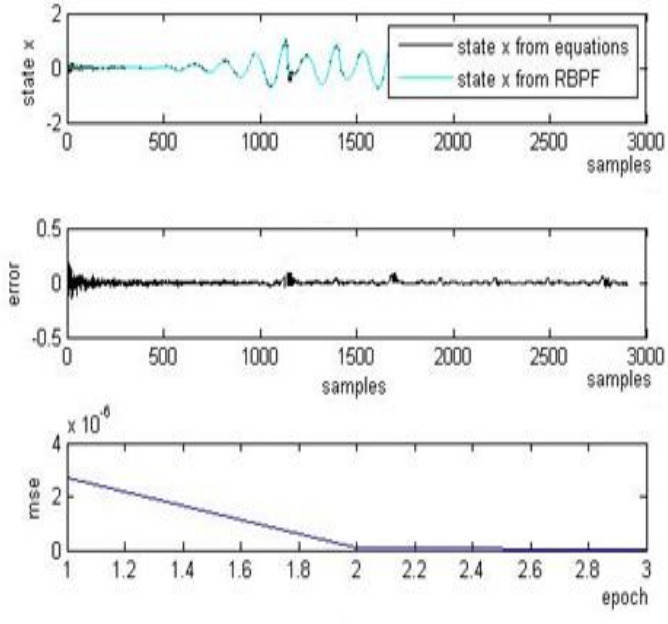

Figure 3-8 Rossler model with RBPF

3.4.3 Chen system

Chen proposed a new chaotic system in 1999 [46], described by the following three non-linear equations.

$$\dot{x} = a(y - x) \tag{3.18}$$

$$\dot{y} = (c - a)x - xz + cy \tag{3.19}$$

$$\dot{z} = xy - bz \tag{3.20}$$

The system exhibits chaotic behaviour with the values of a=35, b=3, c=25. Chen systems are most suited for generating hyper chaos. The analysis of Chen system will contribute to a better understanding of a whole family of similar and closely related chaotic systems. The intrinsic dynamics of the Chen system deserves further investigation in the near future.

Figure 3-9 shows the time series 'x' of Chen system. Figures 3-11 to 3-13 show the plot of time series, modeling error and mean square error of Chen system with EKF, SIRPF and RBPF respectively.

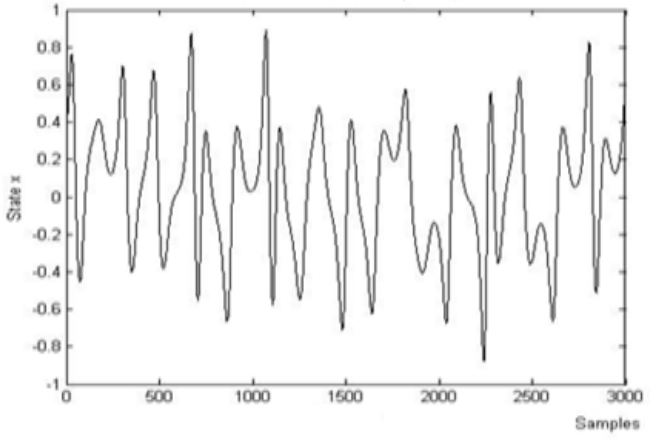

Figure 3-9 Time series 'x' of Chen system

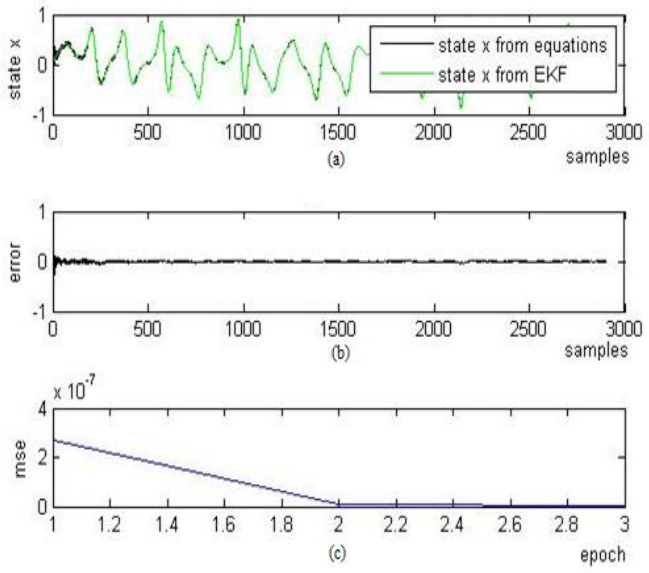

Figure 3-10 Chen model with EKF

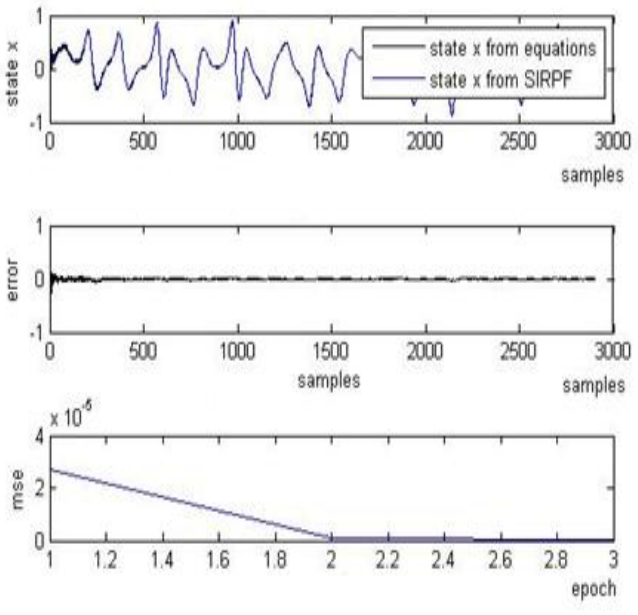

Figure 3-11 Chen model with SIRPF

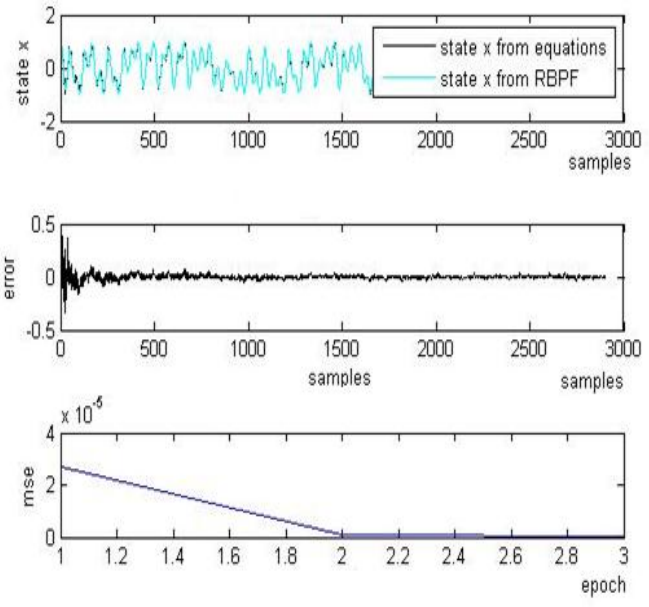

Figure 3-12 Chen model with RBPF

3.4.4 Chua Chaotic Oscillator

The Chua oscillator is a simple electronic circuit conceived by Chua, as shown in Figure3-13. It has 5elements: a linear resistor, a linear inductor, 2 linear capacitors, and a nonlinear 2-terminal resistor (Chua's diode) with piecewise non-linear characteristicsshown in Figure 3-14. The system is defined by the following differential equations and parameter

$$\dot{x} = y - x - f(x) \tag{3.21}$$

where $f(x) = bx + \frac{1}{2}(a-b)\left[|x+1| - |x-1|\right]$

$$\dot{y} = x - y + z \tag{3.22}$$

$$\dot{z} = -\beta y - \gamma x \tag{3.23}$$

$$x = \frac{v_1}{B_p} \qquad y = \frac{v_2}{B_p}, \quad z = i_3 \frac{R}{B_p}, \quad \alpha = \frac{C_2}{C_1},$$

$$\beta = \frac{R^2 C_2}{L}, \quad \gamma = \frac{R R_0 C_2}{L}, \quad a = R G_a, \quad b = R G_b$$

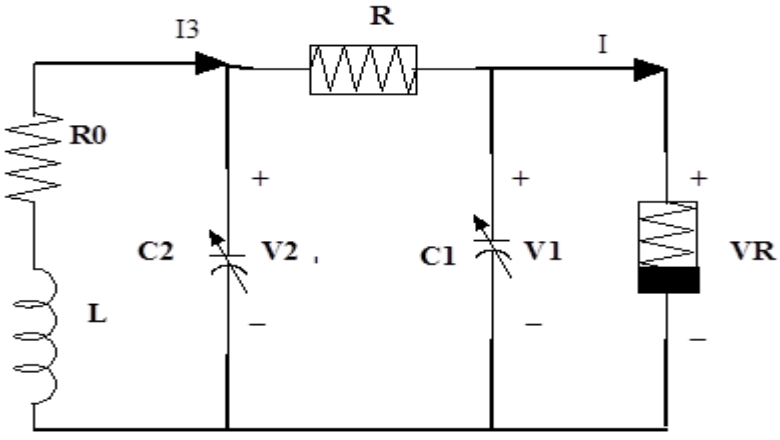

Figure 3-13 Chua's Circuit

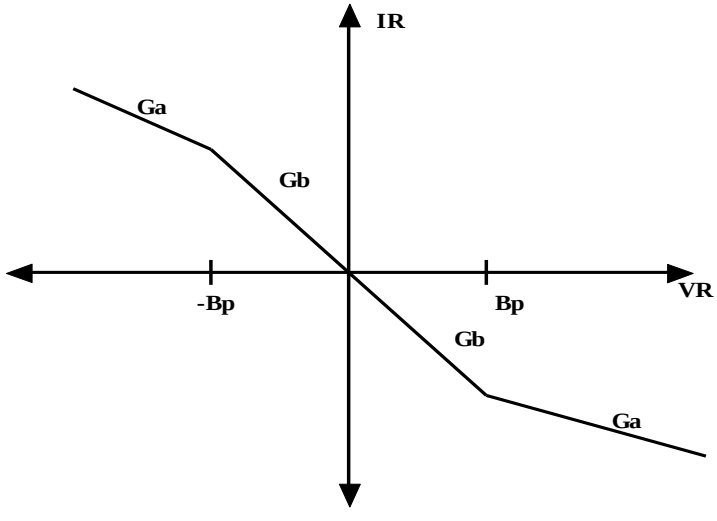

Figure 3-14 Chua diode characteristics

Chuas circuit is considered as the simplest tool for analyzing chaotic systems. It is easy to implement with a few energy storage elements and one non-linear element. The chaotic behaviour of Chua's circuits are verified with laboratory experiments. The system shows chaotic behaviour for the following parameter values

$$R = 1001\,\Omega, \quad R_0 = 20\,\Omega, \quad G_a = \frac{-1}{878.1\,\Omega}, \quad G_b = \frac{-1}{2339\,\Omega} - \frac{1}{878.1\,\Omega},$$

$$B_p = 1\,V, \quad L = 12\ mH, \quad C_1 = 15.06\ nF \quad and \quad C_2 = 178.5\ nF$$

Figure 3-16 shows the time series 'x' of Chua system. Figures 3-17 to 3-19 show the plot of time series, modeling error and mean square error of Chua system with EKF, SIRPF and RBPF respectively.

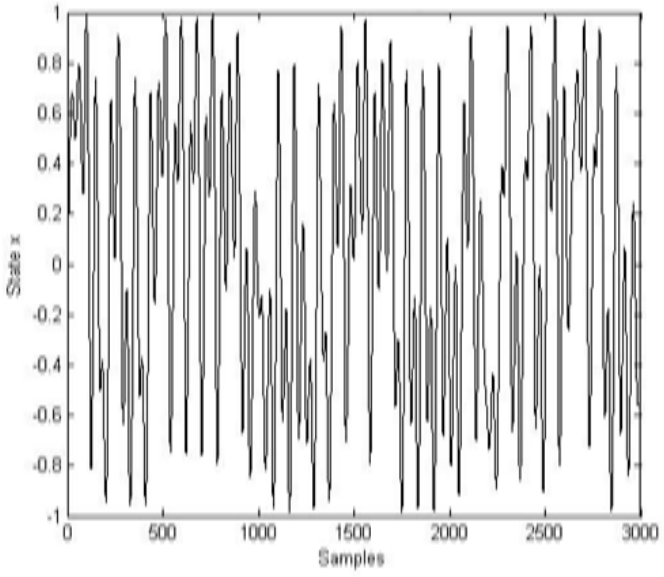

Figure 3-15 Time series x of Chua system

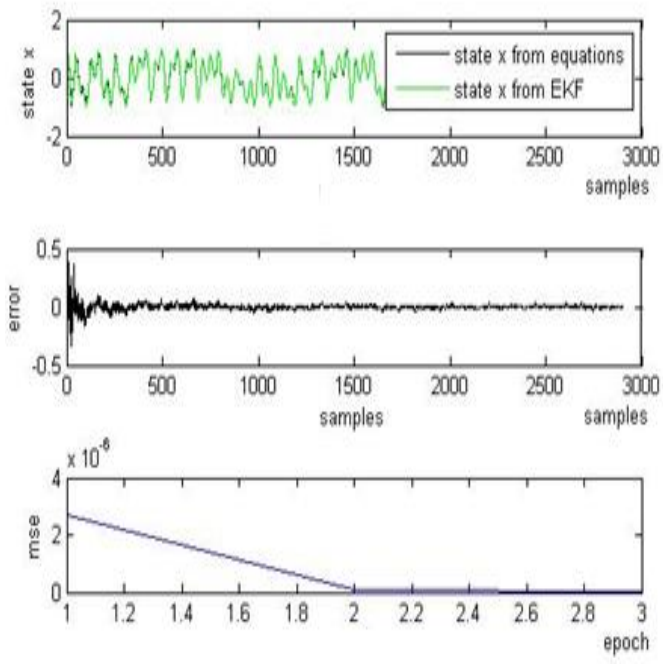

Figure 3-16 Chua model with EKF

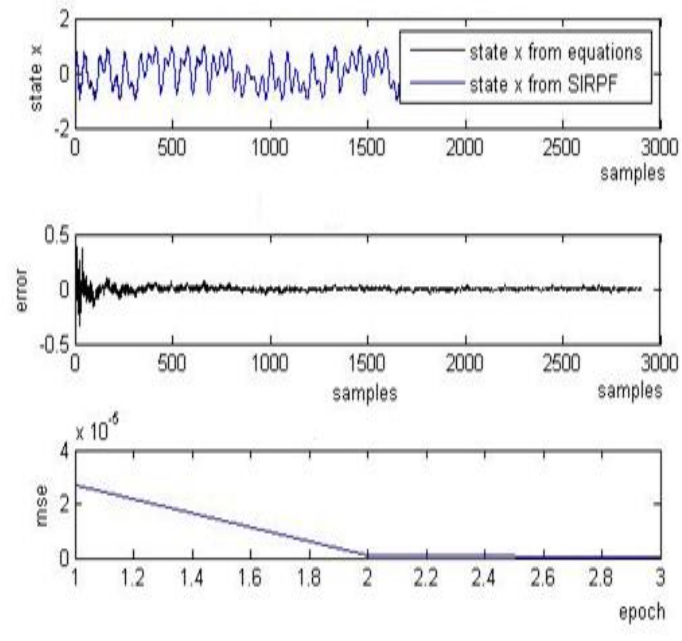

Figure 3-17 Chua model with SIRPF

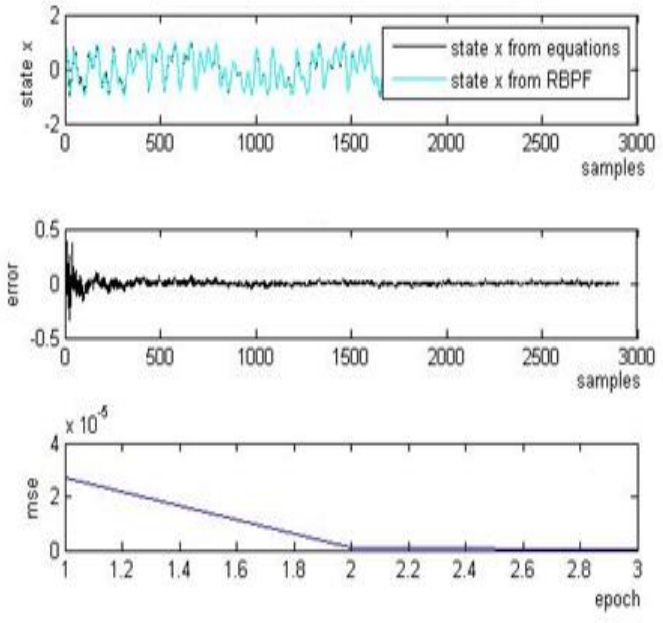

Figure 3-18 Chua model with RBPF

3.5 Selection of best training algorithm for RNN

Four standard chaotic systems - Lorenz, Rossler, Chen and Chua - are generated from the dynamic equations given in Sections 1.4, 3.4.2, 3.4.3 and 3.4.4 respectively. State x of each system is selected and samples of the corresponding time series are given as input to RNN model. The model is trained with the algorithms – EKF, SIRPF and RBPF- discussed in Sections 3.2, 3.3.1, 3.3.2 respectively to produce estimated output. Mean square error between actual output and estimated output is calculated. The MSE corresponding to all the four chaotic systems are tabulated in Table 3.2. . Analysis of the plots of MSE and Table 3.2 shows that EKF is the best among the three algorithms.

Table 3.2 Comparison of Mean Square Error (MSE)

No	Data	**MSE with EKF**	MSE with SIRPF	MSE with RBPF
1	Lorenz	**6.052×10^{-10}**	6.003×10^{-6}	2.803×10^{-7}
2	Rossler	**2.892×10^{-7}**	2.795×10^{-6}	2.788×10^{-6}
3	Chen	**2.888×10^{-7}**	2.899×10^{-5}	2.700×10^{-5}
4	Chua	**2.500×10^{-6}**	2.902×10^{-5}	2.522×10^{-5}

3.6 Conclusion

Chapter presents selection of a best model structure for chaotic. While RNN is selected as the model structure, a suitable training algorithm was to be identified. Three versatile algorithms, EKF with EM, SIRPF and RBPF, are used to train the RNN. Four well known chaotic systems, Lorenz, Rossler, Chen and Chua, with known dynamics are modeled using these algorithms, with a view to demonstrate the correctness of the model structure chosen and the parameter estimation algorithm. The output generated by the freewheeling RNN model , trained using EKF algorithm after parameter estimation match the chosen time series with a MSE as low as 10^{-10}. Hence it is concluded that RNN model can be selected as the best choice for time series modeling of chaotic systems and is adopted herein after. Since the

behaviour of the chaotic system is more manifest in the state space evolution diagram, it is imperative that the model is able to produce correct phase sequence on attaining minimum error after training. The RNN model outlined here is extended to accommodate state transition function of the chaotic system modeled. The chapter to follow introduces and demonstrates the extended model which is able to correctly generate the state space evolution sequence thus facilitating the analysis of chaotic systems from the state space evolution characteristics like Lyapunov exponents, Kaplan Yorke dimension, and Embedding dimension and bifurcation diagram.

Chapter 4

Model Validation with Time Domain Characteristics

4. Model Validation with Time Domain Characteristics

Chaotic systems have the property of sensitive dependence on initial conditions. Therefore analysis and characterization of chaotic systems is unique. The previous chapter describes methods of modeling chaotic system from the output time series. The EKF algorithm is proved to be the best algorithm with minimum modeling error for RNN.

Change in the qualitative character of chaotic systems can be depicted by certain invariant time domain properties like phase plots, strange attractors, Lyapunov exponents, Kaplan - Yorke dimension, embedding dimension and bifurcation diagrams [14] [26]. Phase plots and strange attractors illustrate the state space evolution of the chaotic system. The Lyapunov Exponents and Kaplan - Yorke dimension describe the dynamic content of the system. Embedding dimension gives a proper measure for attractor reconstruction, while bifurcation characterizes growth rate of a perturbation of chaotic systems.

The present chapter describes an extension to time series model of chaotic systems to a complete state estimation process. The invariant parameters are estimated for the systems generated from the RNN model. Since the dynamic equations are known, the estimated values and plots are compared with that of original dynamic systems. The chapter also discusses estimation of Lyapunov exponents along with bifurcation.

4.1 State estimation from RNN model

The RNN model discussed in Section 3.1 is insufficient for state estimation since it generate only one state of the chaotic system and hence only one

output. But the chaotic systems described in Sections 3.4.1 to 3.4.4 has 3 states x, y & z. Hence the RNN model is modified to accommodate 3 outputs. Hence the RNN model in Figure 3-1 is modifies for complete state estimation as depicted in Figure 4-1. The network consists of *n* input neurons and 3 output neurons. Each output neuron represents a state of the chaotic system under consideration. The complete weight vector is $W=[w^m, w^\upsilon, w_p^s]^T$ where *m* is the number of input neurons of NARX model, υ is the number of neurons with noise input & *s* is the number of feedbacks.

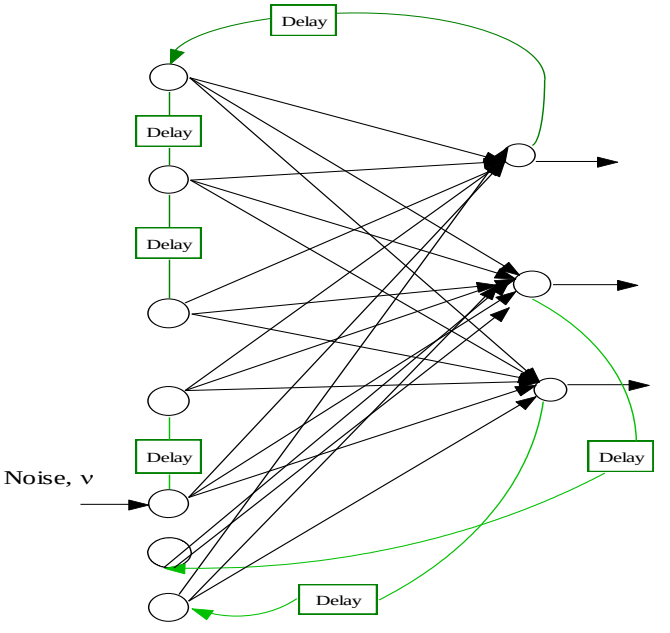

Figure 4-1 RNN model for state estimation

Following the approach developed in modeling of time series, the parameter vector $W=[w^m, w^\upsilon, w_p^s]^T$ corresponding to the weights of the neural network is represented as a state and is augmented with $X=[x_1, x_2 \ldots x_p]$ where p is the number of states. Because of the dynamic characteristic of the model the state transition is expressed as,

$$W_{k+1} = h(W_k) \tag{4.1}$$

$$X_{k+1} = f(W^T X) \tag{4.2}$$

Accordingly, the Jacobean of the state transition function to be used in the EKF algorithm is given by

$$F_k = \begin{bmatrix} I\ 0\cdots\ 0 \\ 0\ \cdots\ \ 0 \\ \vdots \\ 0\ \cdots \dfrac{\partial f(.)}{\partial \hat{X}_k} \end{bmatrix} \tag{4.3}$$

and the Jacobean of the measurement function is given by

$$H_k = \left[\frac{\partial h(.)}{\partial w^m}, \frac{\partial h(.)}{\partial w^\upsilon} \right] \tag{4.4}$$

The corresponding EKF algorithm for state estimation is given below:

EKF Algorithm for state estimation

1. *All the weights and states are initialized to small random values.*
2. *The covariance matrix P(0/-1) is initialized to a diagonal matrix with relatively small values.*
3. *EM algorithm is used to calculate the proper values of W(0), X(0) and P(0/-1) using 3.14 to 3.17.*
4. *Let w_p^s be the weights corresponding to the p states, w^υ be the weights of the feedback layer corresponding to the input time series. NARX model estimates the states $x_1(k)$ from the time series $x_1(k-n)$; n= 1, 2,... q for NARX input and n= 1, 2,... r for noise inputs*

$$x_1(k) = h\left(\sum_{n=1}^{q} w_n^m x_1(k-n) + \sum_{n=1}^{r} w_n^{\upsilon} \upsilon(n) \right) \tag{4.5}$$

5. *Then estimate of state* $\hat{X}(k)$ *at any instant will be*

$$\begin{aligned}
\hat{x}_1(k) &= f(w^s{}_{11}\, x_1(k) + w_{12}^s x_2(k) + w_{13}^s x_3(k)) \\
\hat{x}_2(k) &= f(w^s{}_{21}\, x_1(k) + w_{22}^s x_2(k) + w_{23}^s x_3(k)) \\
&\vdots \\
\hat{x}_p(k) &= f(w^s{}_{p1}\, x_1(k) + w_{p2}^s x_2(k) + w_{p3}^s x_3(k))
\end{aligned} \tag{4.6}$$

Algorithm 4.1

As in the case of modeling time series, the approach here is to estimate the parameters of the RNN model corresponding to w^s, w^m and w^{υ} from the output time series. The state transition function estimated in terms of w^s correctly generates the state space, as the modeling error comes down to acceptable limits. The following sections validate the performance of the technique by implementing the chaotic systems described in Section 3.4 using the Algorithm 4.1 by computing the invariant properties.

4.2 Phase plots and strange attractors

Phase plot of a dynamic system represents the relation between state variables where time is implicit and each axis represents one of the states. The trajectory traversed by a state is called a phase trajectory. The phase plot of a system depends on system parameters and initial conditions. The geometrical shape of phase plots give valuable information about nature of the system. The attractor of a system is an invariant set and a signature of chaotic behaviour. All the four chaotic systems discussed in Chapter 3 are

found to have attractors in their phase plots. Change in dynamics of the systems is described from the state space analysis.

In order to validate the state space model developed in Section 4.1, one of the states of standard systems described mathematically is used as the time series input. The RNN model is trained using the EKF algorithm, along with EM, until the modeling error between the state 1 of RNN and the corresponding state of the given chaotic system falls below an acceptable value ($< 10^{-7}$). Training is carried out with 22,000 samples, so as to ensure the correct reproduction of strange attractors. Subsequently, RNN model is driven by noise over 30,000 samples. Evolution of all the state variables in time in gives the phase plot and are plotted. The phase plot from RNN model is given in green, while the plot from the system of equations describing given chaotic system is plotted in black. Sections to follow illustrate the correctness of the state space evolution RNN model developed as applied to Lorenz, Rossler, Chen & Chua systems.

4.2.1 Phase plots of Lorenz system

According to chaotic system theory, existence of strange attractors in the phase plots is a sufficient condition for chaotic property. The Lorenz system of equatiuons are already proved to have strange attractors in their phase plots. Lorenz system represented by the set of dynamic equations (1.10) to (1.12) is simulated with parameter values $\sigma = 10$, $\gamma = 26.5$, $\beta = \frac{8}{3}$ and initial conditions x_0=0, y_0=0.1, z_0=0. The state x of the Lorenz system is used for modeling. The samples from output time series *'x'* is applied to the RNN model along with noise and recurrent inputs. The model, trained with EKF algorithm generates all the three states: *'x', 'y'* & *'z'*..These states are plotted along with the actual system states as follows.

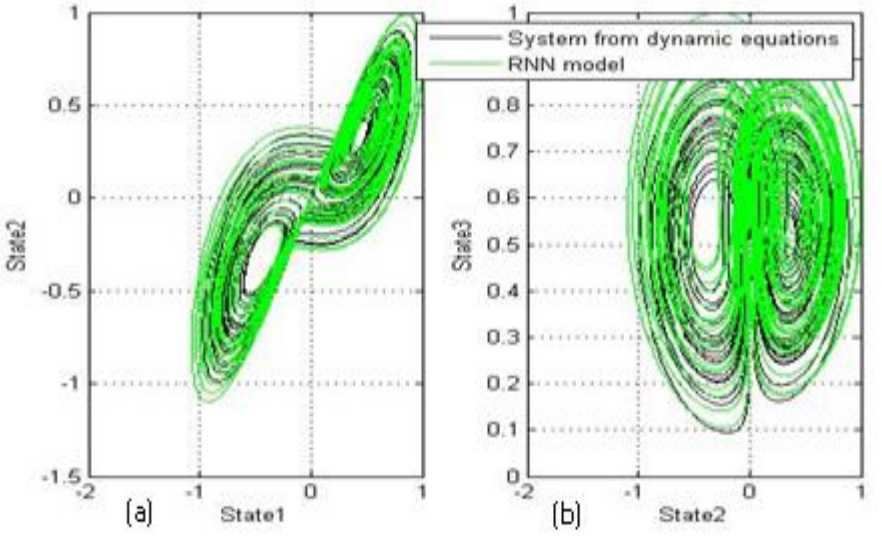

Figure 4-2 Phase plots of Lorenz system: (a) States1 &2 (b) States 2 &3

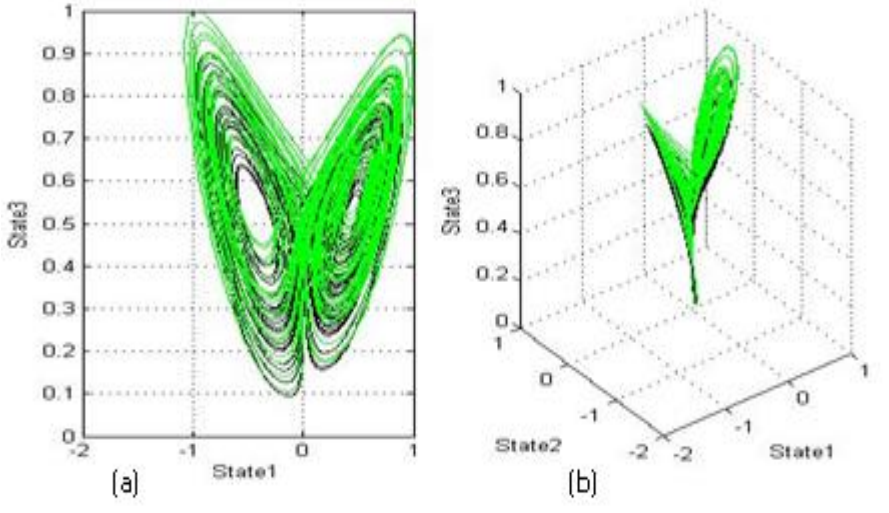

Figure 4-3 Phase plots of Lorenz system: (a) States1 &3 (b) States1, 2 &3

Figures 4-2 and 4-3 show the phase plots of Lorenz system in 2-D with states taken pairwise and 3-D with all the three states together. The state space evolves perfectly as a strange atrractor which brings out chaotic

nature. Further, the superimposed plots of the state space evolution from the mathematical model and the RNN model shows perfect agreement of the state trajectory, thereby confirming the correctness of the RNN model developed.

4.2.2 Phase plots of Rossler system

The Rossler system described by the non-linear dynamic equations (3.15) to (3.17) are simulated in MATLAB, with a= 2, b=0.2, c=5.7and initial conditions x_0= 0, y_0= 0, z_0=0.1 for which the system will be chaotic. The state *x* of the Rossler system is used for modeling. The samples from output time series *'x'* is applied to the RNN model along with noise and recurrent inputs. The model, trained with EKF algorithm generates all the three states: *'x', 'y'* & *'z'*. These states are plotted along with the actual system states as follows.

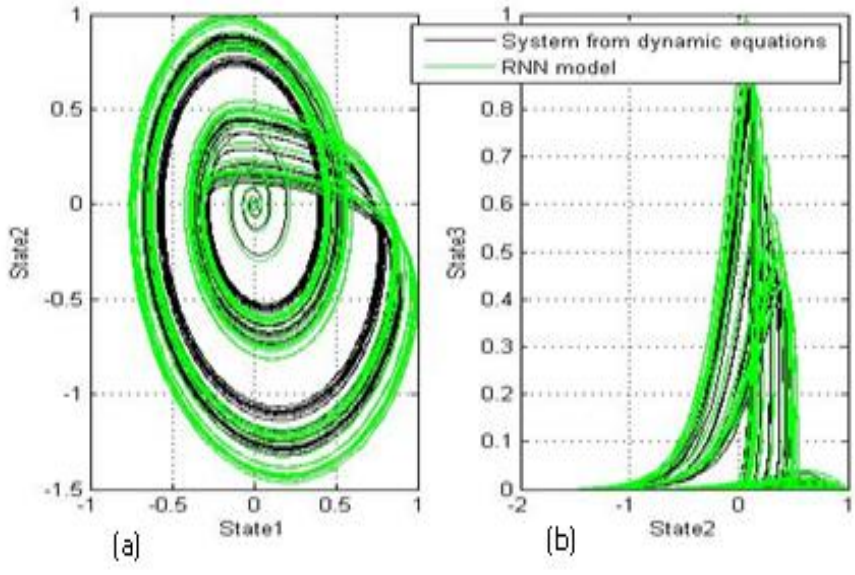

Figure 4-4 Phase plots of Rossler system: (a) States1 &2 (b) States 2 &3

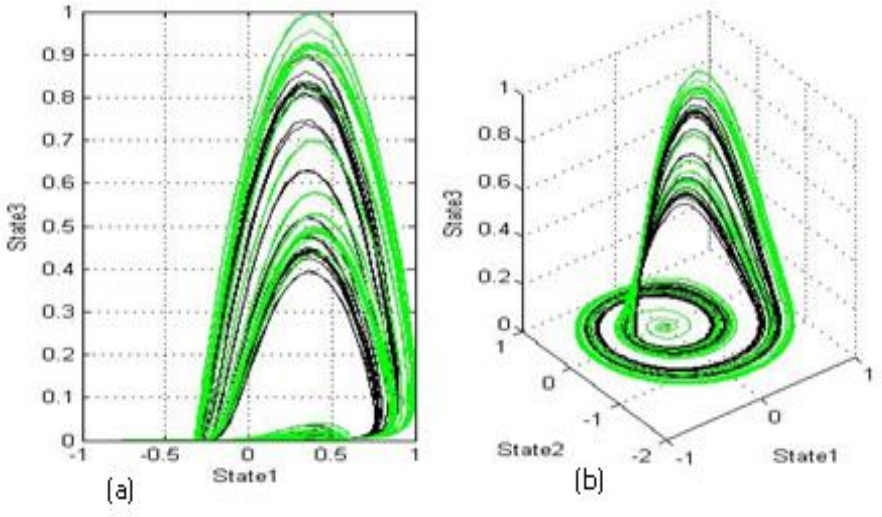

Figure 4-5 Phase plots of Rossler system: (a) States1 &3 (b) States1, 2 &3

The phase plots of RNN model and system generated from dynamic equations are shown respectively in Figures 4-4 and 4-5. The state space progresses as a strange atrractor and the superimposed plots of the state space evolution from the mathematical model and the RNN model shows perfect agreement of the state trajectory.

4.2.3 Phase plots of Chen system

Chen system, described by the three non-linear dynamic equations (3.18) to (3.20), is simulated with the parameter values a=35, b=3, c=25 for which the system exhibits chaotic behaviour. The state *x* of the Chen system is used for modeling as in the case of Lorenz and Rossler. The model, trained with EKF algorithm, generates all the three states: *'x', 'y'* & *'z'*. These states are plotted along with the actual system states as follows.

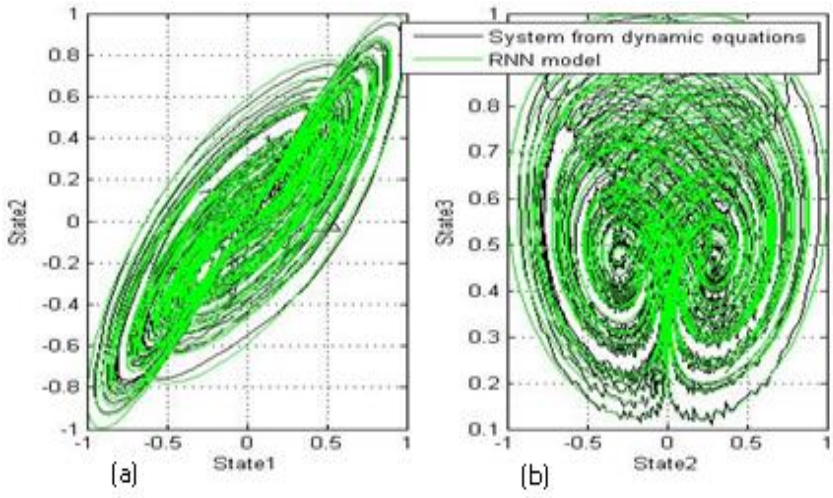

Figure 4-6 Phase plots of Chen system: (a) States1 &3 (b) States1, 2 &3

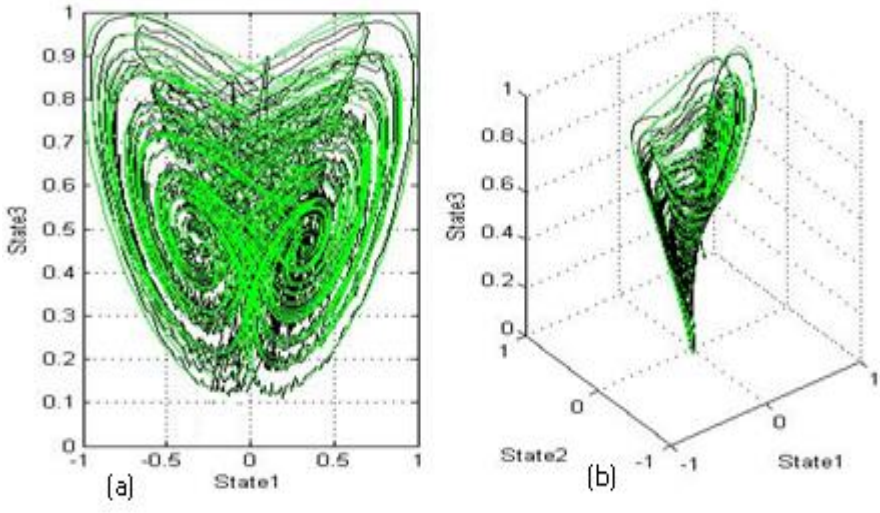

Figure 4-7 Phase plots of Chen system: (a) States1 &3 (b) States1, 2 &3

Figures 4-6 and 4-7 show the phase plots of Chen system. The perfect agreement of the superimposed plots of the state space evolution from the mathematical model and the RNN model is convincingly evident.

4.2.4 Phase plots of Chua system

The Chua system is simulated and the strange attractors are plotted using the dynamic equations and parameters described in Section 3.4.4

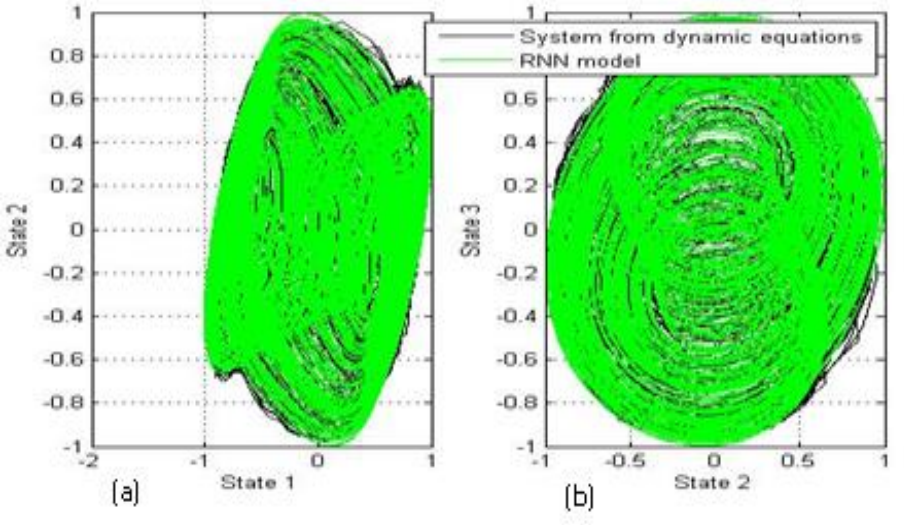

Figure 4-8 Phase plots of Chua system: (a) States 1 & 2 (b) States 2 & 3

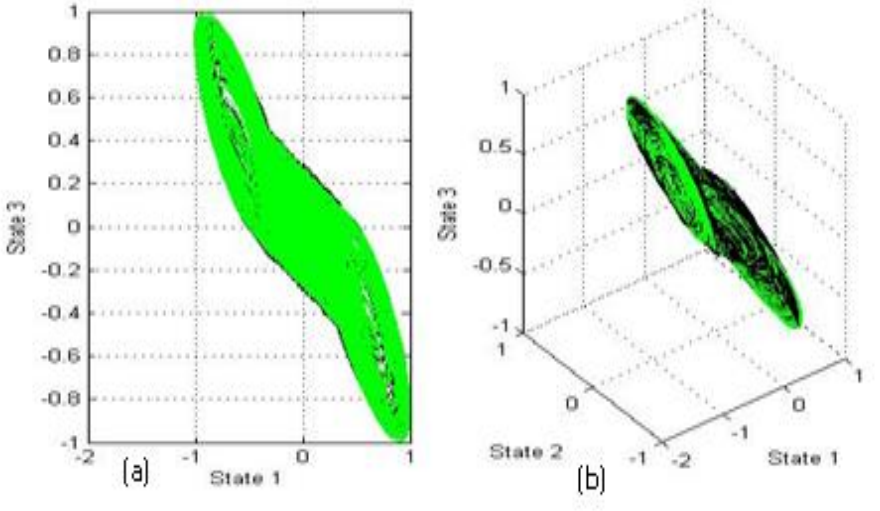

Figure 4-9 Phase plots of Chua system: (a) States 1 & 3 (b) States 1, 2 & 3

Figures 4-8 and 4-9 show the phase plots of Chua system. Obviously enough, the state space evolution from the mathematical model and the RNN model are in perfect covenant.

4.3 Lyapunov Exponents

The most important quantity of chaotic systems, the Lyapunov Exponents (LE) is a set of invariant geometric measures that describe the dynamic content of the system. Lyapunov Exponents quantify the average rate of convergence or divergence of nearby trajectories in a global sense. A positive exponent implies divergence of trajectories and a negative one implies convergence. The more positive the exponent, the faster the trajectories move apart. Similarly, for negative exponents, the trajectories move together. The presence of both positive and negative exponents is an indication of exponential separation of trajectories and is a signature of chaos [12]. The number of exponents is equal to the number of states of the system. A system with m states has m Lyapunov exponents $\lambda_1, \lambda_2, \ldots, \lambda_m$ in descending order. Hence, it can be seen that the Lyapunov Exponents describe the average rate of exponential growth in distance between orthonormal trajectories within the embedding space sense.

Mathematically Lyapunov Exponent can be defined by

$$\lambda_i = \lim_{n\to\infty} \frac{1}{n} \sum_{k=0}^{n-1} \ln \left[\frac{\partial f\left(x_i(k)\right)}{\partial x_i(k)} \right], \; i = 1, 2, \ldots n \tag{4.7}$$

where x_i, is the i^{th} state variable of the system and $f(x_i)$ is the output of the system corresponding to the state x_i. n=3 for Lorenz, Rossler, Chua & Chen systems.

The Lyapunov exponents of the four chaotic systems under consideration are calculated using Equation (4.7), from the state space evolution generated

using the dynamic equations of respective systems. Further, the Lyapunov exponents of the state space evolutions of RNN model, estimated in Section 4.1, are also calculated and compared with the actual values. It is seen from Table 4.1 that the numerical values of the Lyapunov exponents of both the approaches compare very well.

Table 4.1 Lyapunov Exponents: comparison

No	Data	Standard LE	**LE of RNN model**
1	Lorenz	0.906, 0.000, -14.572	**0.902, 0.000, -14.038**
2	Rossler	0.0714, 0.000, -5.394	**0.077, 0.000, -5.809**
3	Chen	2.030, 0.000, -10.035	**2.079, 0.000, -10.819**
4	Chua	0.340, 0.000, -5.989	**0.350, 0.000, -5.890**

4.4 Kaplan - Yorke dimensions

J. Kaplan and J. A. Yorke [6] have conjectured that the dimension of a strange attractor can be approximated from the spectrum of Lyapunov exponents. Such a dimension has been called the Kaplan - Yorke (or Lyapunov) dimension, helpful in the analysis of typical strange attractors.

Let λ_i be the i^{th} Lyapunov exponent. The Kaplan - Yorke Dimension (KYD)

$$D_{KY}=D+ (\lambda_1+\lambda_2+...+\lambda_D)/\text{abs} (\lambda_{D+1}) \quad (4.8)$$

where D is the largest integer for which

$$\lambda_1 + \lambda_2 + ... + \lambda_D > 0$$

The Kaplan - Yorke dimensions of Lorenz, Rossler, Chen and Chua systems are calculated both from the dynamic equations and RNN model. The values so obtained are almost similar as seen from Table 4.2, demonstrates efficiency of the RNN model.

Table 4.2 Kaplan Yorke dimension: comparison

Sl No	Data	Standard KYD	**KYD of RNN model**
1	Lorenz	2.0622	**2.0640**
2	Rossler	2.0131	**2.0135**
3	Chen	2.2024	**2.02083**
4	Chua	2.0208	**2.0394**

4.5 Bifurcation analysis

A bifurcation diagram is a plot that shows the value of a change in parameter, on one axis and the solution to the system on the other axis. In other words, change in the qualitative character of a solution, as a variation in control parameter, is known as a bifurcation. A bifurcation causes the solution of a system to change from a stable fixed point to a chaotic attractor. In the case of chaotic systems, the parameters play an important role in the transition to chaos. If one of the parameter of a chaotic system is varied, the nature of the output varies accordingly. The transition of a given system from non-chaotic

to chaotic state occurs corresponding to the variation in system parameters. For example, σ, β and γ are the parameters of Lorenz system as in equations (1.10) to (1.12). If any one parameter is varied, keeping the others constant, it yields the bifurcation diagram of the system.

4.5.1 Evaluation of Lyapunov Exponents along with Bifurcation

The Lyapunov Exponents of all the chaotic system under analysis are calculated and tabulated in Section 4.3. The exponents are calculated for the whole state space evolution by taking the logarithm of the differences of the states and averaged. In this section it is shown that the average of the derivative of the model function calculated continuously for each point in the state space evolution indicates the Lyapunov exponent. The derivative is given by $f'(x_i(k))\, w_{ii}$, where $f'(\,)$ is the derivative of the non-linearity (tan sigmoid) considered. Figure 4-10 to 4-13 show the values of the Lyapunov exponents as a function of the parameters (changing in time) along with the state variable x_i for Lorenz, Rossler, Chen & Chua systems. The figure shows perfect match of the change in Lyapunov exponent and the onset of bifurcation. When one of the Lyapunov exponents becomes positive and the system shows second bifurcation, the transition from non-chaotic to chaotic state. In the following section, the Lyapunov Exponents are evaluated continuously along with change in parameter β, during the state space evolution, and the correspondence among the parameter and Lyapunov exponent is demonstrated.

4.5.2 Bifurcation analysis of Lorenz system

Figure 4-10 shows the bifurcation diagram and Lyapunov Exponent of Lorenz system. The parameter β is varied from 3 to 4 in 200 steps and corresponding values of state 1 are plotted. It is seen that for β = 3 the system

state starts its first bifurcation. When the value of β is 3.45 the system further bifurcates and for the value β=3.6 the complete transition to chaos take place. As the plot of the Lyapunov exponent is observed, it is clear that for the values of β between 3 to 3.45 the Lyapunov exponent is negative, which prove that the system is not chaotic at this time interval. Near to β=3.5 the Lyapunov exponent becomes positive and remains positive. The bifurcation diagram and Lyapunov exponents are justifying each other.

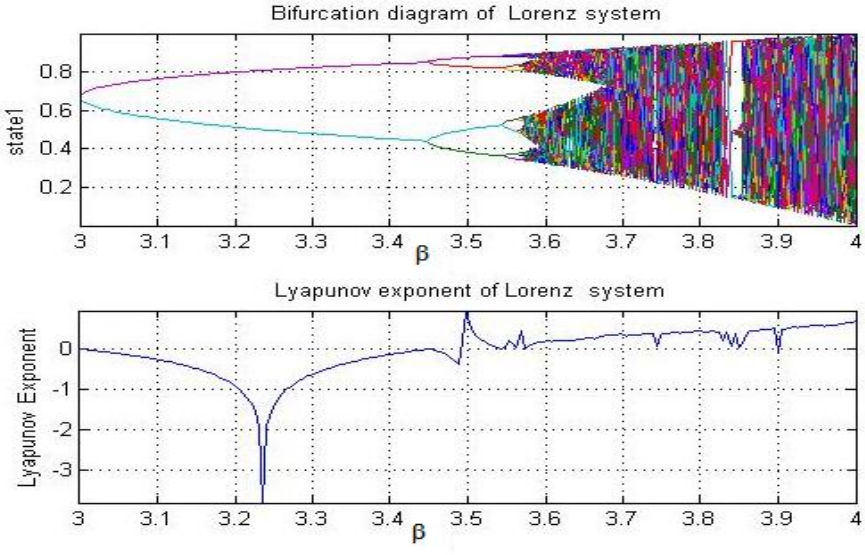

Figure 4-10 Bifurcation and Lyapunov exponents: Lorenz system

4.5.3 Bifurcation analysis of Rossler system

Figure 4-11 shows the bifurcation diagram and Lyapunov Exponent of Rossler system. The parameter c is varied from 3.5 to 8.55 in 200 steps and corresponding values of state 1 are plotted. It is seen that for c = 3.5 the system state shows its first bifurcation. When the value of c is 5.75, the system further bifurcates and for the value c=6.4 the complete transition to chaos take place. As the plot of the Lyapunov exponent is observed, it is clear that for the values of c between 3.5 to 5.75 the Lyapunov exponent is

negative, which prove that the system is not chaotic at this time interval. When the value of c is 5.75, the Lyapunov exponent becomes positive and remain positive till the final value of c. The bifurcation diagram and Lyapunov exponents are justifying each other.

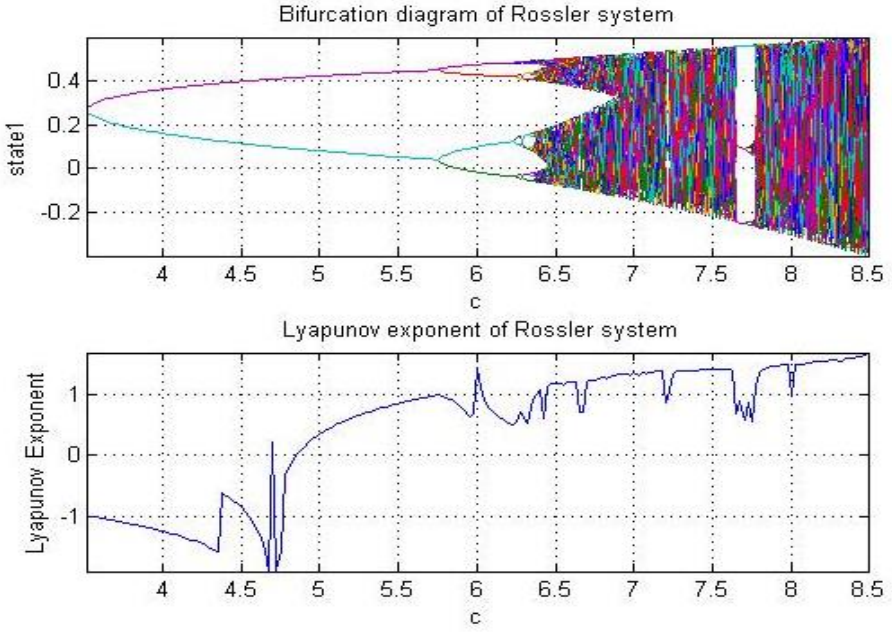

Figure 4-11 Bifurcation and Lyapunov exponents: Rossler system

4.5.4 Bifurcation analysis of Chen system

Figure 4-12 shows the bifurcation diagram and Lyapunov Exponent of Chen system. The parameter b is varied from 1 to 5 in 200 steps and corresponding values of state 1 are plotted. It is seen that for b = 1, the system state shows its first bifurcation. When the value of b is 2.8 the system further bifurcates and for the value b= 3.25 the complete transition to chaos take place. Since the Lyapunov exponent is negative for the values of b between1 to 2.8 system is not chaotic at this time interval. When the values of b is 3.25 the Lyapunov exponent becomes positive and remain positive till the final value

of b. The bifurcation diagram and Lyapunov exponents are justifying each other.

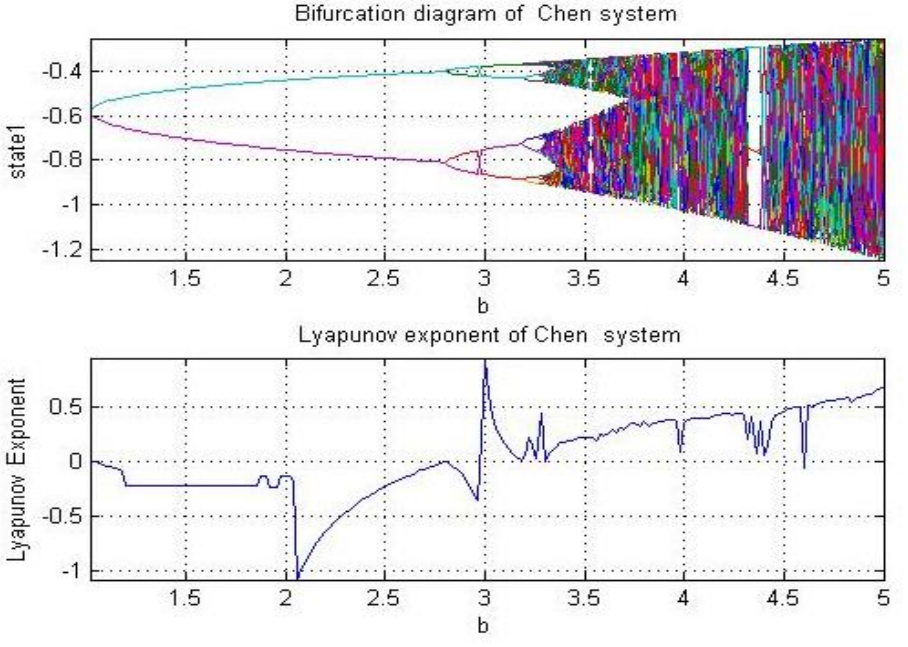

Figure 4-12 Bifurcation and Lyapunov exponents: Chen system

4.5.5 Bifurcation analysis of Chua system

Figure 4-13 shows the bifurcation diagram and Lyapunov Exponent of Chua system. The parameter β is varied from 10 to 20 in 200 steps and corresponding values of state 1 is plotted. It is seen that for β = 10 the system state starts its first bifurcation. When the value of β is 15 the system further bifurcates and for the value β=15.6 the complete transition to chaos take place. As the plot of the Lyapunov exponent is observed, it is clear that for the values of β between 3 to 3.45 the Lyapunov exponent is negative, which prove that the system is not chaotic at this time interval. Near to β = 15 the Lyapunov exponent becomes positive and remain positive till the final value of β. The bifurcation diagram and Lyapunov exponents are justifying each

other. It can be concluded that the online evaluation of Lyapunov exponents if an efficient method to characterize the transition to chaos.

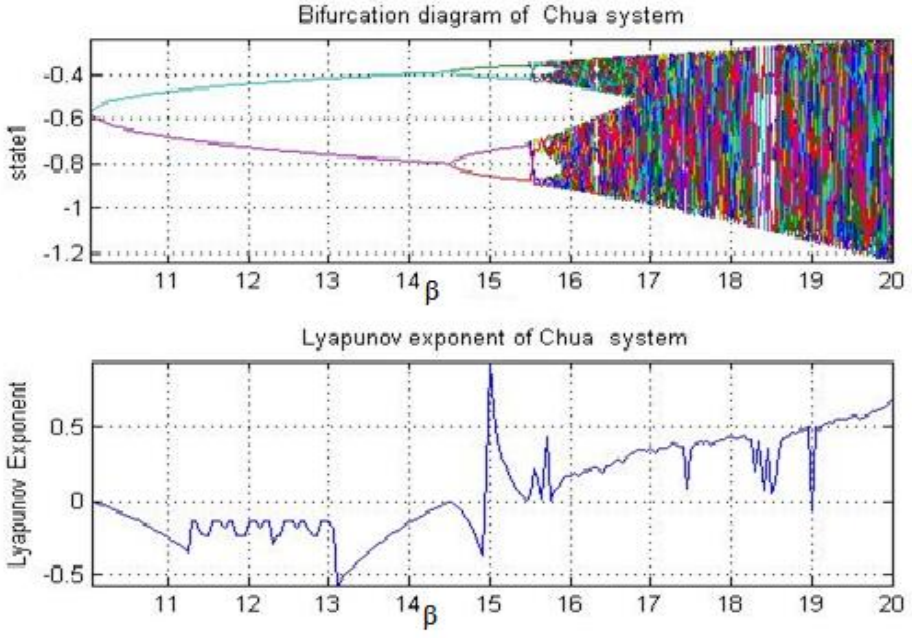

Figure 4-13 Bifurcation and Lyapunov exponents: Chua system

4.6 Minimum Embedding Dimension

One of the basic questions to be answered when modeling an unknown system is the number of states. The technique based on the minimum self-embedding dimension due to Takens [8] provides a fool proof method to calculate the number of states from the time series. There are three important dimensions for a dynamic system - geometric dimension or box counting dimension, attractor dimension or state space dimension and embedding dimension. The first two are invariant sets, calculated from the dynamic equations of the system. The embedding dimension is the smallest integer for which the system states can be embedded into, without intersecting itself

[40]. An efficient model of a dynamic system can be derived by selecting a proper embedding dimension capable of embedding all the properties of actual dynamic system. Reconstructed system may preserve only some of the properties, if the selected dimension is not optimum and does not preserve the geometric shape of structures in phase space.

Taken's theorem [8] [9] states that the original dynamic properties of the attractor can be retained as long as the embedding dimension $d_e \geq 2d+1$ where d is the correlation dimension of the attractor, equivalent to Kaplan Yorke dimension. It is already estimated for the systems under observation. It is sufficient to find the minimum embedding dimension so as to reconstruct the dynamic system with all the properties. The minimum embedding dimension can be obtained from the following algorithm based on The Method of False Nearest Neighbours [33]:

Algorithm for Minimum Embedding Dimension

1. Dimension of the attractor is assumed as *'d=1'* and the k^{th} state is assumed as '*x(k)'*.

2. Each state *x(k)* is sampled, in dimension 'd', into time lagged set - *{(s(k), s(k+T), s(k+2T), . . . , s(k+(d-1)T)}* - where T is a small time lag.

3. Each state *x(k)* has a Nearest Neighbour (NN), $x^{NN}(k)$ with nearness in the sense of distance function norm, $R_d^2(k) = [x(k) - x^{NN}(k)]^2$

4. $R_d^2(k)$ is calculated in terms of time lagged sets as.

$$R_d^2(k) = [s(k) - s^{NN}(k)]^2 + [s(k+T) - s^{NN}(k+T)]^2 + \ldots + [s(k+(d-1)T - s^{NN}(k+(d-1)T]^2 \quad (4.9)$$

5. Dimension is incremented as d= d+1. Correspondingly the new state is $x(k+dT)$ and its nearest neighbour is $x^{NN}(k+dT)$. Then the distance is changed due to the $(d+1)^{st}$ samples as $s(k+dT)$ and $s^{NN}(k+dT)$. The new distance is calculated as

$$R_{d+1}^2(k) = R_d^2(k) + [s(k+dT) - s^{NN}(k+dT)]^2 \tag{4.10}$$

Relative change in distance can be used to check whether the points are really close together or a projection from a higher state space.

6. The criteria for false nearest neighbours is chosen as the threshold given by

$$R_T < \frac{\left|[x(k+dT) - x^{NN}(k+dT)]\right|}{R_d(k)} \tag{4.11}$$

Algorithm 4.2

Using this criterion all the sequence of samples are tested. The sample, where percentage of false nearest neighbours goes to zero is calculated. A graph is plotted between the percentage of false nearest neighbours and embedding dimension. The lowest point in the graph gives the minimum embedding dimension [40]. The four chaotic systems under analysis are subjected to the method of false nearest neighbours and minimum embedding dimensions are calculated. Figure 4-14 shows the plot of embedding dimension and percentage of false nearest neighbours.

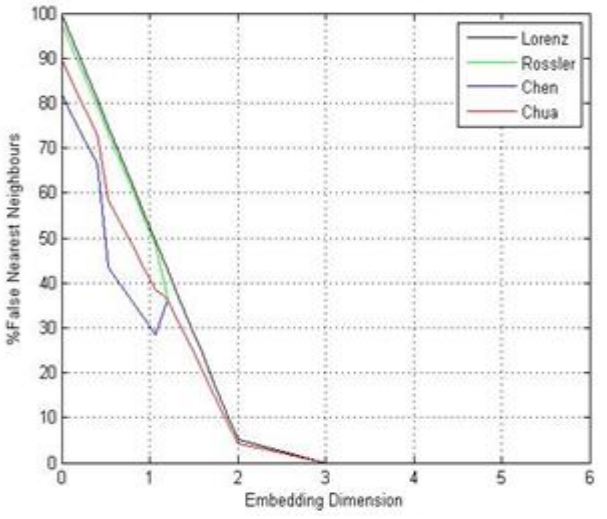

Figure 4-14 Estimation of embedding dimension

The figure shows that the minimum embedding dimension of the model for Lorenz, Rossler, Chen and Chua systems is 3. The percentage of false nearest neighbours vanishes when the value of embedding dimension approaches 3.

4.7 Conclusion

The method of identifying a chaotic system, by building a model from the time series of the system output, has been developed and demonstrated in the present Chapter. Important characteristics of the chaotic systems, phase plots, strange attractors, Lyapunov exponents, Kaplan Yorke dimensions and bifurcation diagrams of the RNN model output are calculated from the state space evolution from the model developed and compared with actual values calculated from the dynamic equations. It is observed that the selected model structure retains all the properties of the original chaotic system, thereby further validating the model structure. The bifurcation plots show the transition of the system from non-chaotic to chaotic behavior. This is further identified from the plot of the Lyapunov Exponents calculated online from analytic expression derived from the state transition function estimated by

the technique developed in the thesis. Since chaotic dynamical systems are broadband signals, the analysis in the frequency domain is complicated. Some important frequency domain characteristics of chaotic systems using Fourier transform (FT), wavelet transform (WT) and Mapped real transform (MRT) are presented in the next chapter.

Chapter 5

Frequency Analysis of Chaotic Systems

5. Frequency Domain Analysis of Chaotic Systems

Fourier analysis is the traditional method in frequency domain and is very powerful in revealing the periodicity of time series. However, a chaotic time series has broad-band power spectra for which the Fourier spectrum gives no indication about the deterministic origin. As a result, they have been mainly investigated using time-domain techniques. Various time domain characteristics of chaotic systems are presented in Chapter 4. The Fourier spectrum is not capable of representing the non-stationary nature of a chaotic signal. But the fundamental invariants of the underlying dynamical system can be analysed using Fourier representation. Time-frequency distributions are powerful set of tools specifically designed for non-stationary signal analysis. It is helpful in the study of time-frequency pattern present in non-linear dynamics. One of the competing approaches for time-frequency analysis is Wavelet Transform. Mapped Real Transform (MRT) is an alternate form of signal representation in the frequency domain, which makes use of real additions only. In this chapter chaotic systems are analyzed in the frequency domain using Fourier Transform (FT), Wavelet Transform and MRT.

5.1 Analysis using Fourier Transform

Fourier transform, explained in Appendix B, of chaotic systems is analyzed in order to study the spectrum and nature of coefficients. The Lorenz system behaviour changes from non-chaotic to chaotic according to changes in parameters. In the present analysis, the value of 'σ' in Equations (1.10) to (1.12) is chosen as 1 &10. The system generate non-chaotic time series for

σ = 1, whereas chaotic time series for σ = 10. Behaviour of the system in both cases under the Fourier domain is illustrated in Figures 5-1 to5-4.

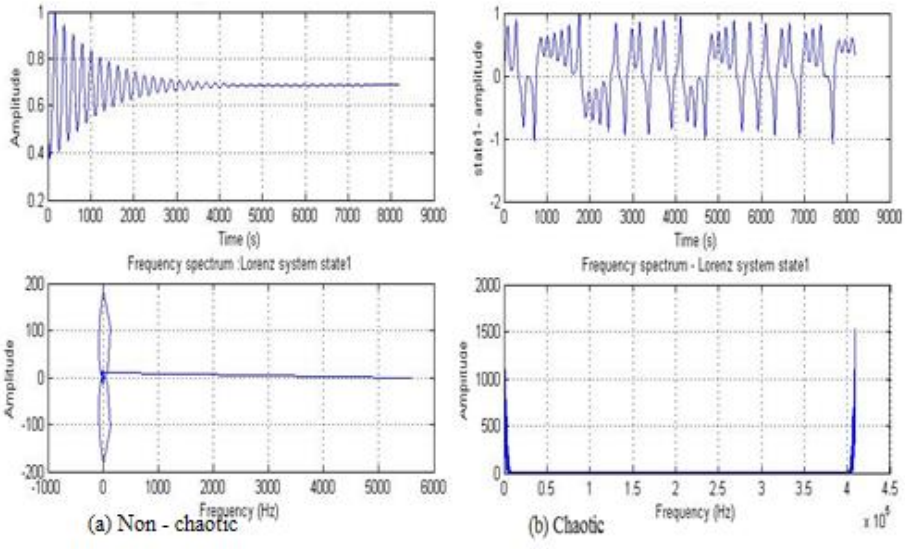

Figure 5-1 Time series and frequency spectrum of Lorenz system

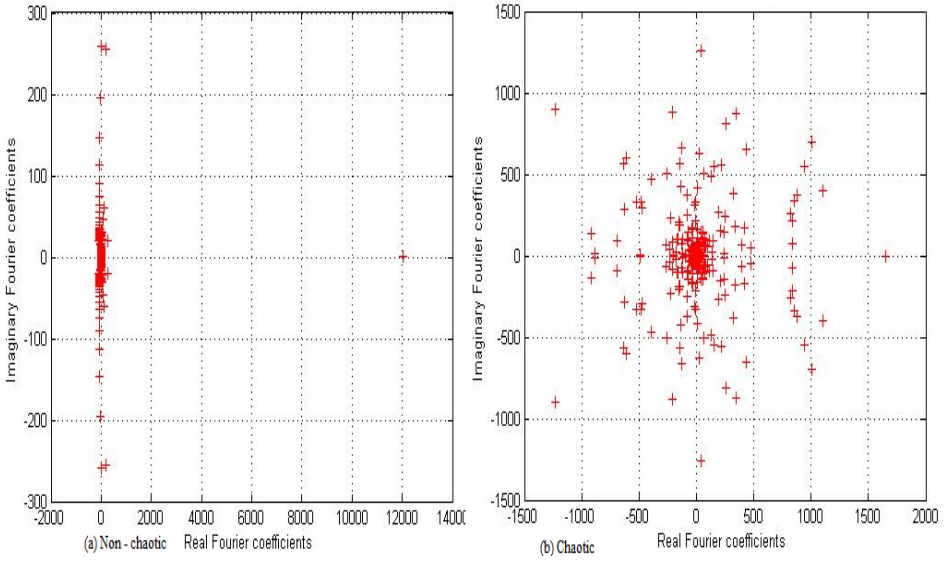

Figure 5-2 Scatter plot of Fourier coefficients

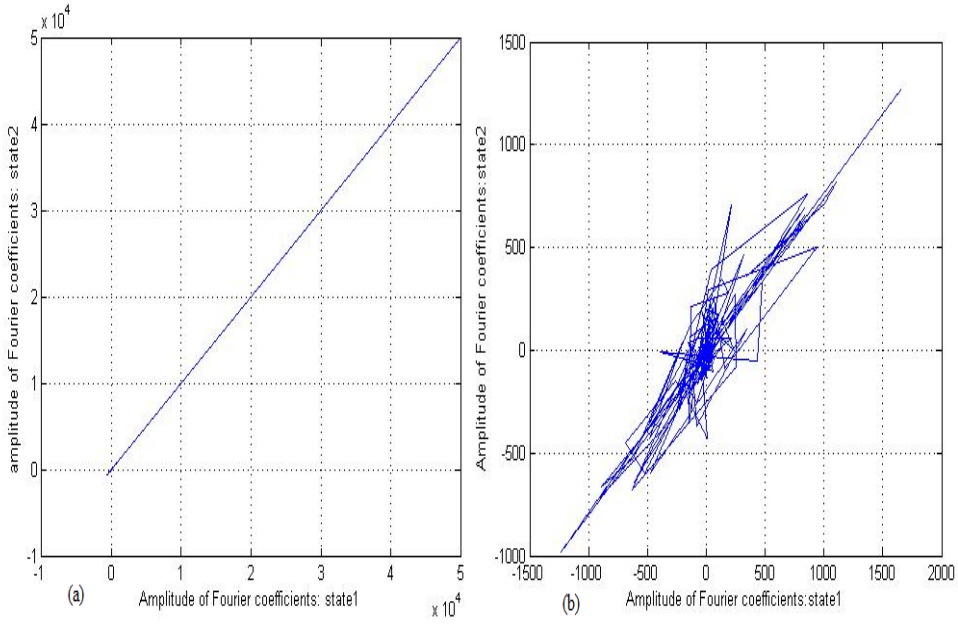

Figure 5-3 Phase plot of amplitude of Fourier coefficients States 1 &2 Lorenz system: (a) Non-chaotic & (b) chaotic

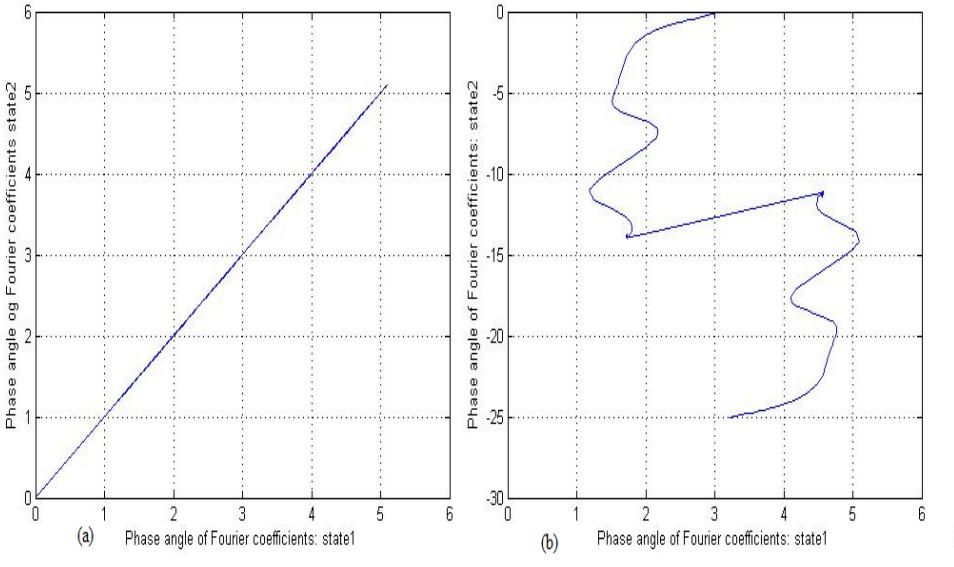

Figure 5-4 Phase plot of phase angle of Fourier coefficients States 1 &2 Lorenz system: (a) Non-chaotic & (b) chaotic

Figure 5-1 show the time series and corresponding frequency spectrum of Lorenz system for $\sigma = 1$ & 10 respectively in which 5.1 (a) is non-chaotic and narrow banded whereas 5.1 (b) is chaotic and broad banded. Figure 5-2 demonstrate the scatter plot of Fourier coefficients in which the real part of the Fourier transform is represented on the X axis and imaginary part on Y axis. The figures show that Fourier coefficients of the non-chaotic time series are spread more or less linearly, whereas that of chaotic state are in a scattered manner.

Figures 5-3 (a) and (b) show the the phase plot of amplitude of Fourier coefficients whereas Figures 5-4 (a) and (b) show the corresponding phase angles of state1 and state 2 on X and Y axes, in comparison with the phase plots illustrated in Figure 4-2. The above figures show that phase plot of the two states is linear for non-chaotic and non-linear for chaotic systems. Comparison of Figures 5-3 & 5-4 with Figure 4-2 shows that Fourier representation is not capable of explicitly representing the chaotic behaviour. The following section explores the feasibility of wavelet analysis of Lorenz system.

5.2 Analysis using wavelet transform

The Fourier technique decomposes a signal into harmonically related complex exponential signals. Another tool for analysing time series is the wavelet transform, detailed in Section B.2. It has been introduced and developed to study a large class of phenomena such as image processing, data compression, chaos, fractals, etc.

The basic features of the wavelet transform are localization in time (or space) and in frequency. There are different types of mother wavelets available in the literature like Haar, Daubechies, and Mayer etc. Daubechies wavelets are

used for analysis of chaotic time series following the work reported in [88]. In general, Daubechies wavelet can be chosen to have the highest number of vanishing moments and have the property of very low shift invariance.

Wavelet transform is applied for the analysis of chaotic and non-chaotic states of Lorenz time series. The work reported in [65] had optimized the number of levels for decomposition as 14 for chaotic system representation and hence the present work is implemented using Daubechies wavelet with 14 levels of decomposition. The energy of each level coefficients are calculated and the coefficients with highest energy are analysed. Chaotic time series are mainly characterized by the strange attractors evolved from the phase plots. Hence the analysis of detailed coefficients with highest energy level is done based on the phase plots. The following analysis reveals the characteristics of wavelet coefficients of chaotic time series.

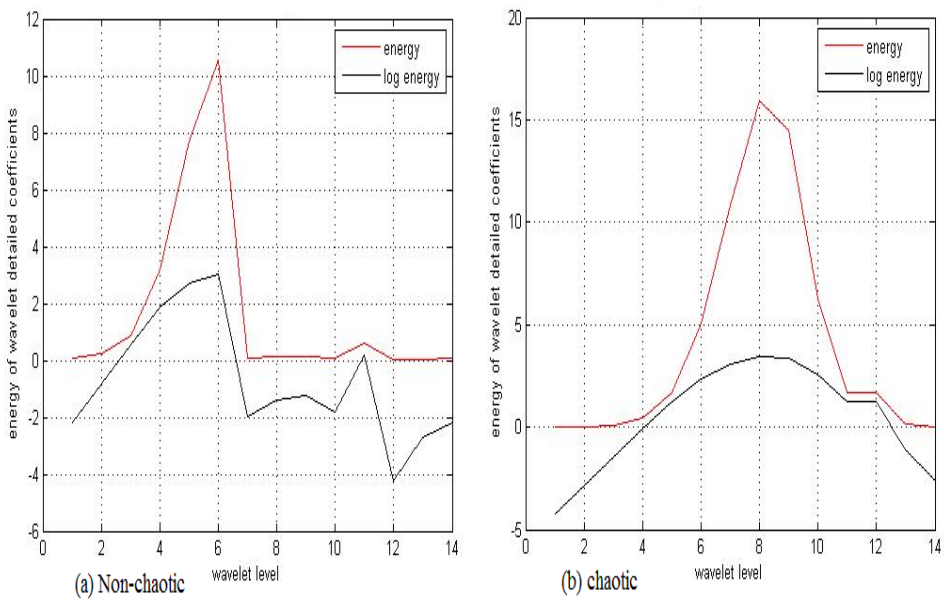

Figure 5-5 Energy content vs wavelet levels of Lorenz system

The variation in energy corresponding to each level for non- chaotic and chaotic states of Lorenz system is shown in Figure 5-5 (a) and (b). It is seen that when the Lorenz system is non-chaotic (ie. σ =1) the plot presents a peak energy at level 6 whereas for the chaotic time series (ie. σ=10), the peak energy is at level 8. Hence, level 6 detailed coefficients of non-chaotic and level 8 detailed coefficients of chaotic time series are used for analysis and plotted in Figure 5-6 (a) and (b).

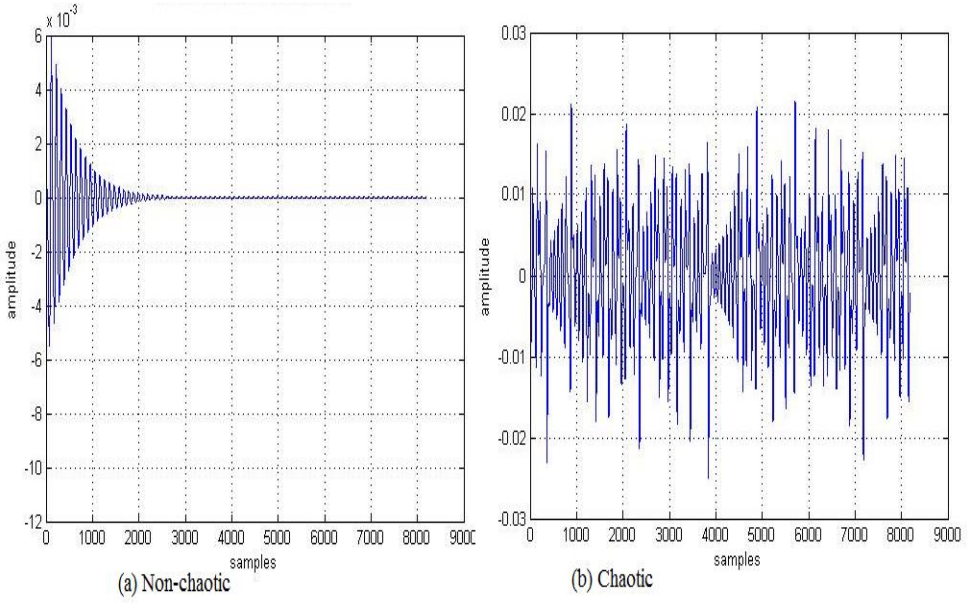

Figure 5-6 Level 6 and 8 wavelet detailed coefficients of Lorenz system

It is evident from the plot that the detailed coefficients of level 6 and level 8 resembles that of the original time series shown in Figure 5-1 and 5-2 to an extent. Even though the non-chaotic time series is reconstructed with a good level of accuracy, the chaotic time series is not well replicated by the wavelet coefficients. It is required to observe how the phase plots are reconstructed by wavelet coefficients. The wavelet coefficients corresponding to state 1 and state 2 are plotted on X & Y axes respectively for σ =1 and σ =10 in Figures 5-7 (a) & (b).

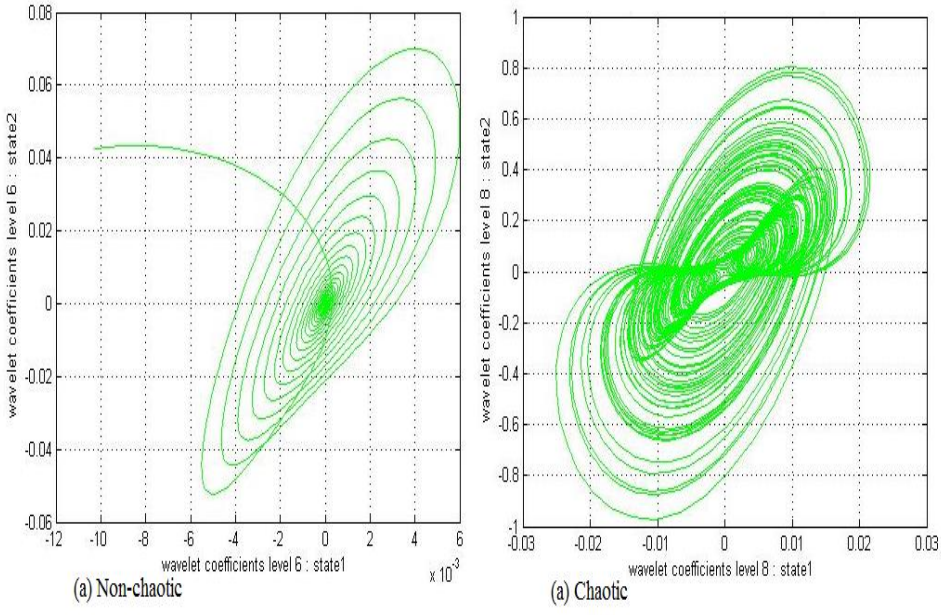

Figure 5-7 Wavelet coefficients' phase plots of Lorenz system

The phase plot for σ =1 in Figure 5-7 (a), follows the non- chaotic nature of the time series. Interestingly the phase plot for σ =10 shown in Figure 5-7 (b), unfolds the strange attractor like behaviour presented in Figure 4-2. However a close comparison of Figure 4-2 and Figure 5-7 (b) reveals the fact that the wavelet coefficients' phase plot does not exactly follow the actual strange attractor. Even though wavelet transform is comparatively more effective than the Fourier transform in representation of chaotic behaviour of systems, it is not able to completely reconstruct the strange attractors. Hence it is important to search for a better transform to completely represent the chaotic behaviour. MRT, being a newly developed transform to map signals from time domain to frequency domain in terms of real additions, is chosen as a new tool.

5.3 Analysis using MRT

MRT (Mapped Real Transform, originally M-dimensional Real Transform) is an evolving transform [5] [7] that can be used for the frequency domain analysis of signals. It is evolved by modifying DFT computations in terms of real additions, exploiting the symmetry and periodicity properties of the twiddle factor. Sequency based unique MRT (SMRT) [8] is a new representation of MRT applicable for both 1-D and 2-D signals.

In the present section 1-D SMRT is used for analysis non-chaotic and chaotic systems. Non-overlapping rectangular window of size 16 is applied over a data array of size 10240 samples from the system and the SMRT coefficients are obtained for each block. There are 16 SMRT coefficients corresponding to each block representing different computations as illustrated in Appendix B.3.5.1. An array is formed from a selected coefficient of the same type from each block. Thus there will be 640 coefficients in each array. A detailed analysis of all the 16 arrays of SMRT coefficients are performed for different chaotic systems.

5.3.1 SMRT analysis of Lorenz system

The energy content of all 16 SMRT arrays are plotted in Figure 5-8. The aim of this experiment was to observe which array of SMRT coefficients is having the highest level of energy content. It was deduced that the array with highest energy content will contain the most appropriate coefficients for chaotic time series analysis as observed in wavelet analysis. Interestingly it is observed that the energy content in all 16 arrays are identical and a notion

that all arrays of SMRT coefficients may have sufficient information to reconstruct the chaotic system was underlined from this investigation.

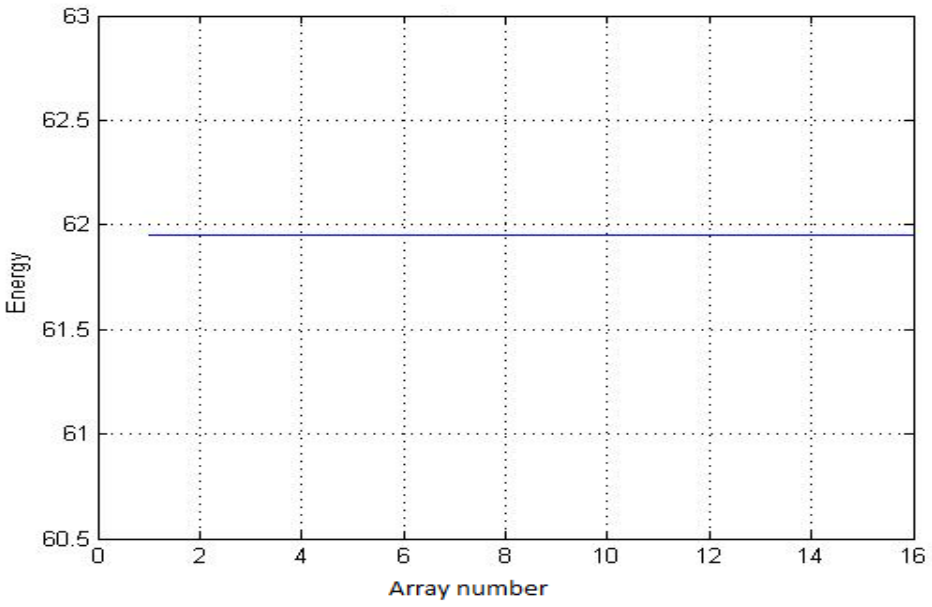

Figure 5-8Energy content vs array number of Lorenz system

Figure 5-8 above illustrate the fact that all arrays of SMRT coefficients are having the same energy content. This finding gives an impression to select any array for analysis of chaotic systems with SMRT coefficients. This property is explicitly different from that of wavelet coefficients in which the energy content of different level of decompositions were different and hence a particular level was found to be sufficient for representing non-chaotic and another one for representing chaotic system.

The selection of any array of SMRT coefficients may yield the same results. The validation of this can be done only by testing the capability of SMRT coefficients to reconstruct the time series and phase plots.

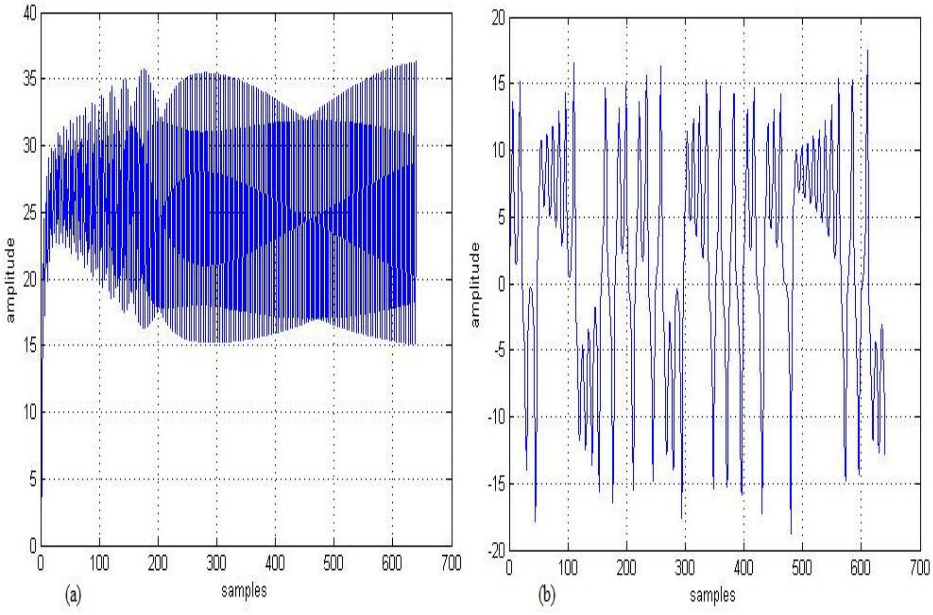

Figure 5-9 Array1 SMRT coefficients of Lorenz system (a) non-chaotic &(b) chaotic states

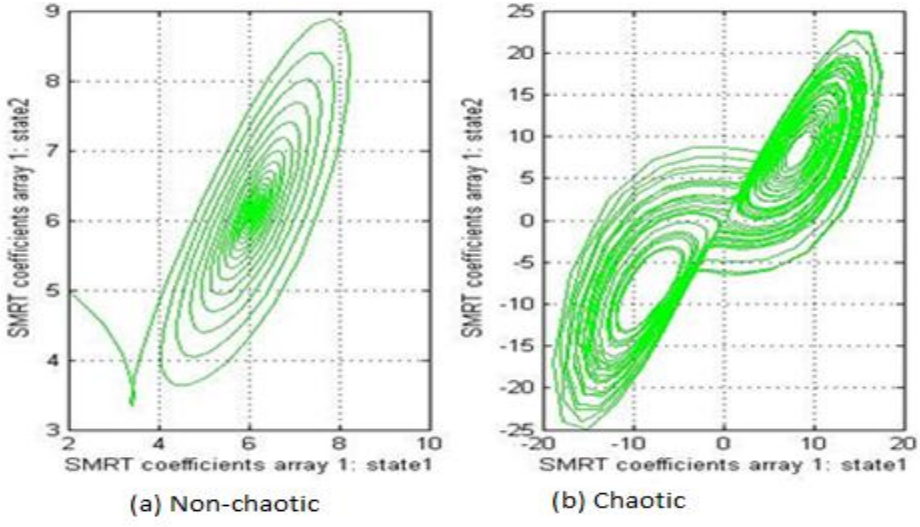

Figure 5-10Phase plot of array1 SMRT coefficients of Lorenz system

The array1 SMRT coefficients of non-chaotic Lorenz system does not match with the actual time series in Figure 5-1 whereas the array1 SMRT coefficients of the chaotic state exactly matches the actual time series as in Figure 5-2.

The phase plot of SMRT coefficients of the non-chaotic and chaotic states are surprisingly similar to the actual Lorenz system phase plots as in Figure 4.2.

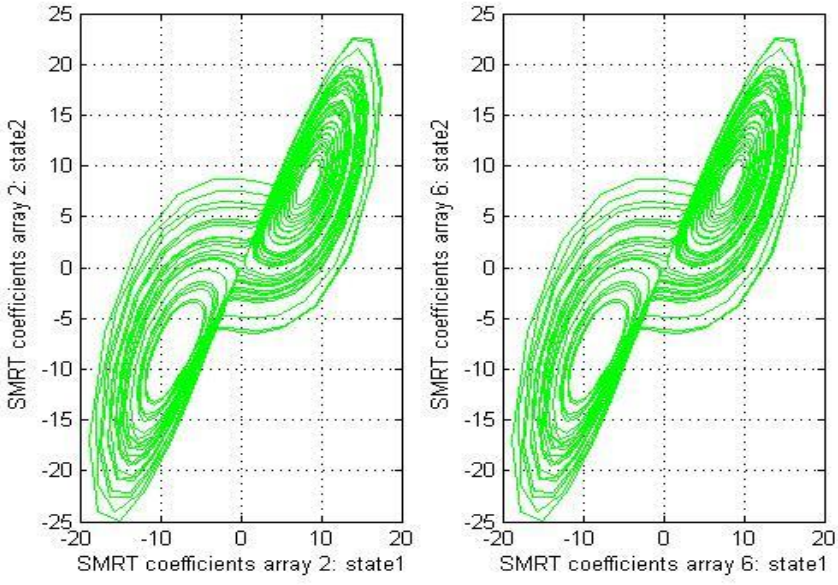

Figure 5-11 Phase plot of array 2&6 SMRT coefficients, chaotic Lorenz system

It is evident from the phase plots of Fourier, wavelet and SMRT coefficients that the SMRT coefficient retains the actual nature of the system under chaotic transformation. It is proved that all the 16 arrays are having the same energy level as shown in Figure 5-8. It will be interesting to analyze whether all arrays are able to unfold the strange attractor of the chaotic system under

consideration. Hence phase plots of array2, array 6, array13 and array16 are analyzed to verify the consistency in different categories of SMRT coefficients.

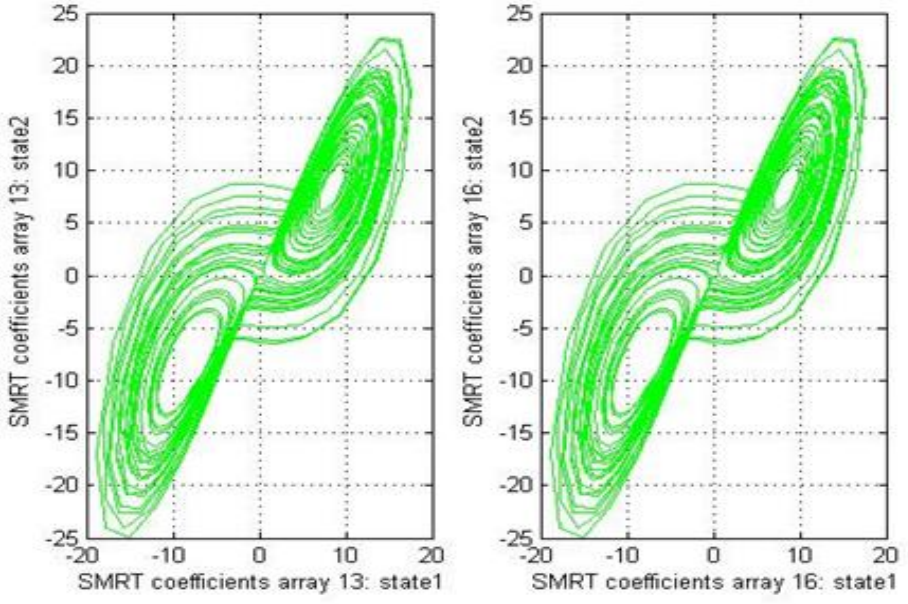

Figure 5-12 Phase plot of array 13 &14 SMRT coefficients, chaotic Lorenz system

Figures 5-11 and 5-12 clearly show that all arrays of SMRT coefficients retains the inherent properties of the chaotic system. Hence it is sufficient to compute one SMRT coefficient per window to extract the chaotic behaviour of systems. The validation of the intuition that SMRT coefficients, under transformation retains the property in all arrays is well established by these observations.

It is also worthy to note that SMRT representation is more informative when the system behaviour is chaotic. As the same system shows non-chaotic behaviour, the SMRT coefficients fails in exact reproduction of time series.

The placement of SMRT coefficients in a scattered plot is appreciable, in order to note the property of these coefficients. Hence the scattered plot of SMRT coefficients for chaotic and non-chaotic states of Lorenz system is simulated in MAtlab and observed as shown in the following figure.

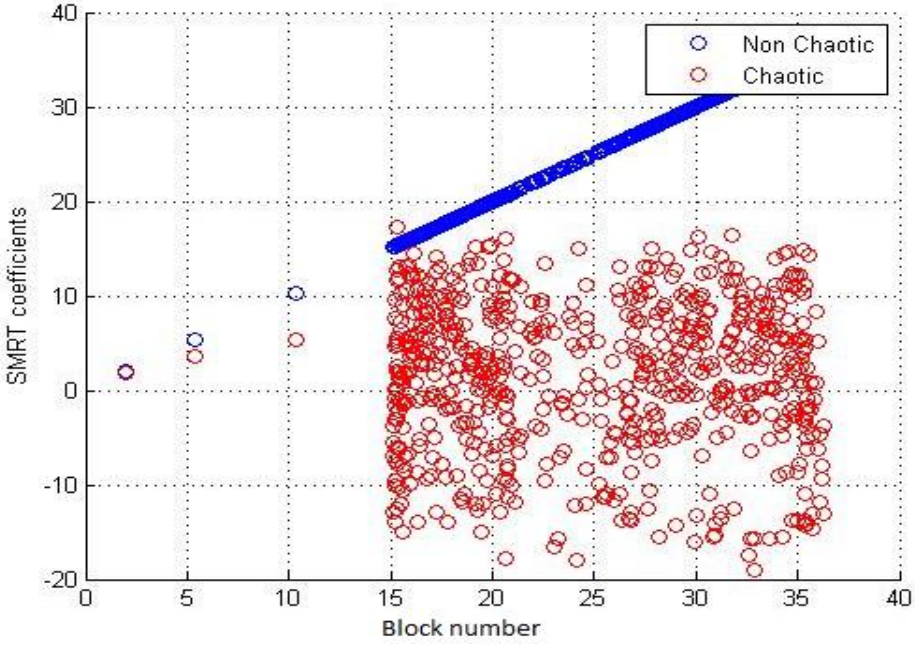

Figure 5-13 SMRT coefficients scatter plot: Lorenz non-chaotic &chaotic

Figure 5-13 shows the combined scatter plot of SMRT coefficients for both non- chaotic (plotted in blue) and chaotic (plotted in red) states. As in the original system, the coefficients corresponding to non- chaotic state are linear and that of chaotic state are scattered.

From these observations it is clear that the SMRT coefficients retains the original property of chaotic systems and are well suited for the analysis. The analysis of chaotic systems based on SMRT is extended to validate other chaotic systems such as Rossler, Chen and Chua.

The Rossler system is defined by the non-linear equations (3.15) to (3.17).The system is simulated in Matlab and the resulting time series is transformed to obtain the SMRT coefficients. As in the case of Lorenz system, there are 16arrays of SMRT coefficients each containing 640 samples.

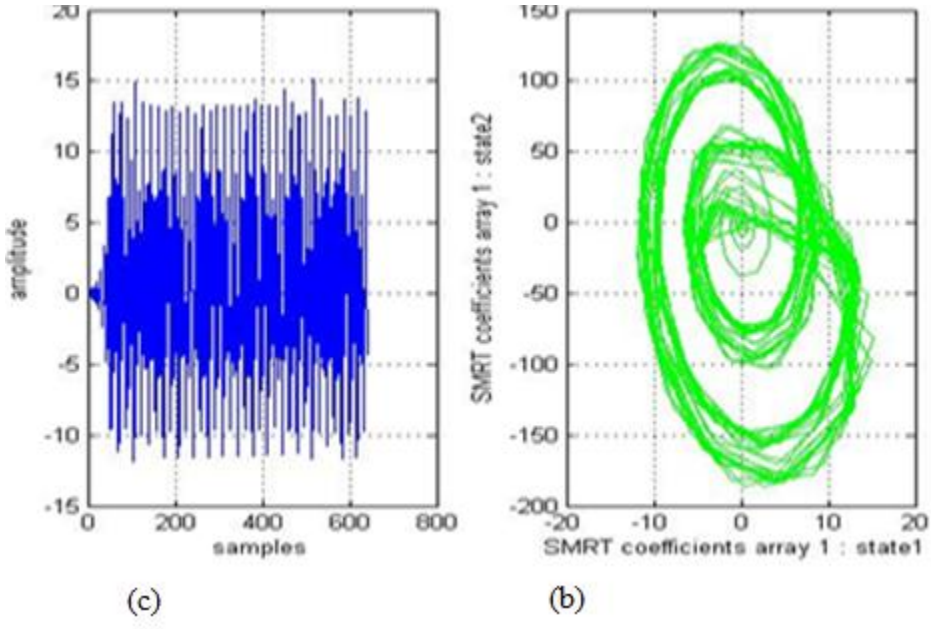

Figure 5-14 SMRT coefficients of chaotic Rossler system (a) array 1 samples& (b) phase plot

The array1 SMRT coefficients and the corresponding phase plots of Rossler system are plotted in Figures 5-14 (a) and (b) respectively. Comparing these with Figures 3-5 and 4-4 respectively it can be observed that the SMRT coefficients of Rossler system retain the original system properties.

Similarly Chen system &Chua system, defined by (3.18) to (3.20) & (3.21) to (3.23) respectively, are also subjected to SMRT transformation. The time series and phase plots of array 1 alone of the above systems under chaotic behaviour are considered for a crisp analysis.

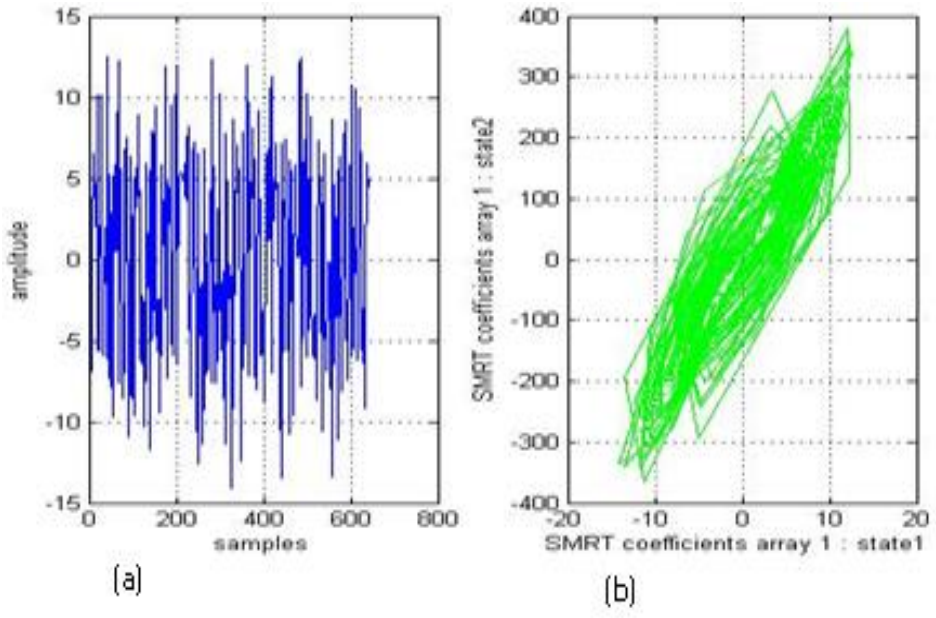

Figure 5-15 SMRT coefficients of chaotic Chen system (a) array 1 samples & (b) phase plot

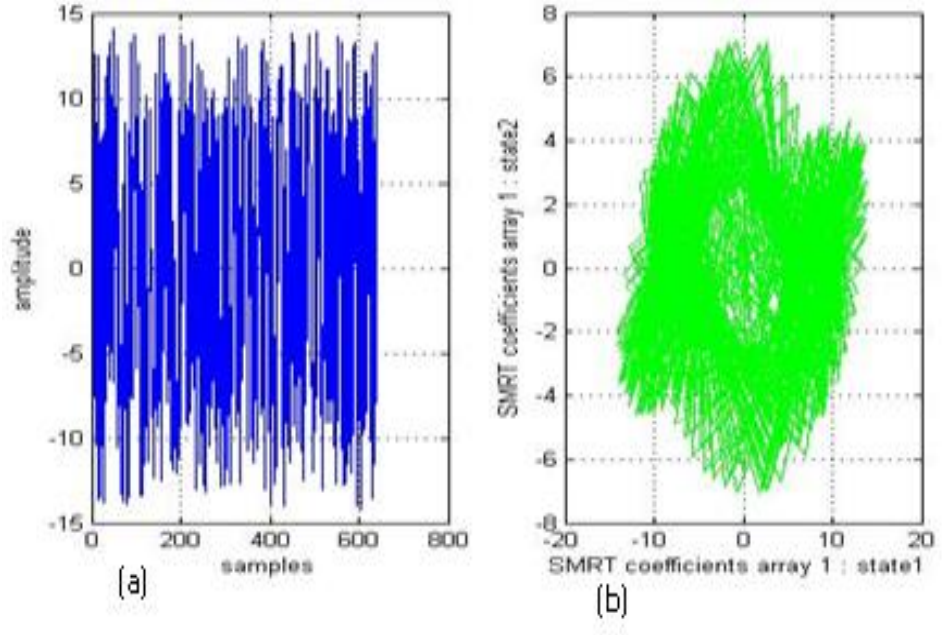

Figure 5-16 SMRT coefficients of chaotic Chua system (a) array 1 samples & (b) phase plot

Comparison of these with Figures 3-9 and 4-6 show the consistency of the SMRT technique.

Chua system is also analyzed in the SMRT domain and plotted in Figures 5-16 (a) & (b). Figures 3-15 and 4-8 are also in agreement with this as in other cases of chaotic systems. The power of SMRT coefficients in analyzing the chaotic behaviour of non-linear system is excellently demonstrated from all these investigations.

Thus all the 16 arrays of SMRT coefficients are capable to retain each and every properties of the original time series as observed from Figures 5-14 to 5-16. Hence, 640 SMRT coefficients are sufficient to extract important properties of a long time series of length 10240. If the length of the time series is still higher the array size can be increased, thereby further reducing the number of samples. These observations are important in the analysis of chaotic systems in the frequency domain. Comparing to Fourier and transforms, SMRT is proved to be the best tool for frequency domain analysis of chaotic systems.

5.4 Conclusion

Frequency domain analysis of chaotic systems is presented in this chapter. Three important transforms -Fourier, wavelet and SMRT- are used. The Lorenz system with non - chaotic and chaotic states are analyzed by varying one of the parameter σ. The frequency spectrum is band limited for non-chaotic and is broad banded for chaotic systems. The amplitude and phase of Fourier coefficients under non-chaotic state are linear while the same under chaotic state is non-linear. Attempt is made to construct the phase plot of Fourier coefficients of two states and has been futile as it did not reveal the original system properties.

The wavelet analysis proved to be more fruitful in many aspects. Initially the wavelet level with highest energy concentration is selected from energy plot. It is found that when the system is non-chaotic & chaotic, level 6 and level 8 respectively are suitable for analysis. Interestingly the coefficients seemed to be in line with the actual time series. Further, the phase plot of wavelet detailed coefficients is plotted and is found to be having some of the properties of the original phase plots.

The SMRT analysis is found to be the promising one in frequency domain. In the present analysis, there are 16 arrays of SMRT coefficients and each array is found to have the same energy level. Further, the plot of coefficients of each array is exactly similar to the actual time series. Then the phase plots of SMRT coefficients are investigated and found to be surprisingly coinciding with the actual phase plots. Also a scatter plot of non- chaotic and chaotic SMRT coefficients showed distinguishing features. Thus it is concluded that the SMRT analysis is the best method for analysis of time series in frequency domain. Modeling and analysis of some important weather systems like sunspot time series, Venice Lagoon time series and North Atlantic Oscillations are presented in the next chapter.

Chapter 6

Modeling and Analysis of Chaotic systems in Nature

6. Modeling and Analysis of Chaotic Systems in Nature

There are a number of weather systems which are chaotic in nature. Chaotic dynamical systems are present in the nature in various forms such as weather, oceanic oscillations, flows and turbulence. Modeling and analysis gives detailed understanding of a system in an effective way. In the present chapter three important weather systems - the Sunspot time series, the Venice lagoon time series and the North Atlantic Oscillations - are modeled and analyzed. A few important features are extracted and certain observations are made on the three weather systems which will contribute to further analysis of these systems.

6.1 Sunspot time series

Sunspot data are available since 1818 in the Greenwich series obtained from daily photographic images of the sun. Although, sunspots themselves produce only minor effects on solar emissions, the magnetic activity that accompanies the sunspots can produce dramatic changes in the ultraviolet and soft X-ray emission levels. These changes over the solar cycle have important consequences for the Earth's upper atmosphere. Sunspot number is calculated by first counting the number of sunspot groups and then the number of individual sunspots. The "sunspot number" is then given by sum of the number of individual sunspots and ten times the number of groups since most sunspot groups have about ten spots. This formula for counting sunspots gives reliable numbers even when the observing conditions are less than ideal and small spots are hard to see. The sequence of sunspot numbers [116] available as a time series, from year 1818 to 2013 has been utilized in

the present study. The model and the algorithms developed in Chapter 4 are utilized to characterize the sunspot time series.

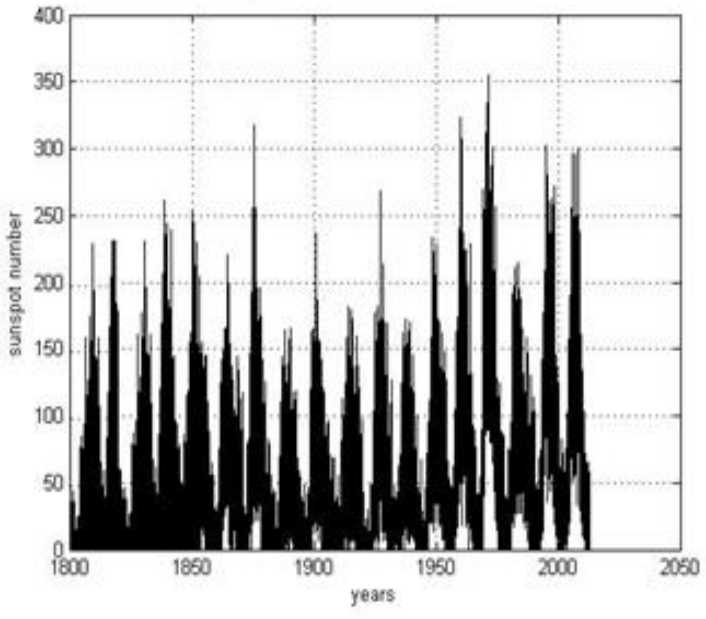

Figure 6-1 Sunspot time series 1818-2013

Figure 6-1 shows the sunspot time series. The steps followed in modeling and analysis of sunspot time series include:

1. Estimation of minimum embedding dimension
2. Computation of modeling error
3. Phase plots reconstruction
4. Computation of Lyapunov exponents
5. Computation and analysis of SMRT coeffcients

The behaviour of sunspot time series in the time and frequency domain are analysed following the above mentioned steps and explained.

6.1.1 Estimation of minimum embedding dimension of sunspot time series

Number of states of the sunspot time series is to be computed to facilitate proper modeling. Minimum embedding dimension is the parameter that reveals the number of states of unknown dynamical system.As explained in Section 4.6 the minimum embedding dimension of the sunspot timeseries is estimated using the method of false nearest neighbours.

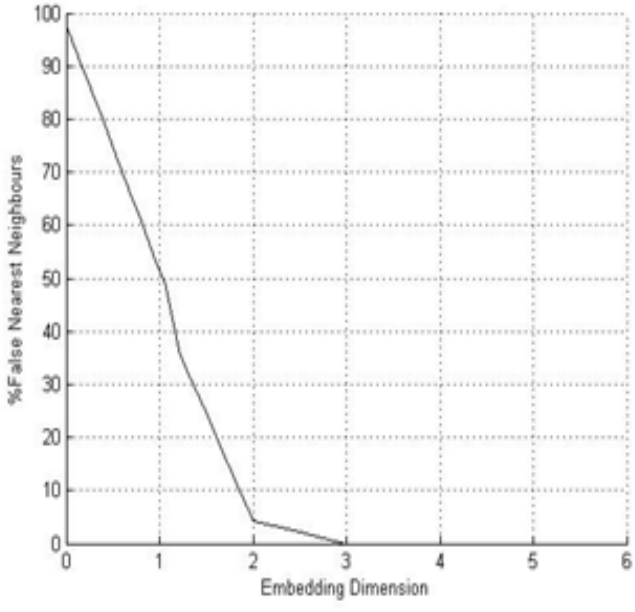

Figure 6-2 Minimum embedding dimension of sunspot time series

Figure 6-2 shows the estimation of embedding dimension of sunspot timeseries. It is evident from the plot of percentage false nearest neighbours and embedding dimension that the minimum embedding dimension is 3, which corresponds to three states.

6.1.2 Phase plots of Sunspot time series

The given timeseries is modeled using the RNN model structure with three states after estimating the minimum embedding dimension. The recurrent

Neural networks are trained with a single channel time series data of the sunspot. All the three sets of weights are updated using Algorithm 4.1. The training is continued until the modeling error comes to an appreciable level of 2.54×10^{-6} as shown in Figure.6-3.

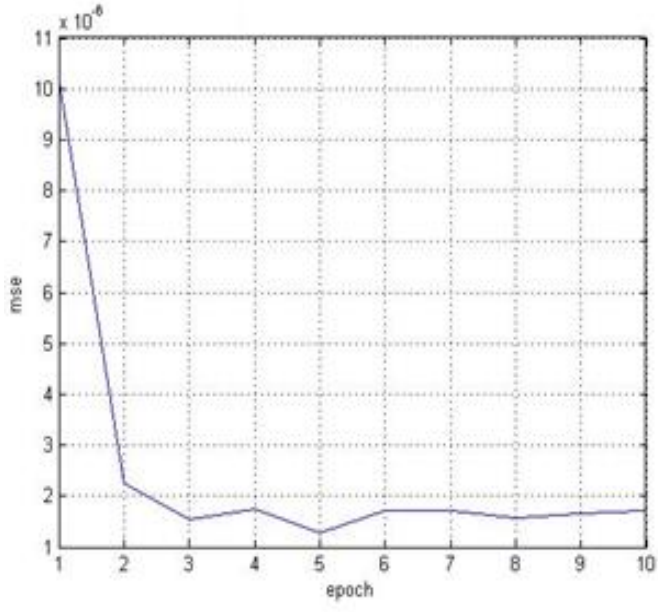

Figure 6-3 Modeling error-sunspot

The training of the sunspot time series with the selected RNN structure trained with the EKF algorithm is proved to satisfying the mean square error criterion and can be adopted for state space modeling of the same system. The sunspot time series is nonlinear, but in extreme situations the system may show chaotic behaviour. Also the phenomena causing sunspot originating in the sun can also be chaotic in nature. A verification of these facts can be derived from phase plots.

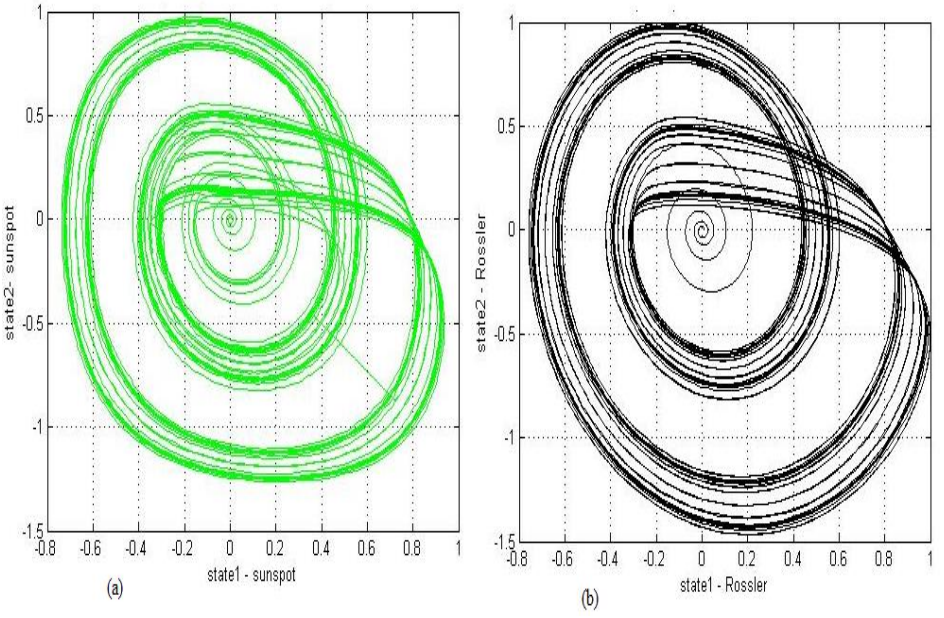

Figure 6-4 Phase plots, states 1 &2 (a) sunspot & (b) Rossler

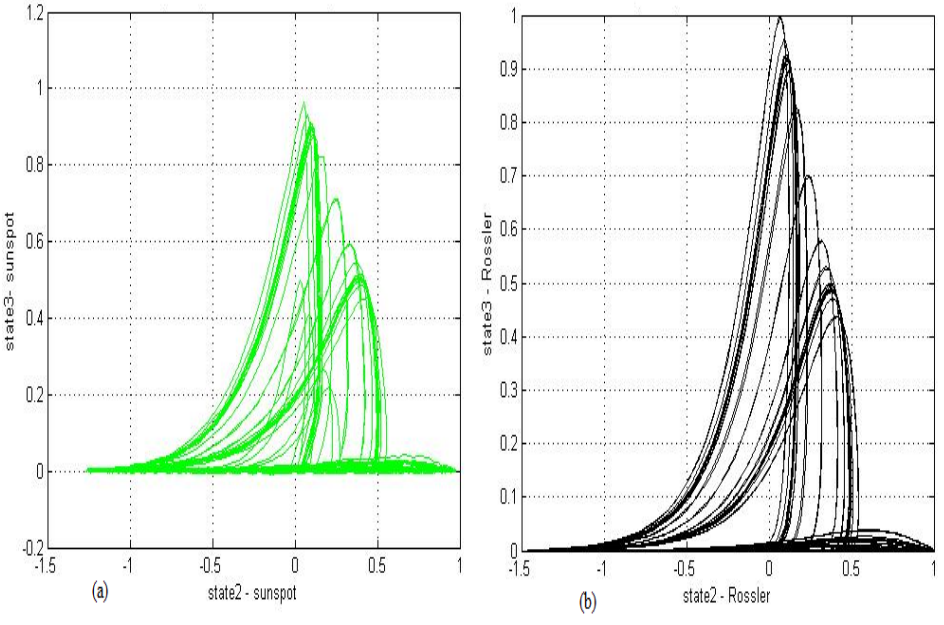

Figure 6-5 Phase plots, states 2 &3 (a) sunspot & (b) Rossler

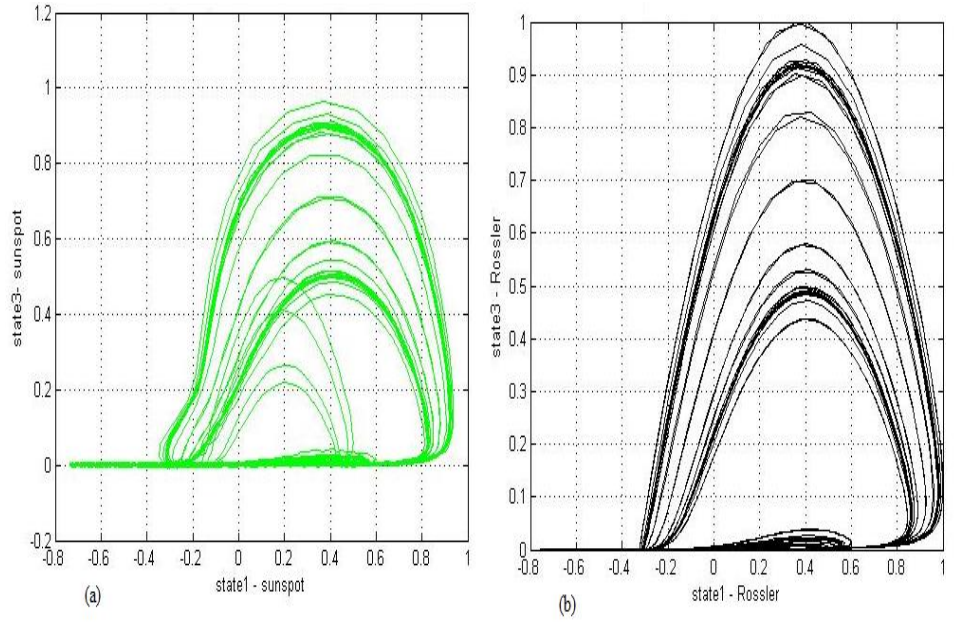

Figure 6-6 Phase plots, states 1 &3 (a) sunspot & (b) Rossler

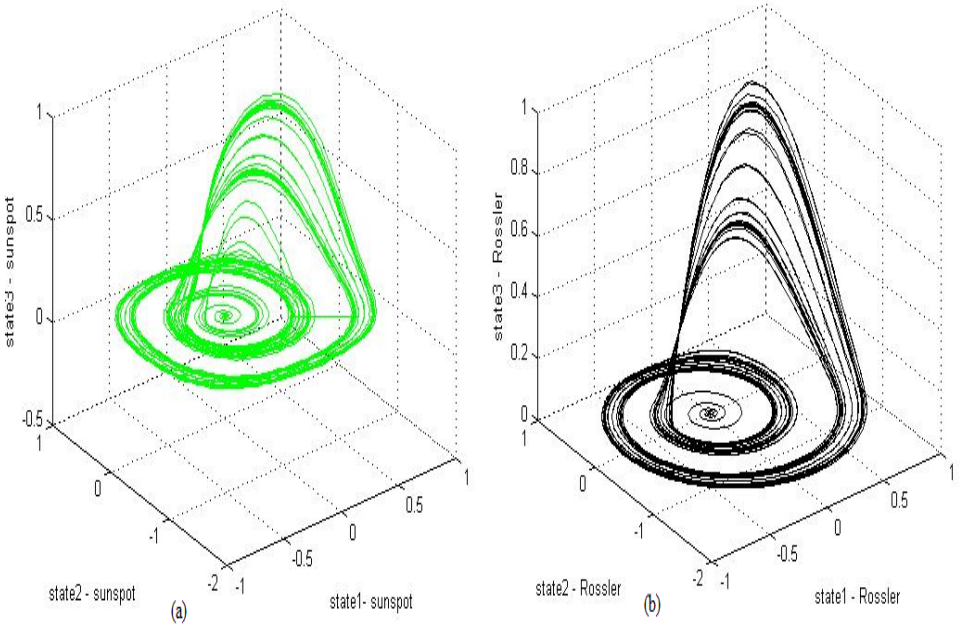

Figure 6-7 Phase plots, states 1, 2 &3 (a) sunspot & (b) Rossler

The state space evolved has demonstrated strange attractors which confirm the chaotic nature of the source of time series. Interestingly enough, the state space evolution shows that the system modelled from the sunspot time series using the method in Section 4.1 has a close semblance to the famous chaotic system developed by Otto Rossler, Section 4.1. In Figures 6-4 to 6-7, the phase plots of Rossler system and sunspot time series (in black) are plotted along with that of the (in green) to facilitate comparison.

6.1.3 Lyapunov exponents of sunspot time series

Lyapunov Exponents of the Sunspot time series are calculated using the method described in Section 4.3 and is given in Table 6.1. The phase plots of sunspot time series showed a close resemblance with that of Rossler system. Hence a comparison of Lyapunov Exponents of sunspot time series and Rossler system is essential.

Table 6.1 Lyapunov exponents of sunspot time series

Sunspot	-5.2446	0	0.0694
Rossler	-5.394	0	0.0714

One of the Lyapunov exponent is negative, one is zero and the other one is positive in the case of sunspot, verifying its chaotic behaviour. Table 6.1 shows that the Lyapunov exponents of the Rossler system and sunspot are closely matching, thereby establishing the correlation between them.

6.1.4 SMRT analysis of Sunspot time series

Frequency analysis of chaotic systems is done with the help of three important transforms viz - Fourier, wavelet & SMRT. Sections 5.1 to 5.3 covers a detailed analysis of behaviour of chaotic systems in frequency

domain. It was found that SMRT is the best tool for chaotic system analysis since all the SMRT coefficients retain the property of original chaotic systems and preserve the shape of time series and phase plots

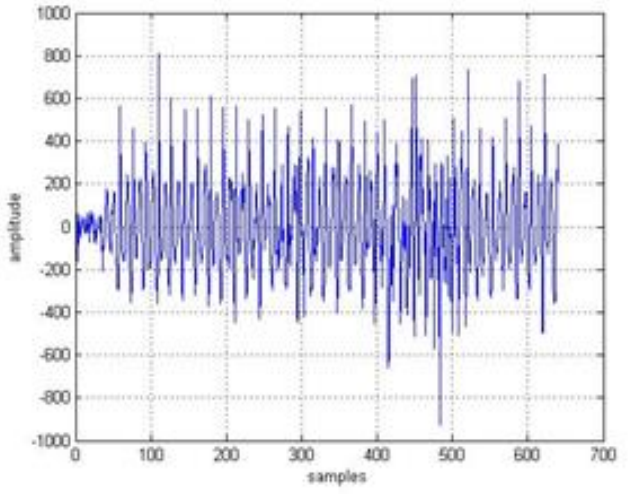

Figure 6-8 SMRT coefficients sunspot

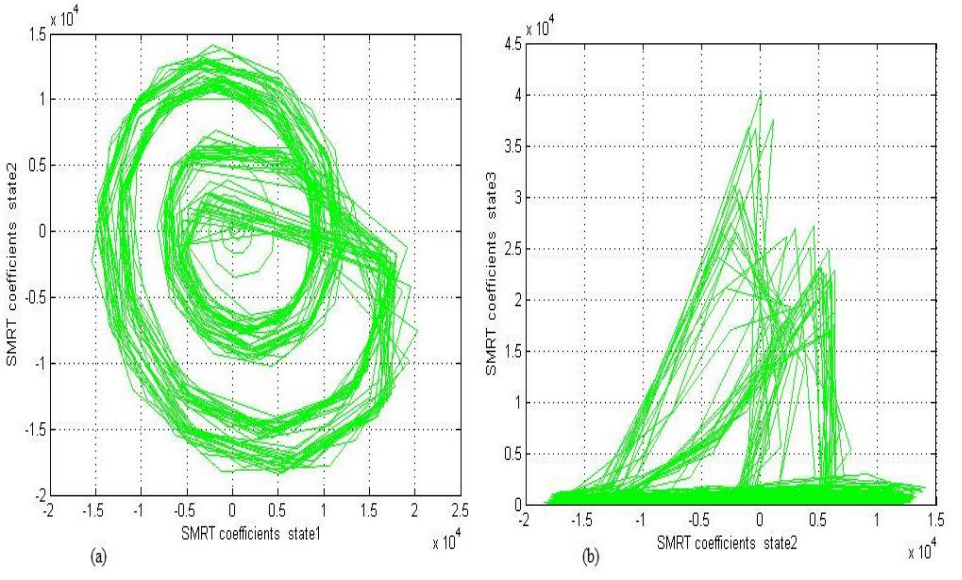

Figure 6-9 Phase plot of SMRT coefficients, sunspot (a) states1 &2 (b) states 2 & 3

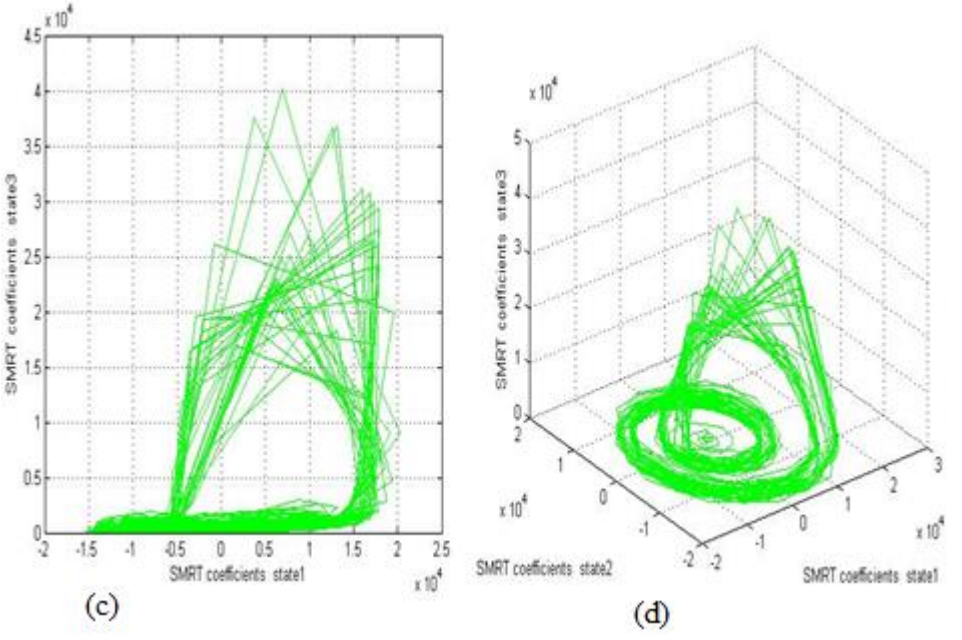

Figure 6-10 Phase plot of SMRT coefficients, sunspot (c) states 1 &3 and (d) states 1, 2, &3

Figures 6-9 and 6-10 shows the phase plots of SMRT coefficients. From the comparison of these figures with Figures 6-4 to 6-7 it is validated that the SMRT coefficients are completely capable of retaining the chaotic properties of the system after the transformation under SMRT domain. The phase plots of SMRT coefficients are investigated and found to be surprisingly coinciding with the actual phase plots of the sunspot time series.

6.2 Venice Lagoon time series

The Venice Lagoon time series is a measure of the level of water in the lagoon in centimetres each hour along the years 1940-2013. Non-linear stochastic models are used for modeling the system. Unusually high tides and other climatic condition drive the time series to show chaotic behaviour. Modeling and analysis of such events has always been subject of intense interest to mankind, not only from human point of view, but also from an economic sense.

The most famous example of flooding in the Venice Lagoon occurred in November 1966 when, driven by strong winds, the Venice Lagoon rose by nearly 2 m above the normal water level. The damage to the city's homes, churches and museums ran into hundreds of millions of Euros. Such behaviour is difficult to be modeled, because they depends on too much factors, like the astronomic and atmospheric agents.

The problem has been approached by numerical models and statistical methods, familiar to climatologists. Such numerical modeling requires computation of meteorological forcing functions on each point of finite difference grid and hence are computationally expensive. The model developed may be applied to explore the feasibility of characterizing this time series with unusual events.

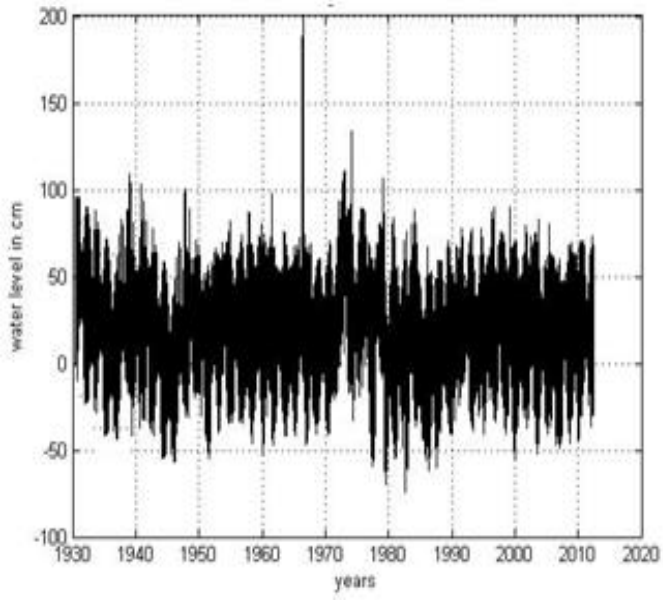

Figure 6-11 Time series: Venice lagoon water level

6.2.1 Estimation of minimum embedding dimension of Venice lagoon time series

Venice lagoon time series is modled with RNN model structure. As a first step the minimum embedding dimension is to be calculatedand estimated using the method of false nearest neighbours.

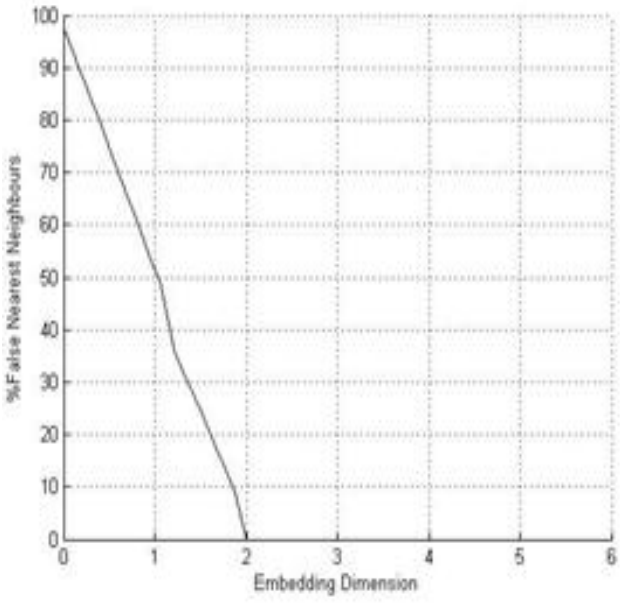

Figure 6-12 Minimum embedding dimension of Venice lagoon time series

The minimum embedding dimension of Venice lagoon time series is found to be two from Figure 6-12.

6.2.2 Phase plots of Venice lagoon time series

After estimating the minimum embedding dimension the given timeseries is modeled using the RNNmodel structure. The system is modeled with two states. The systems analysed so far are all proved to be with three states, but the present system- Venice lagoon time series exhibits properties of a system with only two states.

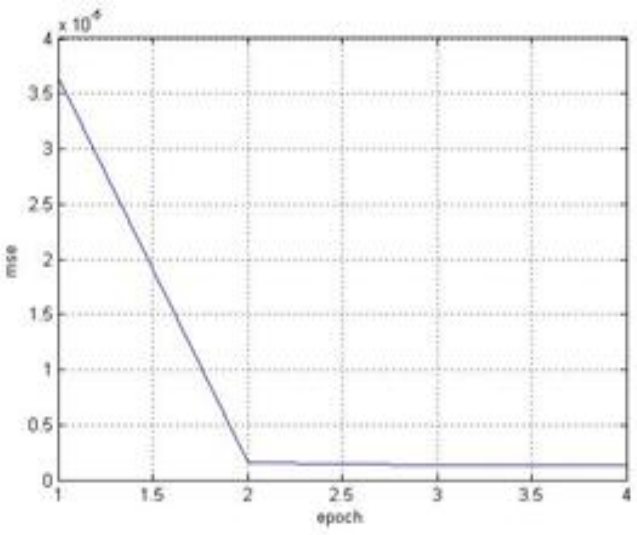

Figure 6-13 Modelling error: Venice lagoon time series

The recurrent neural networks are trained with a single channel time series data of the Venice lagoon. All the three sets of weights are updated using the EKF equations. The initial values of P(0/-1) and x(0) are obtained using EM method. The training is continued until the modelling error comes to an appreciable level of 0.254×10^{-6} as shown in Figure 6-13. Further the phase plot of the two states of the given time series is plotted.

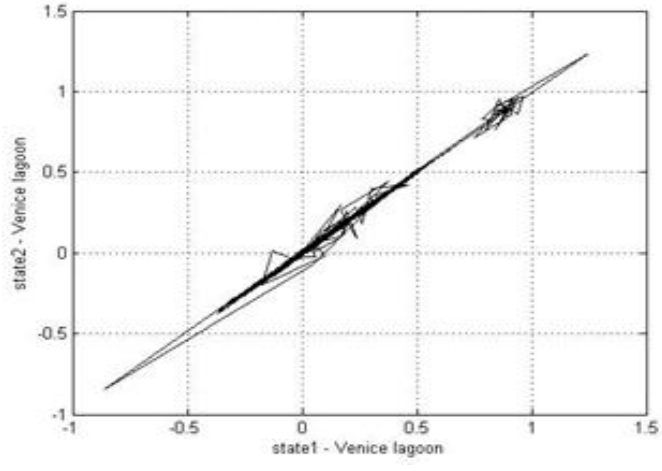

Figure 6-14 Phase plot: Venice lagoon

Figure 6-14 illustrate the phase plot of Venice lagoon time series. In chaotic system theory, the identification of chaotic systems by phase plots is applicable only to systems with three or more states. Since the system has got only two states there is no possibility of a strange attractor. From the phase plot it is not possible to understand the chaotic behaviour of the system. For a detailed investigation into the chaotic nature the Lyapunov exponents are to be studied

6.2.3 Lyapunov exponents of Venice lagoon time series

The Lyapunov Exponents of the Venice lagoon time series is calculated and is given in table 6.2.

Table 6.2.Lyapunov exponents of

Venice lagoon time series

Lyapunov exponents	
0	0.05

It can be seen that one of Lyapunov exponent is zero and the other one is positive verifying the chaotic behaviour. The chaotic nature of the Venice lagoon time series is verified from the above modeling.

6.2.4 SMRT analysis of Venice Lagoon time series

As explained in Section 6.1.4, SMRT analysis of Venice lagoon time series is done and the results are plotted in Figures 6-15 and 6-16. The time series is well reconstructed with SMRT and phase plot does not reveal much about the underlying dynamics.

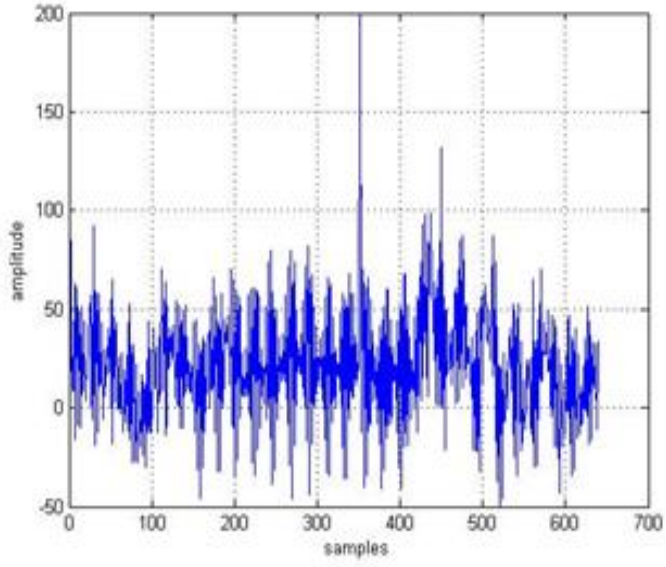

Figure 6-15 SMRT coefficients: Venice lagoon time series

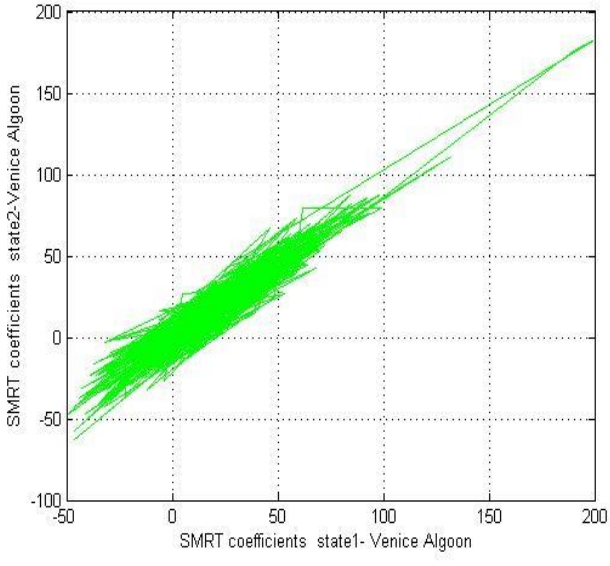

Figure 6-16 Phase plot of SMRT coefficients: Venice lagoon time series

6.3 North Atlantic Oscillation

The North Atlantic Oscillation (NAO) is characterized by an oscillation of atmospheric mass between the Arctic and the subtropical Atlantic. It is usually defined through changes in surface pressure. A permanent low-pressure system over Iceland (the Icelandic Low) and a permanent high-pressure system over the Azores (the Azores High) control the direction and strength of westerly winds into Europe. The relative strengths and positions of these systems vary from year to year and this variation is known as the NAO. NAO measures the strength of the westerly winds blowing across the North Atlantic Ocean between 40^{o}N and 60^{o}N. Studies reveal that the NAO accounts for 31% of the variance in hemispheric winter surface air temperature north of 20^{o}N[49].

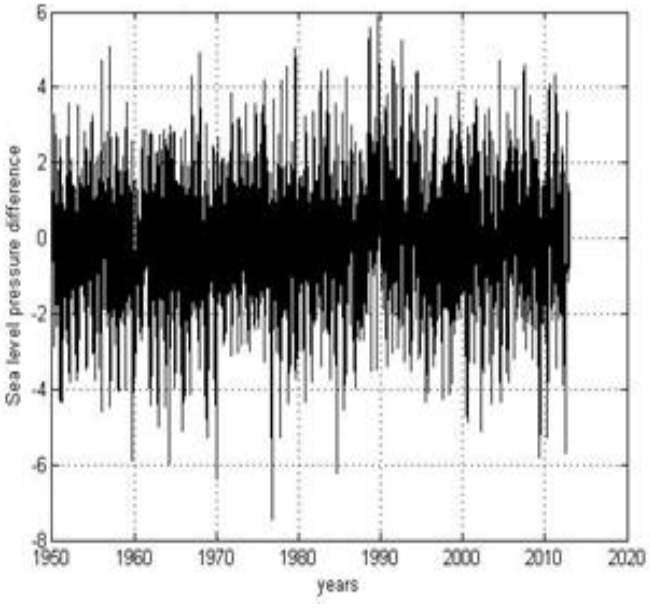

Figure 6-17 Time series: NAO

There is an index for the NAO as the difference between normalised mean winter (December to February) sea level pressure (SLP) anomalies at Ponta Delgadas, Azores and Akureyri, Iceland [73]. The normalisation is achieved by dividing the SLP anomalies at each station by the long term (1864-2014) standard deviation [114] [115].The modeling and analysis of NAO index considered as a time series - Figure 6-17 - can throw light on the behaviour of the system responsible for the oscillations. In the forthcoming section the modeling and analysis of origins of the NAO index series is presented

6.3.1 Estimation of minimum embedding dimension of NAO time series

In order to model the NAO time series with RNN model structure, it is required to estimate the minimum embedding dimension. As explained in Section 4.6 the minimum embedding dimension of the NAO timeseries is estimated using the method of false nearest neighbours.

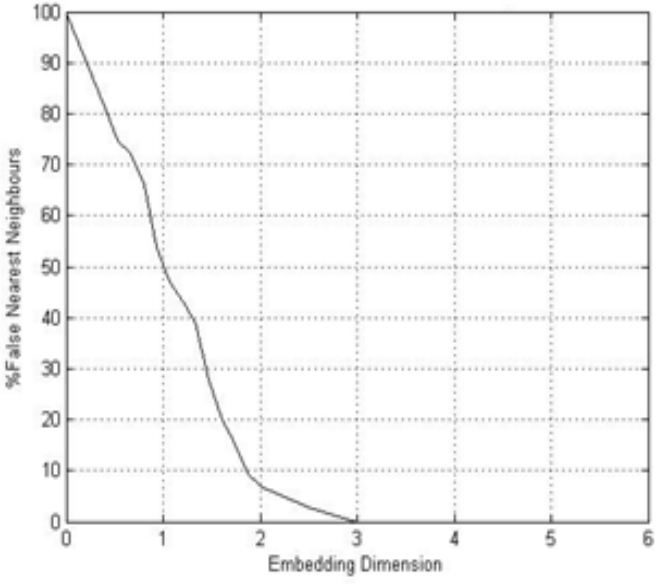

Figure 6-18 Minimum embedding dimension of NAO time series

Figure 6-18 shows the estimation of embedding dimension of NAO timeseries. From the plot of percentage false nearest neighbours and embedding dimension it is evident that the minimum embedding dimension is 3, which decides the number of states.

6.3.2 Phase plots of NAO time series

After estimating the minimum embedding dimension the given timeseries is modeled using the RNN model structure. The system is modeled with three states. The recurrent neural networks are trained with a single channel time series data of the NAO. All the three sets of weights are updated using the EKF equations. The initial values of P(0/-1) and x(0) are obtained using EM method. The training is continued until the modelling error comes to an appreciable level of 2.54×10^{-6} as shown in Figure 6-19. Further the phase plots of the three states of the given time series are plotted.

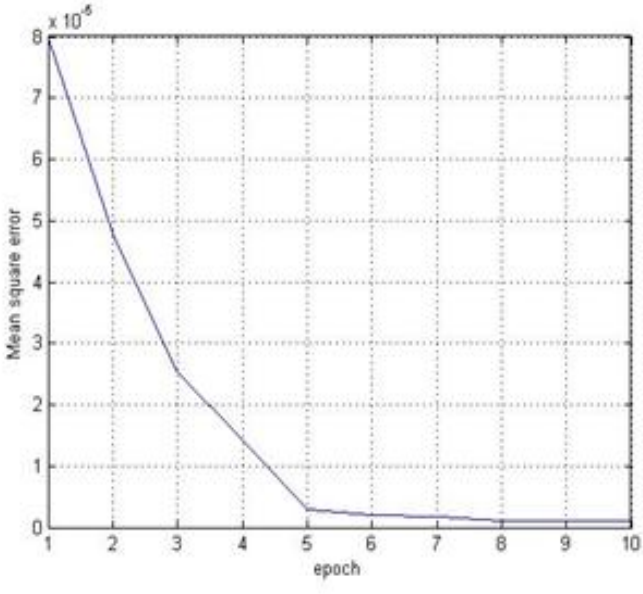

Figure 6-19 Modelling error: NAO time series

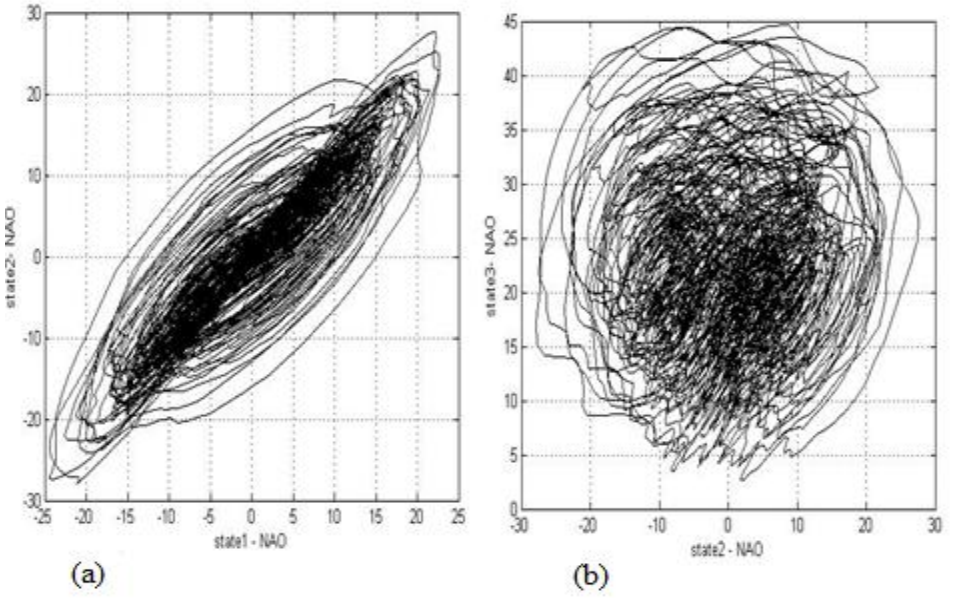

Figure 6-20Phase plots of NAO (a) states 1&2, (b) states 2&3

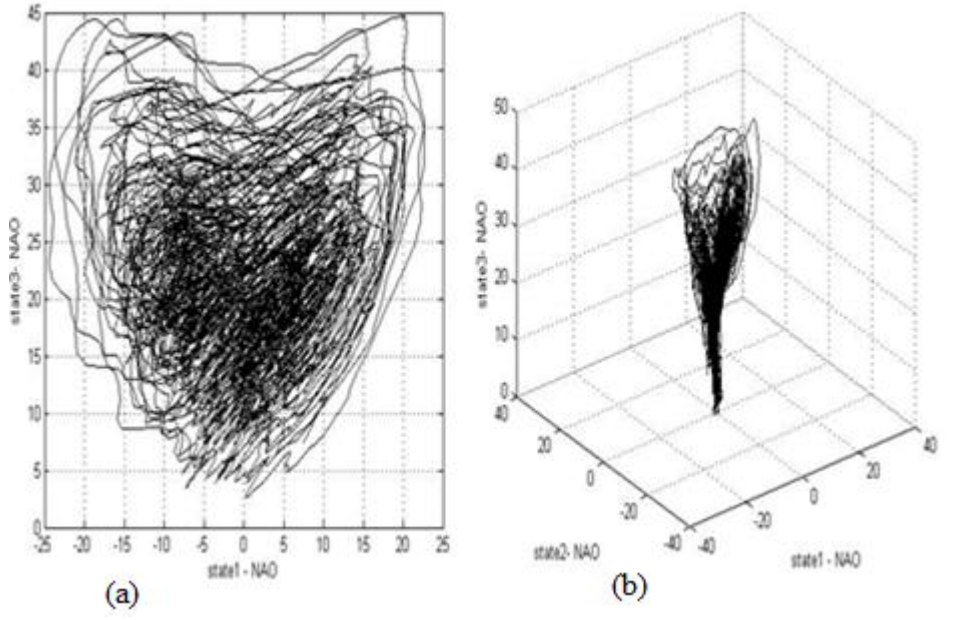

Figure 6-21 Phase plots of NAO (a) states 1 &3 and (b) states 1, 2 &3

Figures 6-20 and 6-21 illustrate the phase plots of NAO time series. The state space evolution shows that the system modelled from the NAO time series using the method reported here exhibits chaotic behaviour characterized by strange attractors. Also a mild similarity of these phase plots with Lorenz system (Figures 4-2 & 4-3) appears to indicate the possibility of deriving a mathematical model similar to that of Lorenz system. With the possibility of chaotic behaviour from strange attractors, the Lyapunov exponents of the time series are to be calculated.

6.3.3 Lyapunov exponents of NAO time series

The Lyapunov Exponents of the NAO time series is calculated using the method described in Section 4.2 and is given in table 6.3.

Table.6.3.Lyapunov exponents of NAO time series

Lyapunov exponents		
-15.2446	0	0.00127

It can be seen that one of Lyapunov exponent is negative, one is zero and the other one is positive, which shows the chaotic behaviour of the system responsible for NAO.

6.3.4 SMRT analysis of NAO time series

SMRT analysis of NAO time series is done and the results are plotted in Figures 6-22 to 6-24. As already observed in the cases of standard chaotic systems like Lorenz, Rossler, Chen & Chua and natural chaotic systems like sunspot time series, it is expected that the SMRT coefficients of NAO time series will be able to preserve the system properties and analysed by the following figures.

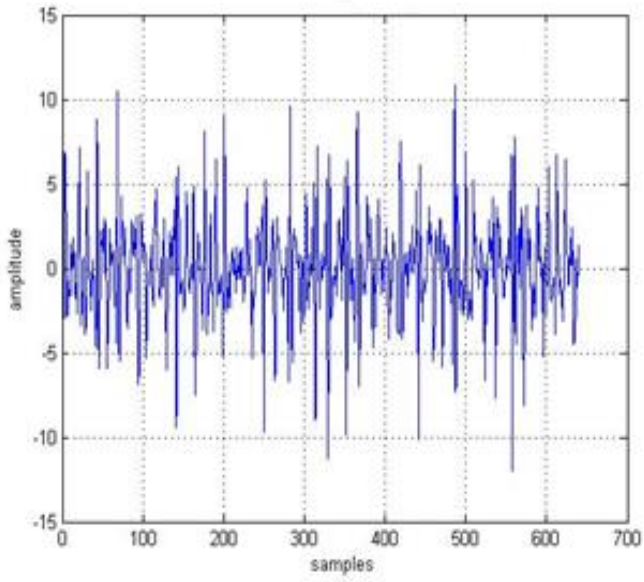

Figure 6-22 SMRT coefficients NAO

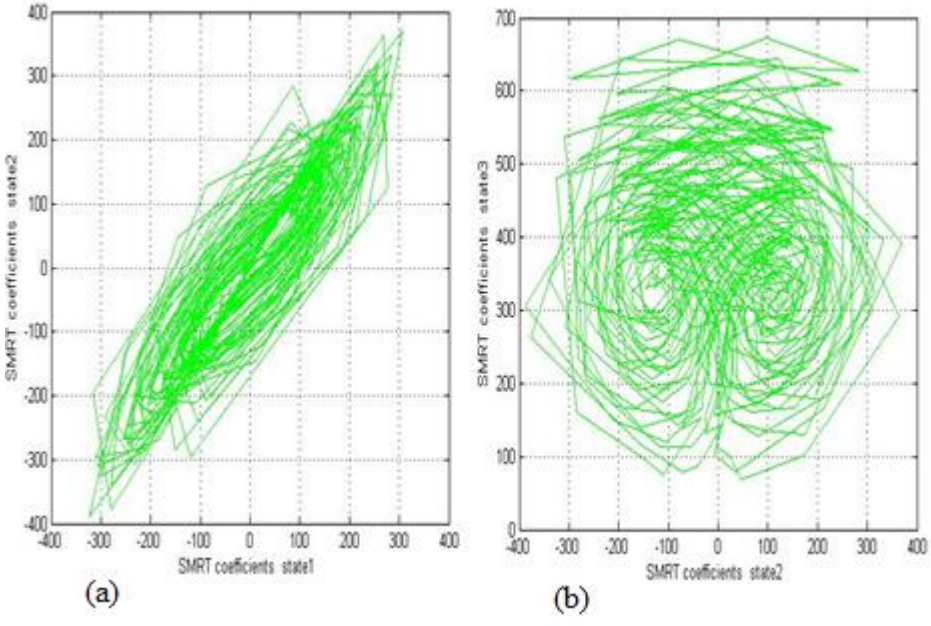

Figure 6-23 Phase plot of SMRT coefficients, NAO (a) states1 &2 (b) states 2 &3

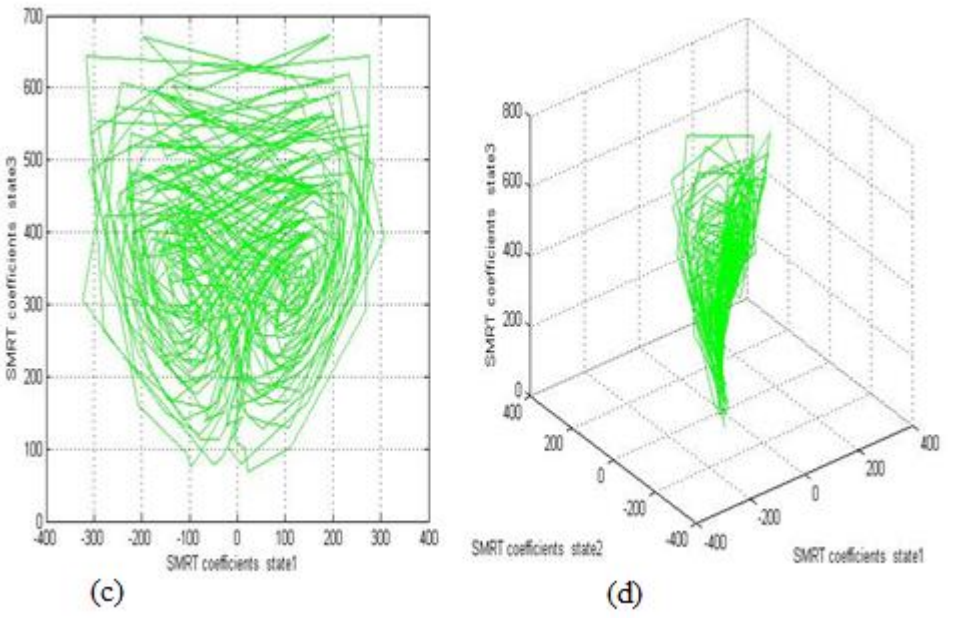

Figure 6-24 Phase plot of SMRT coefficients, NAO (c) states 1 &3 and (d) states 1,2, &3

From Figures 6.22 to 6-24 it is validated that the SMRT coefficients are completely capable of retaining the chaotic properties of the system after the transformation under SMRT domain. The phase plots of SMRT coefficients were investigated and fou nd to be surprisingly coinciding with the actual phase plots of the NAO time series.

6.4 Conclusion

Analysis and characterization of three important weather systems are presented in this chapter. The Sunspot, Venice lagoon and the North Atlantic Oscillation are modelled using the RNN model structure with a very low modeling error. The important characteristics of these systems like embedding dimension, phase plots, strange attractors and Lyapunov exponents are calculated. It is observed that the Sunspot time series has a minimum embedding dimension of three and the phase plot of Sunspot series evolve as strange attractor. Also the strange attractors of Sunspot time series

hold a significant similarity with the famous Rossler chaotic system. The Lyapunov exponents of Sunspot series are calculated and the chaotic behaviour is confirmed. The Venice lagoon time series is found to have a minimum embedding dimension of two. It has two Lyapunov exponents and one of which is positive verifying the chaotic nature. Finally the NAO index time series is analysed and found to have an embedding dimension of three. It's phase plots show strange attractors signifying chaotic nature. Also a close observation of the strange attractors of NAO time series reveals a significant similarity with the phase plots of Lorenz system. The Lyapunov exponents of NAO time series also verified the chaotic nature. The SMRT coefficients of all the three natural chaotic systems are calculated. Section 5.4 concludes that SMRT analysis is the most promising method for time series in frequency domain and inherent properties of the chaotic systems are well preserved in these coefficients. This fact is again verified from phase plots of SMRT coefficients of natural chaotic systems.

Chapter 7

Conclusions and Suggestions for Future work

7. Conclusion and Suggestions for Future Work

The study of chaotic systems have become very topical over the past few decades, since they have ramifications in diverse disciplines like Engineering, Ecology, Climatology, Biology and Finance. Modeling of chaotic systems, based on output time series, is quite promising since the output often represents the characteristic behavior of the total system. Growing importance of chaotic systems has motivated the researchers to look for various tools to model and analyze such systems. Artificial neural networks, with their exceptional self-learning capacity, have always presented themselves as one of the best tool for modeling highly non-linear and chaotic systems. Choice of a good training algorithm to estimate the weights of artificial neural networks so as to model chaotic systems remained a challenging problem in this field. The thesis addresses this aspect by examining different estimation techniques and finally establishes that the EKF algorithm, with EM technique to estimate the initial values, is the right candidate for estimate. Current research is also very active in the analysis of chaotic systems in time and frequency domain. Accordingly, the present thesis addresses modeling and analysis of chaotic systems and puts forward many important observations and conclusions.

Neural network based modeling, identification, and characterization of chaotic systems in nature are discussed in the previous chapters. The thesis discusses the concept of linear, non-linear and chaotic systems in Chapter 1. A brief description about chaotic weather systems, which are later modelled, is introduced here. An introduction to recurrent neural networks and training strategies are also discussed. Chapter 2 deals with a review of important

publications relevant to the present work. Choosing RNN as the model to represent chaotic systems, described by NARX model, selection of the best training algorithm to estimate the weights and application of the same on standard chaotic systems is developed systematically in Chapter 3. EKF algorithm along with EM technique to estimat the initial values and Particle Filter algorithm with its two variants are evaluated to train the RNN model. Performance of the three training algorithms, for modeling the time series emanating out of chaotic systems modelled using RNN structure, is systematically evaluated based on least mean square error criterion. Samples of the time series is given as input to the RNN model. The output time series from four standard chaotic systems, Lorenz, Rossler, Chen and Chua, are modeled producing a modeling error as low as 10^{-7}. It is observed that the lowest modeling error is obtained for the EKF algorithm with EM technique for estimating initial values and therefore it is concluded that RNN, trained with EKF algorithm along with EM technique, can be selected as the best structure to model chaotic systems.

Extending the results on modeling the time series, the complete modeling of the chaotic system involving the state transition and output in the form of time series is taken up, with a view to identify the chaotic system. The RNN model is modified to accommodate both the aspects. The complete set of weights are then estimated, based on the time series of the output. The consequent demonstration on the time series generated from standard chaotic systems resulted in the truthful reproduction of state space evolution of the system (with modeling error as low as 10^{-7}). The model and the resultant state space evolution lead to the computation of various parameters representing the properties of chaotic system, viz. strange attractors, Lyapunov exponents, Kaplan - Yorke dimensions and bifurcation diagrams. All these properties are seem to be perfectly in agreement with the state space

evolution and resulting properties computed on the four standard chaotic systems using the cross coupled mathematical equations. The values obtained for Lyapunov exponents and Kaplan - Yorke dimensions of the modelled output, closely comparable to what is reported in literature, proved to be very convincing on the correctness of the modeling approach developed. The analysis of the bifurcation plots reveals the transition, of the system from non-chaotic to chaotic behaviour, in response to change in the parameter describing the system. The online evaluation of Lyapunov exponents directly from the model along with the bifurcation diagram brings out the close correspondence between the two, thereby highlighting the ability of the model developed.

The analysis in the frequency domain is complicated since chaotic dynamical systems are broadband signals. Some important frequency domain characteristics of chaotic systems using Fourier Transform, wavelet transform and Mapped Real Transform (MRT) turned out to be a set of significant findings of the thesis. The fact that Fourier spectrum is not able to well represent the non-stationary nature is established from the studies chaotic signals. The Lorenz system with non-chaotic and chaotic states are analyzed by varying one of the parameters. The Fourier coefficients of Lorenz system demonstrated different characteristics under non- chaotic and chaotic states. The frequency spectrum is band limited for the former state and is broad banded for latter. The Fourier coefficients under non-chaotic state are linear while the same under chaotic state is non-linear. Attempt is made to construct the phase plot of Fourier coefficients of two states and the attempt has been futile as it did not reveal the original system properties.

The wavelet analysis is proved to be more fruitful in many aspects. From the energy plot of different wavelet decomposition levels, one with highest

energy concentration is selected and the detailed coefficients are taken for analysis. It is found that level 6 and 8 are suitable for non-chaotic and chaotic states respectively. The corresponding detailed coefficients are plotted. Interestingly, the coefficients seemed to be in line with the actual time series. Further, the phase plot of wavelet detailed coefficients is found to be somewhat similar to the original phase plot.

There were 16 arrays of SMRT coefficients and each array is found to have the same energy level. Further the plot of coefficients of each array is exactly similar to the actual time series. Then the phase plots of all the 16 arrays of SMRT coefficients are investigated and all are found to be surprisingly coinciding with the actual phase plots. Thus any one array of SMRT coefficients is capable to represent all the properties of the complete time series. Thus it is sufficient to compute only one SMRT coefficient corresponding to the selected window and hence it also reduces the computation time and complexity. Scatter plot of SMRT coefficients from non-chaotic and chaotic systems revealed distinguishing features. Thus it is concluded that the SMRT analysis is the most promising methods for chaotic system analysis in transform domain from among the three transforms considered. Validity of the SMRT analysis is established using other standard chaotic systems like Rossler, Chen and Chua.

The techniques based on output time series developed using standard chaotic systems is extended to model and identify unknown natural systems. There are a number of natural systems which are non-linear in nature with probability of exhibiting chaotic behaviour. Analysis and characterization of three important weather systems are performed. The time series of Sunspot, Venice lagoon and North Atlantic Oscillation index are modeled using RNN model structure with a modeling error as low as 10^{-6}. The number of states

required to model an unknown source has been calculated using the self-embedding dimension due to Takens. The important characteristics of these systems like strange attractors and Lyapunov exponents are calculated directly from the model. It is interesting to observe that the Sunspot time series has a minimum embedding dimension of three and the phase plot of Sunspot series evolve as strange attractor. Also the strange attractors of Sunspot time series hold a significant similarity with the famous Rossler chaotic system. The Lyapunov exponents of Sunspot series are calculated and the chaotic behaviour is confirmed.

The Venice lagoon time series is found to have a minimum embedding dimension of two. There is no possibility to find any strange attractor since there are only two states. It has two Lyapunov exponents and one of which is positive verifying the chaotic nature.

Finally the NAO index time series is analyzed and found to have an embedding dimension of three. Its phase plots show strange attractors signifying chaotic nature. Phase plots of NAO show some similarities to that of Lorenz system. The three Lyapunov exponents of the system show that one is a large negative value, another is zero and the third one is positive, verifying the chaotic nature as observed from the phase plots.

The results obtained in the thesis are regularly submitted for peer review in national/international conferences and international journals. On the whole a total of 9 papers have been published based on the investigations reported in the thesis, attached as list of papers published.

The investigations and findings of the thesis suggest the way ahead for further work in the areas of modeling, time and frequency domain analysis of chaotic systems. Other modeling structures and algorithms for chaotic

systems are worth exploring. Recent literature highlights extensive use of frequency domain approaches for the analysis of chaotic systems. However the broadband nature of such systems is a major concern in the frequency domain. A detailed research on SMRT technique to analyze chaotic systems could trigger some further investigation. Derivation of a mathematical model for unknown natural systems will be helpful in the prediction of events like Tsunami, earthquake, etc. The efficacy of the proposed method can be extended in the modeling of hyper chaotic systems. There are a number of such systems like hyper chaotic Chen, Lorenz and Rossler systems. The analysis of other natural chaotic systems like sea clutter, EL Nino Southern Oscillation index, business data like stock market index etc. will prove to be a flourishing continuation of the work.

Appendix A

A RNN Learning Algorithms

A.1 System representation

Consider a discrete time non-linear dynamic system, described by a vector difference equation with additive white Gaussian noise that models "unpredictable" disturbances. The dynamic system equation is given by the following non-linear equations

$$x_k = f(x_{k-1}, u_k, w_{k-1}) \qquad (A.1)$$

where x_k is an n dimensional state vector u_k is an m dimensional known input vector, and w_k is a sequence of independent and identically distributed zero mean white Gaussian process noise with covariance

$$E(ww^T) = Q \qquad (A.2)$$

The measurement equation is

$$z_k = h(x_k, v_k) \qquad (A.3)$$

where v_k is the measurement noise with covariance

$$E(vv^T) = R \qquad (A.4)$$

The functions *f* and *h* and the matrices Q and R are assumed to be known.

A.2 Extended Kalman Filter

The Kalman filtering process has been designed to estimate the unknown states in a linear stochastic system with apriory knowledge of known states and noise statistics. The Kalman filter may be extended for non-linear systems also by a linearization procedure. The resulting filter is referred to as Extended Kalman Filter (EKF)

Consider the actual state and measurement equations (A.1) and (A.3).

Let the approximate state and measurement equations be

$$\tilde{x}_k = f(\hat{x}_{k-1}, u_k, 0) \qquad (A.5)$$

and

$$\tilde{z}_k = h(\tilde{x}_k, 0) \qquad (A.6)$$

Where $\tilde{x}_k$ is a posterior estimate of the state from a previous time step k. The equations that linearize the estimate about (A.5) and (A.6) are given as

$$x_k = \tilde{x}_k + A(x_{k-1} - \hat{x}_{k-1}) + Ww_{k-1} \qquad (A.7)$$

$$z_k = \tilde{z}_k + H(x_k - \tilde{x}_k) + Vv_k \qquad (A.8)$$

where x_k and z_k are the actual state and measurement vectors, $\tilde{x}_k$ and $\tilde{z}_k$ are the approximate state and measurement vectors, $\hat{x}_k$ is a posterior estimate of the state at step *k*, w_k and v_k are random variables and represent the process and measurement noise. *A* is the Jacobian matrix of partial derivatives of f with respect to *x*, W is the Jacobian matrix of partial derivatives of f with respect to *w*. H is the Jacobian matrix of partial derivatives of *h* with respect to x and *V* is the Jacobian matrix of partial derivatives of *h* with respect to *v*.

A.2.1 EKF time update equations

Project the state ahead

$$\hat{x}_k^- = f(\hat{x}_{k-1}, u_k, 0) \qquad (A.9)$$

Project the error covariance ahead

$$\bar{P}_k = A_k P_{k-1} A_k^T + W_k Q_{k-1} W_k^T \qquad (A.10)$$

A.2.2 EKF measurements update equations

Compute the Kalman gain

$$K_k = P_k^- H_k^T (H_k P_k^- H_k^T + V_k R_k V_k^T)^{-1} \quad \text{(A.11)}$$

Update estimate with measurement

$$\hat{x}_k = \hat{x}_k^- + K_k (z_k - h(\hat{x}_k^-, 0)) \quad \text{(A.12)}$$

Update error covariance

$$P_k = (I - K_k H_k \bar{P}_k) \quad \text{(A.13)}$$

One of the basic problems in the implementation of the Kalman filter is the choice of the initial values of the state x and the state co-variance P. Since arbitrary choices can lead to the divergence of the filter, the present work has used the EM algorithm [44] to compute the initial values of state and the state co variance.

A.2.3 EM Algorithm

The EKF Algorithm for training Multi-Layer Perceptrons (MLPs) suffers from serious shortcomings, namely choosing the initial states and covariance $(x, Q \text{ and } R)$. Following backward recursions are done after computing the forward estimates in EKF.

$$J_{k-1} = P_{k-1} A^T P_{k-1}^{-1} \quad \text{(A.14)}$$

$$x_{k-1} = \hat{x}_{k-1} J_{k-1} \left(\hat{x}_{k-1} - A \hat{x}_{k-1} \right) \quad \text{(A.15)}$$

$$P_{k-1} = \hat{P}_{k-1} + J_{k-1} \left(\hat{P}_k - \hat{P}_{k-1} \right) J_{k-1}^T \quad \text{(A.16)}$$

$$P_k = P_{k-1} J_{k-1}^T + J_k \left(P_{k-1} - A P_{k-1} \right) J_{k-1}^T \quad \text{(A.17)}$$

A.3 Particle filters

Particle filters are suboptimal filters. They perform Sequential Monte Carlo (SMC) estimation based on point mass (or "particle") representation of probability densities. The SMC ideas in the form of sequential importance sampling had been introduced back in the 1950s. Although these ideas continued to be explored during the 1960s and 1970s, they were largely overlooked and ignored. Most likely the reason for this was the modest computational power available at the time. In addition, all these early implementations were based on plain sequential importance sampling, which degenerates over time. The major contribution to the development of the SMC method was the inclusion of the re-sampling step, which, coupled with ever faster computers, made the particle filters useful in practice for the first time. Since then research activity in the field has dramatically increased, resulting in many improvements of particle filters and their numerous applications.

A.3.1 Monte Carlo Integration

Monte Carlo integration is the basis of SMC methods. Suppose we want to numerically evaluate a multidimensional integral:

$$I = \int g(x) dx \quad \text{(A.18)}$$

where $x \in R^{nx}$. Monte Carlo (MC) methods for numerical integration factorize g(x) =f(x).π(x) In such a way that π(x) is interpreted as a probability density satisfying π(x) ≥0 and $\int$ π(x) dx=1. The assumption

is that it is possible to drawN>>1 samples $\{x^i; i = 1\ldots N\}$distributed according to $\pi(x)$. The MC estimate of integral

$$I = \int f(x)\,\pi(x)\,dx \tag{A.19}$$

Is the sample mean

$$I_N = \frac{1}{N}\sum_{i=1}^{N} f(x^i) \tag{A.20}$$

If the samples x^i are independent then I_N is an unbiased estimate and according to the law of large numbers I_N will almost surely converge to I. If the variance of f(x),

$$\sigma^2 = \int (f(x) - I)^2 \pi(x) dx \tag{A.21}$$

Is finite, then the central limit theorem holds and the estimation error converges in distribution: $\lim_{n\to\infty} \sqrt{N}(I_N - 1) \sim N(0, \sigma^2)$. The error of the MC estimate, $e = I_N - I$, is of order $0(N^{-1/2})$, meaning that the rate of convergence of the estimate is independent of the dimension of the integrand. In contrast, any deterministic numerical integration has a rate of convergence that decreases as the dimensions n_x increases. This useful and important property of MC integration is due to the choice of samples $\{x^i, i = 1\ldots N\}$, as they automatically come from regions of the state space that are important for the integration result. In the Bayesian estimation context, density $\pi(x)$ is posterior density. Unfortunately, usually it is not possible to sample effectively from the posterior distribution, being multivariate, nonstandard, and only known up to a proportionality constant. A possible solution is to apply the importance sampling method.

A.3.2 Importance Sampling

Ideally we want to generate samples directly from $\pi(x)$ and estimate I using (A.19). Suppose we can only generate samples from a density q(x), which is similar to $\pi(x)$. Then a correct weighting of the sample set still makes the MC estimation possible. The PDF q(x) is referred to as the importance or proposal density. Its "similarity" to $\pi(x)$ can be expressed by the following condition:

$$\pi(x)>0 \Rightarrow q(x)>0 \text{ forall } x \in R^{nx} \qquad \text{(A.22)}$$

which means that q(x) and $\pi(x)$ have the same support. Condition (3.4) is necessary for the importance sampling theory to hold and, if valid, any integral of the form (A.17) can be rewritten as

$$I = \int f(x)\pi(x)dx = \int f(x)(\tfrac{\pi(x)}{q(x)})dx \qquad \text{(A.23)}$$

provided that $\pi(x)/q(x)$ is upper bounded. A Monte Carlo estimate of I is computed by generating N>>1 independent sample $\{x^i, i=1 \ldots N\}$ distributed according to q(x) and forming the weighted sum:

$$I_N = \frac{1}{N\sum_{i=1}^{n} X_i} I_N = \frac{1}{N}\sum_{i=1}^{N} f(x^i)\,\tilde{w}(x^i) \qquad \text{(A.24)}$$

where $\tilde{w}(x^i) = \frac{\pi(x)}{q(x)}$ are the importance weights. If the normalizing factor of the desired density $\pi(x)$ is unknown, we need to perform normalization of the importance weights. Then we estimate I_N as follows;

$$I_N = \frac{\frac{1}{N}\sum_{i=1}^{N} f(x^i)\,w(x^i)}{\frac{1}{N}\sum_{i=1}^{N} w(x^i)} \tag{A.25}$$

where the normalized importance weights are given by:

$$w(x^i) = \frac{w(x^i)}{\sum_{j=1}^{N} w(x^j)} \tag{A.26}$$

This technique is applied to the Bayesian framework, where $\pi(x)$ is the posterior density.

A.3.3 Sequential Importance Sampling

Importance sampling is a general MC integration method that we now apply to perform non-linear filtering specified by the conceptual solution. The resulting sequential importance sampling (SIS) algorithm is a Monte Carlo method that forms the basis for most sequential MC filters developed over the past decades; this sequential Monte Carlo approach is known variously as bootstrap filtering, the condensation algorithm, particle filtering, interacting particle approximation, and survival of the fittest. It is a technique for implementing a recursive Bayesian filter by Monte Carlo simulations. The key idea is to represent the required posterior density function by a set of random samples with associated weights and to compute estimates based on these examples and weights. As the number of samples becomes very large, this Monte Carlo characterization becomes an equivalent representation to the usual functional description of the posterior PDF, and the SIS filter approaches the optimal Bayesian estimator:

SIS Particle Filter Algorithm

At time n=1

Sample $X_1^i \sim q_1(x_1)$

Compute the weights $w_1(X_1^i)$ *and* $W_1^i \propto w_1(X_1^i)$

At time $n \geq 2$

Sample $X_n^i \sim q_n(x_n \mid X_{1:n-1}^i)$

Compute the weights

$$w_n(X_{1:n}^i) = w_{n-1}(X_{1:n-1}^i)\alpha_n(X_{1:n}^i)$$

$$w_n^i \propto w_n(X_{1:n}^i)$$

Algorithm A.1

A.3.4 Sequential Importance sampling Resampling (SIR)

SIS provides estimates whose variance increases with 'n'. Employing the technique of resampling this problem can be solved. Consider an IS approximation $\hat{\pi}_n(x_{1:n})$ of the target distribution $\pi_n(x_{1:n})$.This approximation is based on the weighted samples from $q_n(x_{1:n})$. This approximation does not provide samples distributed according to $\pi_n(x_{1:n})$.To obtain approximate samples from $\pi_n(x_{1:n})$, sample from its IS approximation $\hat{\pi}_n(x_{1:n})$.This operation is called resampling as it corresponds to sampling from an approximation $\hat{\pi}_n(x_{1:n})$ which was itself obtained from sampling. In order to obtain N samples from $\hat{\pi}_n(x_{1:n})$

resample N times from $\hat{\pi}_n(x_{1:n})$ and associate a weight of $\frac{1}{N}$ with each sample. The approximate measure of $\hat{\pi}_n(x_{1:n})$ is given by

$$\bar{\pi}(x_{1:n}) = \sum_{i=1}^{N} \frac{\overset{i}{N}}{\frac{n}{N}} \delta x^{i}_{1:n} (x_{1:n}) \qquad \text{(A.27)}$$

SIR Particle Filter Algorithm

At time n=1

Sample $X_1^i \sim q_1(x_1 \mid y_1)$

Compute the weights $\frac{\mu(X_1^i) g(y_1 \mid X_1^i)}{q(X_1^i \mid y_1)}$ *and* $W_1^i \propto w_1(X_1^i)$

Resample $\{W_1^i, X_1^i\}$ *to obtain N equally weighted particles* $\left\{\frac{1}{N}, \bar{X}_1^i\right\}$

At time n ≥ 2

$X_n^i \sim q(x_n \mid y_n, \overline{X_{n-1}^i})$ *and set* $X_{n-1}^i \leftarrow (\overline{X_{1:n-1}^i}, X_n^i)$

Compute the weights $\propto_n (X_{n-1:n}^i) = \frac{g(y_n \mid X_n^i) f(X_n^i \mid X_{n-1}^i)}{q(X_n^i \mid y_n, X_{n-1}^i)}$

and $W_1^i \propto w_1(X_{n-1:n}^i)$

Resample $\{W_1^i, X_1^i\}$ *to obtain N equally weighted particles* $\left\{\frac{1}{N}, \bar{X}_{1:n}^i\right\}$

Algorithm A.2

A.3.5 Rao Blackwellised Particle Filter

One of the major drawbacks of PF is that sampling in high-dimensional spaces can be inefficient. In some cases, however, the model has "tractable substructure", which can be analytically marginalized out, conditional on certain other nodes being imputed, The analytical marginalization can be carried out using standard algorithm like such as the Kalman filter, the HMM filter, the junction tree algorithm for general DBNs [ ] or, any other finite-dimensional optimal filters. The advantage of this strategy is that it can drastically reduce the size of the space over which we need to sample. Marginalizing out some of the variables is an example of the technique called Rao-Blackwellisation, because it is related to the Rao-Blackwell formula.

A.3.6.1 Rao-Blackwell Theorem

Let $\hat{\theta}$ be an estimator of θ with E ($\hat{\theta}$2) <∞ for all θ. Suppose that T is sufficient for $\hat{\theta}$, and let $\hat{\theta}$ = E ($\hat{\theta}$| T). Then for all θ

$$E(\overset{*}{\theta}-\theta)^2 \le E(\hat{\theta}-\theta)^2 \qquad (A.28)$$

The inequality is strict unless $\hat{\theta}$ is a function of T. In many cases, it may be possible to divide the problem into linear-Gaussian and non-linear parts. Suppose that the state vector may be partitioned as $x_k = \begin{pmatrix} x_k^L \\ x_k^N \end{pmatrix}$ so that the required posterior may be factorized into Gaussian and non-Gaussian terms:

$$p(x_k/z_k) = p(x_k^L, x_k^N/z_k) = p((x_k^L/x_k^N, z_k)\, p((x_k^N/z_k) \qquad (A.29)$$

Where $p((x_k^L/x_k^N, z_k)$ is Gaussian and $p((x_k^N/z_k)$ is non-Gaussian. The Gaussian

term may be calculated from a Kalman filter and non- Gaussian term from a particle filter. The Rao- Blackwell zed Particle Filter (RBPF) algorithm is given below.

RBPF Particle Filter Algorithm

x_k =*state of the given system*

y_k =*measurement*

θ_k = *arbitrary latent variable*

The probability distribution

$$p(x_{k-1} \mid \theta_{k-1}) = N(x_k \mid A_{k-1}(\theta_{k-1})x_{k-1}, Q_{k-1}(\theta_{k-1}))$$

$$p(y_k \mid x_k, \theta_k) = N(y_k \mid H_k(\theta_k)x_k, R_k(\theta_k))$$

$p(\theta_k \mid \theta_{k-1})$ = *any given form*

Initialization: for i=1: N draw samples $\theta_0(i)$ *from the initial pdf* $p(\theta_0) = p(\theta \mid y)$ *and set* $\hat{x}_0(i) = \hat{x}_0, P_0(i) = P_0,$ *where* $\hat{x}_0$ *the initial state estimate is and* P_0 *is the initial state estimation covariance matrix*

For k=1, 2… repeat the following steps

for i=1: N draw samples $\hat{\theta}_k(i)$ *from* $p(\theta_k \mid \theta_{k-1}(i))$

for i=1, 2, …, N propagate the mean $\hat{x}_{k-1}(i)$ *and covariance* P_{k-1} *of the state* x_{k-1} *as follows*

$$\tilde{x}_{k|k-1}(i) = \Phi(\tilde{\theta}_k(i))\,\hat{x}_{k-1}(i)$$

$$\tilde{P}_{k|k-1}(i) = \Phi(\tilde{\theta}_k(i))P_{k-1}(i)\Phi^T(\tilde{\theta}_k(i)) + \Gamma(\tilde{\theta}_k(i))Q_w\Gamma^T(\tilde{\theta}_k(i))$$

for i= 1, 2, …, N evaluate and normalize the importance weights

$$\tilde{\alpha}_k(i) = p(y_k \mid Z_{k-1}, \tilde{\theta}_k(i)) \sim N(y_{k|k-1}(i), \tilde{R}_k(i))$$

$$\alpha_k(i) = \frac{\tilde{\alpha}_k(i)}{\sum_{j=1}^{N}\tilde{\alpha}_j(i)}, \text{ where } \tilde{y}_{k|k-1}(i) = H\,\tilde{x}_{k|k-1}(i)$$

$$\tilde{R}_k(i) = H\,\tilde{P}_{k|k-1}(i)H^T + Q_v$$

Resample particles $\{\tilde{x}_{k|k-1}(i), \tilde{P}_{k|k-1}(i), \tilde{\theta}_k(i) : i = 1, \ldots\ldots, N\}$

Sampling probabilities proportional to $\tilde{\alpha}_k(i)$ *to obtain N particles*

$$\{\hat{x}_{k|k-1}(i), P_{k|k-1}(i), \theta_k(i) : i = 1, \ldots\ldots, N\}$$

for i= 1, 2, …, N perform measurement update for state vector x using Kalman recursion to obtain particles $\{\hat{x}_k(i), P_k(i), \theta_k(i)\}$ *given*

$$\{\hat{x}_{k|k-1}(i), P_{k|k-1}(i), \theta_k(i)\}$$

where

$$\hat{x}_k(i) = \hat{x}_{k|k-1}(i) + K_k(i)(yk - H\,\hat{x}_{k|k-1}(i))$$

$$P_k(i)(I - K_k(i)H)\,P_{k|k-1}(i)$$

$$K_k(i) = P_{k|k-1}(i)H^T R_k^{-1}(i)$$

$$R_k(i) = H\,P_{k|k-1}(i)H^T + Q_v$$

Algorithm A.3

In RBPF the dimension of x_k for the particle filter is less than the full state vector x_k and so fewer particles are needed for satisfactory performance. Thus the computational cost of particle filter is reduced but complexity of RBPF is more than that of the SIR particle filter though RBPF requires only less number of particle.

The EKF, SIR and RBPF algorithms are presented in detail. The work reported in chapter 3 is based on the theory of these three algorithms.

Appendix B

B Fourier, Wavelet & Mapped Real Transforms

B.1 Fourier transform

Fourier transform represents signal as a linear combination of harmonically related complex exponential function. The resulting set of coefficients as a function of frequency is called the Fourier spectrum. The Fourier representation is applicable to both periodic and aperiodic cases of continuous and discrete time signals.

B.1.1 Continuous Time Fourier transform

The Continuous Time Fourier Transform of an aperiodic signal x(t) is defined as

$$X(j\omega) = \frac{1}{2\pi} \int_{-\infty}^{+\infty} x(t) e^{-j\omega t} dt \qquad (B.1)$$

The signal x(t) can be reconstructed by using the inverse Fourier transform relation, defined as

$$x(t) = \frac{1}{2\pi} \int_{-\infty}^{+\infty} X(j\omega) e^{j\omega t} d\omega \qquad (B.2)$$

B.1.2 Discrete Time Fourier Transform

The Discrete Time Fourier Transform (DTFT) of a signal x_n is defined as

$$X(e^{j\omega}) = \sum_{n=-\infty}^{\infty} x_n e^{-j\omega n} \quad \text{(B.3)}$$

$X(e^{j\omega})$ is a complex function of the real variable ω and can be written as

$$X(e^{j\omega}) = X_{re}(e^{j\omega}) + jX_{im}(e^{j\omega}) \quad \text{(B.4)}$$

$X(e^{j\omega})$ can alternately be expressed as

$$X(e^{j\omega}) = \left|X(e^{j\omega})\right| e^{j\theta(\omega)} \quad \text{(B.5)}$$

$\left|X(e^{j\omega})\right|$ is called the magnitude spectrum, $\theta(\omega)$ is called the phase spectrum. When x_n is real, $\left|X(e^{j\omega})\right|$ & $X_{re}(e^{j\omega})$ are even functions of ω, whereas $\theta(\omega)$ & $X_{im}(e^{j\omega})$ are odd functions of ω.

B.1.3 Discrete Fourier Transform

Discrete Fourier transform (DFT) is the sampled version of DTFT. It maps a sequence x_n , $0 \le n \le N-1$, into X_k, $0 \le k \le N-1$

$$X(e^{j\omega})\big|_{\omega=\frac{2\pi k}{N}} = X_k = \sum_{k=0}^{N-1} x_n e^{-\frac{j2\pi nk}{N}} \quad \text{(B.6)}$$

Using the notation $W_N = e^{\frac{-j2\pi}{N}}$, called twiddle factor, the DFT can be expressed as

$$X_k = \sum_{n=0}^{N-1} x_n W_N^{nk} \quad \text{(B.7)}$$

The Inverse DFT is given by

$$x_n = \frac{1}{N}\sum_{k=0}^{N-1} X_k W_N^{-nk},\ 0 \le n \le N-1 \qquad \text{(B.8)}$$

The Fourier transform gives frequency information of the signal but it does not reveal the time information. Time information is not required when the signal is stationary. Dennis Gabor (1946) used Short-time Fourier transform (STFT) to analyse a small section of the signal at a time by windowing the signal. It uses overlapping or non-overlapping sliding window to find the spectrogram, which gives the information of both time and frequency. But the window size limits the frequency resolution. Also the selection of type and size of the window function is an important issue. Wavelet transform gives a better solution to this problem.

B.2 Wavelet Transform

Wavelet Transform gives time - frequency information. Consider a real or complex valued continuous time function ψ(t) with the following properties

1. The function is integrable to zero

$$\int_{-\infty}^{\infty} \Psi(t)\,dt = 0 \qquad (B.9)$$

2. Its square is integrable having finite energy

$$\int_{-\infty}^{\infty} \left|\Psi(t)\right|^2 dt \prec \infty \qquad (B.10)$$

The function ψ(t) is a mother wavelet. Property 1 is suggestive of a function that is oscillatory and property 2 implies that most of the energy in ψ(t) is confined to a finite duration.

The Continuous time Wavelet Transform (CWT) of a signal x(t) is defined as

$$W_{a,b} \equiv \int_{-\infty}^{\infty} x(t) \frac{1}{\sqrt{|a|}} \Psi^* \left(\frac{t-b}{a} \right) dt \qquad (B.11)$$

where a & b are real, * denotes complex conjugate and ψ(t) is the mother wavelet. Thus the wavelet transform is a function of two variables. The signals x(t) & ψ(t) belong to L^2R, the set of all square integrable functions.

If the mother wavelet satisfies the admissibility condition

$$C = \int_{-\infty}^{\infty} \frac{|\Psi(\omega)|^2}{\omega} d\omega, \quad 0 \prec C \prec \infty \qquad (B.12)$$

then the inverse transform is

$$x_t = \frac{1}{C} \int_{a=-\infty}^{\infty} \int_{b=-\infty}^{\infty} \frac{1}{|a^2|} W_{a,b} \frac{1}{\sqrt{|a|}} \Psi \left(\frac{t-b}{a} \right) da \; db \qquad (B.13)$$

B.2.1 The Discrete wavelet transform

Consider the representation of the signal x(t) in the following form

$$x(t) = \sum_{k=-\infty}^{\infty} \sum_{k=-\infty}^{\infty} d(k,l) \, 2^{-k/2} \Psi(2^{-k} t - l) \qquad (B.14)$$

The values *d(k,l)* are related to the continuous wavelet transform *W(a,b)* at $a=2^k$ and $b=2^k l$. This corresponds to sampling the coordinates (a, b) on a grid with sampling intervals with a difference of two. This process is called dyadic sampling. The two dimensional sequence *d(k, l)* is commonly referred to as the Discrete Wavelet Transform (DWT). The DWT is the transform of

actually a continuous time signal. The discretization is only in the ‘a’ and ‘b’ variables.

B.2.3 Concept of scaling and resolution

Consider the case of a function x(t) being scaled as x(t)=x(at), where a>0, then it is contracted if a>1 and expanded if a<1. As the scale increases the filter impulse response becomes spread out in time function, and takes only the long time behaviour of the signal into account. The resolution of a signal is linked to its frequency content. Scale change of continuous time signals does not alter their resolution. In discrete time signals, increasing the scale involves subsampling, which automatically reduces its resolution.

B.2.3 Different types of wavelet functions

There are many versions of wavelets. One of the oldest one is the Haar wavelet. Many other wavelets are derived later, namely Morlet, Meyer, Mallet, Daubechies etc. All these transforms have numerous applications in signal processing.

B.2.4.1 Haar wavelet

The expression for mother wavelet ψ(t) is as follows:

$$\psi(t) = \begin{cases} 1 & 0 \le t \le 1/2 \\ -1 & 1/2 \le t < 1 \\ 0 & otherwise \end{cases} \qquad (B.15)$$

B.2.4.2 Morlet wavelet

$$\psi(t) = e^{-t^2} \cos(\pi \sqrt{\frac{2}{\ln 2}} t \qquad (B.16)$$

B.2.4.3 Mexican hat wavelet

$$\psi(t) = (1-2t)e^{-t^2} \qquad (B.17)$$

B.2.4.4 Daubechies wavelet

The Daubechies family wavelets are referred as dbN, where N is the order. The db1 wavelet is the same as Haar discussed above. These wavelets have no explicit expression except for db1.

Modern technological advancements paved the way for the development of many new transforms. One of the most promising transforms is Mapped Real Transform (MRT).

B.3 Mapped Real Transform

DFT / FFT computations converts a signal into a set of complex coefficients. Exploiting the symmetry and periodicity properties of the twiddle factor and combining the data that are mapped onto a particular twiddle factor axis, the DFT computations are modified in [42] to reduce the complex multiplications. The resulting representation was developed into a new transform MRT (Mapped Real Transform, originally M- dimensional Real Transform) to eliminate the complex multiplications [103]. MRT maps an N ×N data matrix into M matrices of size N × N where N is an even integer and M = N/2.

B.3.1 2-D MRT

The 2-D DFT of a 2-D signal $x_{n1,n2}, 0 \le n_1, n_2 \le N-1$ is given by

$$Y_{k_1,k_2} = \sum_{n_1=0}^{N-1}\sum_{n_2=0}^{N-1} x_{n_1,n_2} W_N^{n_1k_1+n_2k_2},\ 0 \le k_1, k_2 \le N-1 \qquad (B.18)$$

where $W_N = e^{\frac{-j2\pi}{N}}$

Since the twiddle factor W_N is periodic, (B-18) can be expressed as

$$Y_{k_1,k_2} = \sum_{n_1=0}^{N-1}\sum_{n_2=0}^{N-1} x_{n_1,n_2} W_N^{((n_1k_1+n_2k_2))_N} \tag{B.19}$$

The exponent $((n_1k_1 + n_2k_2))_N = p, 0 \le p \le M-1$ is satisfied by a set of (n_1,n_2) for a given (k_1,k_2) Hence, by grouping such data and applying the property that $W_N^{p+M} = -W_N^p$, (B.19) can be expressed as

$$Y_{k_1,k_2} = \sum_{p=0}^{M-1} Y_{k_1,k_2}^{(p)} W_N^p \tag{B.20}$$

where

$$Y_{k_1,k_2}^{(p)} = \sum_{\forall(n_1,n_2)|z=p}^{N-1} x_{n_1,n_2} - \sum_{\forall(n_1,n_2)|z=p+M}^{N-1} x_{n_1,n_2}, \quad 0 \le p \le M-1 \tag{B.21}$$

where $z = ((n_1k_1 + n_2k_2))_N$

The computations of the N^2 DFT coefficients using (B.18) & (B.19) involves M complex multiplications each, and thus a total of $\frac{N^3}{2}$ complex multiplications for any even N. As a result of the combined works reported in [42] and [103] $Y_{k_1,k_2}^{(p)}$ of Eqn. (B.21) was developed as a new transform MRT which involves only real additions rather than complex multiplication. This transform maps the data x_{n_1,n_2} of size NxN into M matrices each of size

NxN with elements $Y_{k_1,k_2}^{(p)}$. The MRT computation is highly redundant and needs to be represented in terms of unique coefficients.

B.3.2 2-D Unique MRT

The MRT of an NxN data matrix in the raw form will have MN^2coefficients and is highly redundant. There are only N^2 coefficients that are unique in the MRT computation. Different arrangements in the form of an NxN matrix were proposed in [103] & [111]. These arrangements were finally developed as Unique MRT (UMRT). Here the coefficients corresponding to (k_1,k_2) be placed at $((k_1.q))_N,((k_2.q))_N$ where q is a non-negative integer, co-prime to $\frac{N}{dm}$ and less than $\frac{N}{dm}$ where $dm=\gcd(k_1,k_2,M)$. A sequency ordered placement of the unique MRT coefficients named SMRT (Sequency based unique MRT) was proposed in [112].

B.3.3 2-D Sequency based unique MRT

MRT coefficients corresponding to a particular (k_1,k_2) are distributed in UMRT. Hence, ordered changes in the signal are reflected in a scattered manner in UMRT. A reordering based on sign changes or sequencies was found to be more advantageous in signal analysis. Hence a new placement technique called Sequency based unique MRT (SMRT) was developed for N a power of 2 [112]. The coefficients are arranged in the order of sequencies

along row, column and diagonal directions. An algorithm to compute the SMRT coefficients, as given in [112] is as follows

2-D SMRT algorithm

Let $x_{n_1,n_2}, 0 \le n_1,\ n_2 \le N-1$ be the elements of data matrix and S_{s_1,s_2}, $0 \le n_1, n_2 \le N-1$ be the corresponding elements of SMRT matrix. In the algorithm presented below, $Y^{(p)}_{k_1,k_2}, 0 \le k_1, k_2 \le N-1,\ 0 \le p \le M-1$ can be computed using (B.17)

1. *Initialization*

   $\upsilon = \log_2 M$

2. *To find divisors of M*

   for i=0 to υ

   $d_{div}(i) = 2^i$

   end

3. *To find DC SMRT coefficient* $S_{0,0}$

   $S_{0,0} = Y^{(0)}_{0,0}$

4. *To compute and place first row and column*

   a=1

   for i=0 to υ

   $j = d_{div}(i)$

   for p= 0 to M-1 in steps of j

   $S_{0,a} = Y^{(p)}_{0,j}$

   $S_{a,0} = Y^{(p)}_{j,0}$

   a=a+1

   end

   end

5. *To compute and place other coefficients*

a=1

for i=0 to υ

b=i, r=a, c=a

for j=0 to υ *-1*

$s_1 = 2\, d_{div}(i)$, $s_2 = d_{div}(i)$

$s_3 = \dfrac{N}{d_{div}(j)}$, $s_4 = d_{div}(j)$

for $k_1 = s_2$ *to* s_3 *in steps of* s_1

$k_2 = d_{div}(i + j)$

for p= 0 to M-1 in steps of s_2

$S(\tau, c) = Y^{(p)}_{k_1, k_2}$

if $i \neq b$ *(% to find related coefficients)*

$S_{\tau, c} = Y^{(p)}_{k_1 . s_4, \frac{k_2}{s_4}}$

end

$\tau = r + 1$

end

$\tau = r - \dfrac{M}{s_2}$, *c=c+1*

end

b=b+1

end

$a = a + \dfrac{M}{s_2}$

end

Algorithm B

B.3.5.1 1-D SMRT

The thesis addresses chaotic system analysis with the knowledge of output time series alone.

Therefore an algorithm to compute 1-D SMRT coefficients of an array of length N is derived from the Algorithm B.1.

1-D SMRT Algorithm

The coefficient $Y_{k_1,k_2}^{(p)}$ & $S_{0,0}$ in 2-D SMRT are replaced by $Y_k^{(p)}$ & S_0

1. *Initialization*

   $M = \frac{N}{2}$

   $\upsilon = \log_2 M$

2. *To find divisors of M*

   for $i=0$ *to* υ

   $d_{div}(i) = 2^i$

   end

3. *To find DC SMRT coefficient* S_0

   $S_0 = Y_0^{(0)}$

4. *To compute and place other coefficients*

   $a=1$

   for $i=0$ *to* υ

   $j = d_{div}(i)$

   for $p= 0$ *to* $M-1$ *in steps of* j

   $S_a = Y_j^{(p)}$

   $a=a+1$

   end

   end

Algorithm B.2

The 16 point 1-D SMRT for *n= 0, 1… 15*coefficients can be calculated as follows.

$x_n = x_0 , x_1 , x_2 , x_3 , x_4 , x_5 , x_6 , x_7 , x_8 , x_9 , x_{10} , x_{11} , x_{12} , x_{13} , x_{14} , x_{15}$

The 1-D SMRT coefficients $S_0 , S_1 , \ldots , S_{15}$ are computed using Algorithm A.2 as follows

$S_0 = x_0 + x_1 + \ldots + x_{15}$

$S_1 = x_0 - x_8$

$S_2 = x_1 - x_9$

$S_3 = x_2 - x_{10}$

$S_4 = x_3 - x_{11}$

$S_5 = x_4 - x_{12}$

$S_6 = x_5 - x_{13}$

$S_7 = x_6 - x_{14}$

$S_8 = x_7 - x_{15}$

$S_9 = x_0 - x_4 + x_8 - x_{12}$

$S_{10} = x_1 - x_5 + x_9 - x_{13}$

$S_{11} = x_2 - x_6 + x_{10} - x_{14}$

$S_{12} = x_3 - x_7 + x_{11} - x_{15}$

$S_{13} = x_0 - x_2 + x_4 - x_6 + x_8 - x_{10} + x_{12} - x_{14}$

$S_{14} = x_1 - x_3 + x_5 - x_7 + x_9 - x_{11} + x_{13} - x_{15}$

$S_{15} = x_0 - x_1 + x_2 - x_3 + x_4 - x_5 + x_6 - x_7 + x_8 - x_9 + x_{10} - x_{11} + x_{12} - x_{13} + x_{14} x_{15}$

The illustration of 1-D SMRT shows an ordered arrangement of the terms according to sign change / sequency. This arrangement and the fact that it is

an integer to integer transform makes it suitable for time series analysis. The Fourier, wavelet and SMRT concepts are discussed here. MRT, being a comparatively new transform, is explained from basic concepts. The algorithms to compute 2-D and 1-D SMRT coefficients are also listed. The chaotic systems are analysed in frequency domain by exploiting these techniques in Chapters 5 &6.

References

[1] Bray R. J., Longhead R. E., “The lifetime of sunspot penumbra filaments”, Australian Journal of Physics, vol. 11, pp 185-190, 1958

[2] Edward Norton Lorenz, “Deterministic non- periodic flow”, Journal of Atmospheric Science, no.20, pp.130-141, 1963

[3] J. W. Cooley, J. W. Tukey, "An algorithm for the machine computation of complex Fourier series," Mathematics of Computation., vol.19, pp. 297-301, 1965

[4] G. E. Box, G. M. Jenkins, “Time series analysis, forecasting and control”, Holden Day, Sanfrancisco, 1970

[5] O. E. Rossler, “An equation for continuous chaos.” Physics Letters A, vol. 35, pp.397-398, 1976

[6] J. Kaplan, J.A.Yorke, “Chaotic behaviour of multidimensional difference equations”, Springer Lecture Notes in Mathematics, vol.730, pp.204 -227, 1979

[7] L. O. Chua, “Dynamic non-linear networks: state of the art”, IEEE Transactions on Circuits and Systems, vol. CAS-27, pp. 1059-1087, 1980

[8] Takens F. “On the numerical determination of dimension of an attractor”, Springer Lecture notes on Mathematics, vol. 898 pp.230-241, 1981

[9] Takens F, “Detecting strange attractors in turbulence” Springer Lecture Notes in Mathematics”, vol. 898, pp. 366–381, 1981

[10] A. J. Izenman, “J R Wolf and H AWolfer: A Historical note on the Zurich Sunspot relative numbers”, Journal of Royal Statistical Society A, vol.136, part 3, pp.311-318, 1983

[11] T. Matsumoto, “A Chaotic Attractor from Chua’s Circuit”, IEEE Transactions on Circuits and Systems, vol. CAS-31, no.12, pp. 1059-1087, 1984

[12] A. Wolf, J. B. Swift, H L Swinney, J A Vastano, “Determining Lyapunov exponents from a time series”, Physica D:Non-linear Phenomena, vol.16,Issue 3, pp. 285–317, 1985

[13] S. Masaki, Y. Sawada. "Measurement of the Lyapunov spectrum from a chaotic time s series." Physical review letters 55.10, pp. 1082-1085, 1985

[14] Arun V. Holden, “Chaotic behaviour in systems” -Manchester University Press, 1986

[15] Lennart Ljung, “System identification – Theory for the user” , Prentice Hall, 1987

[16] Wittmann A. D, Wu Z T, “A catalogue of sunspot observations from165 B C to 1684 A D”, Astronomy and Astrophysics. Supplement series. no.70, pp.83-94, 1987,

[17] I.Daubechies, “Orthonormal bases of compactly supported wavelets,” Communications on Pure and Applied Mathematics, vol. 41, no. 7, pp. 909–996, 1988.

[18] S. G. Mallat,“ A theory for multiresolution signal decomposition: the wavelet representation”, IEEE Transactions on Pattern Analysis and Machine Intelligence, *Vol. 11*,No.7, *pp. 674-693, 1989*

[19] Huang Anshan, “Period doubling and period plus one law – Chaotic phenomena in similar Chua’s circuit”, IEEE International Conference on Circuits and Systems, Senzen, China, pp. 4–7, 1991

[20] M. Arbib, D. Ballard, J. Bower, and G. Orban, "Neural Networks Algorithms, Applications and Programming Techniques", Computation and Neural systems series, California Institute of Technology, 1991

[21] Casdagli M., Eubank S., Farmer J D, & Gibson, J. "State space reconstruction in the presence of noise", Physica D: Non-linear Phenomena,51(1), pp. 52-98, 1991

[22] S. Chen and S.A billings, "Neural networks for non-linear dynamic system modeling and identification", International journal of control, vol.56, no.2, pp. 319-346, 1992

[23] Thomas J. H., Weiss N O, "Sunspots: Theory and Observations", NATO ASI series C, vol.375, Kluwer academic publishers, Dordrecht, 1992

[24] Si-Zhao, Quin Hong, Thomas J Mc Avoy "Comparison of four Neural network learning methods for dynamic system modeling", IEEE Transactions on neural networks, vol.3, pp 192-198, 1992

[25] I. Daubechies, "Ten lectures on wavelets" CBMS-NSF Regional Conference Series in Applied Mathematics, Society for Industrial and Applied Mathematics (SIAM), Philadelphia, 1992.

[26] Devaney, "A first course in chaotic dynamical systems Theory and Experiments", Perseus book publishing, 1992

[27] M. T. Rosenstein, J. J. Collins, C. J. De Luca, "A practical method for calculating largest Lyapunov exponents from small data sets", Physica D: Non-linear Phenomena, vol.65, no.1, pp. 117-134, 1993.

[28] Yakov Bar-Shalom, Xiao-Rong Li, "Estimation and Tracking-Principles and software" Artech House, Boston, London, 1993.

[29] Leon O. Chua, Chai Wah Wu, Anshan Huang, Guo-Qun, "A Universal Circuit for Studying and Generating Chaos-Part 11:

Strange Attractors", IEEE transactions on Circuits and systems-1:Fundamental Theory and Applications, vol. 40, no. 10, pp. 740-761, 1993

[30] H. D. I. Abarbanel, R Brown, J Sidorowich, L S Tsimring, "The analysis of observed chaotic data in physical systems", Review of Modern Physics, vol. 65, pp.1331-1392, 1993

[31] Puskorius G.V., L. A. Feldkamp, "Neurocontrol of non-linear dynamical systems with Kalman filter trained recurrent networks", IEEE Transactions on Neural Networks, vol. 5, no.2, pp. 279-297, 1994

[32] P. Chen, "Study of chaotic dynamical systems via time-frequency analysis", Proceedings of IEEE-SP International. Symposium on Time- Frequency and Time-Scale Analysis, pp. 357–360, 1994

[33] P. Hong, C. Peterson. "Finding the embedding dimension and variable dependencies in time series", Neural Computation, vol.6, no.3, pp.509-520, 1994

[34] D. Kugiumtzis, B. Lillekjendlie, N. Christophersen, "Chaotic time series Part I: Estimation of some invariant properties in state space 1 Introduction", Institutt of infirmatik, Oslo, pp. 1–23, 1995

[35] Rucklidge, A. M., H. U. Schmidt, N. O. Weiss. "The abrupt development of penumbrae in sunspots", Monthly Notices of the Royal Astronomical Society 273.2, pp. 491-498, 1995

[36] S. H. Isabelle, "A Signal Processing Framework for the Analysis and Application of Chaotic Systems, "Ph.D Thesis, R L E Technical reports, The Research Laboratory of Electronics, Massachussetts Institute of Technology, no.593, 1995

[37] C. Lamarque, J Malasoma, "Analysis of Non-linear Oscillations by Wavelet Transform : Lyapunov Exponents", Journal of Non-linear dynamics, vol.9, no. 3, pp. 333–347, 1996

[38] R. G. Hutchins, "Neural network chaotic system identification", IEEE Conference. Record of the Thirtieth Asilomar Conference on Signals, Systems and Computers, pp. 809–812, 1997

[39] H. Dedieu, M. J. Ogorzalek, "Identifiability and identification of chaotic systems based on adaptive synchronization", IEEE Transactions on Circuits and Systems-I Fundamental Theory and Applications, vol. 44, no. 10, pp. 948–962, 1997

[40] Liangyue Cao, "Practical method for determining the minimum embedding dimension from a scalar time series", Physica D: Non-linear Phenomena, vol. 1, no.10, pp. 43-50, 1997

[41] Schmeider B., Toro, Iniesta J C, Vazques M, "Advances in the Physics of Sunspots" , Astronomic Society, Pacific Conference, vol. 118, pp. 178-183, 1997

[42] R Gopikakumari, "Investigations on the development of an ANN model and visual manipulation approach for 2D DFT computation in image processing", Ph.D Dissertation, Cochin University of Science and Technology, Kochi, 1998

[43] M Bask, R Gencay, "Testing chaotic dynamics via Lyapunov exponents", Physica D, vol. 114, pp. 1–2, 1998

[44] J F G De Freitas, M Niranjan and A H Lee, "The EM algorithm and neural networks for non-linear state estimation" Cambridge University Engineering department, CUED/F-INFENG/TR 313, 1998

[45] Simon Haykin, "Neural Networks – a comprehensive foundation", 2nd edition, Pearson Education, 1999

[46] J. C. Robinson, “Takens’ embedding theorem for infinite-dimensional dynamical systems”, Non-linearity, vol2, pp. 1–10,1999

[47] G Chen, T Ueta. “Yet another chaotic attractor”, International. Journal of, Bifurcation and Chaos, vol. 9, pp. 1465-1466, 1999

[48] A Mertins, “Wavelet Transform”, Lecture notes, pp.210-264, 1999

[49] J C Sprott, “Strange Attractors: Creating Patterns in Chaos”, M&T press, 2000.

[50] R J Greatbatch, “The North Atlantic Oscillation,” Stochastic Environmental Research and Risk assessment, no.14, pp. 213-242, 2000

[51] R Washington, “Quantifying chaos in the atmosphere,” Progress in Physical Geography, vol. 24, no. 4, pp. 499–514, 2000

[52] K Ramasubramanian, M S Sriram, "A comparative study of computation of Lyapunov spectra with different algorithms", Physica D: Non-linear Phenomena 139.1 pp. 72-86, 2000

[53] A Doucett, N De Freitast, S Russent, “Rao-Blackwellised Particle Filtering for Dynamic Bayesian Networks”, Proceedings of the Sixteenth conference on Uncertainty in artificial intelligence, Morgan Kaufmann Publishers Inc., 2000

[54] F C Hoppensteadt, “Analysis and Simulation of Chaotic Systems, Second Edition”, Springer, 2000

[55] V Gorlovka, N Maniakov, “Modeling Non-linear Dynamics using Multilayer Neural Networks”, Proceedings of the international workshop on intelligent data acquisition and advanced computing systems, pp. 4–9, 2001

[56] Shuhi Li, “Comparative Analysis of back propagation end extended

Filter in pattern and Batch forms for Training Neural Networks",IEEE transactions on Neural Network, vol.2, no.4, pp. 144-149, 2001

[57] Greg Welch and Garry Bishop and N. Carolina, "An Introduction to the Kalman Filter," cc.cs.unc.edu/~tracker/s2001/Kalman, 2001

[58] L. Palma, "Application of an Extended Kalman Filter for On-line Identification with Recurrent Neural Networks," Proceedings of the seventh journadas Hispano-Lusas de Ingeneniria Electrica Madrid, pp. 4-6.2001

[59] Alan V. Oppenheim, Allan S Willsky, "Signals and Systems" Pearson Education 2002.

[60] M. S. Arulampalam, S. Maskell, N. Gordon, T. Clapp, "A tutorial on particle filters for online non-linear/non-Gaussian Bayesian tracking," IEEE Transaction on Signal Processing., vol. 50, no. 2, pp. 174–188, 2002

[61] H. Broer, C. Sim, R. Vitolo, "Bifurcations and strange attractors in the Lorenz-84 climate model with seasonal forcing,", Institute of Physics Publishing, Non-linearity vol. 15, pp. 1205–1267, 2002.

[62] J. Lü, T. Zhou, G. Chen, and S. Zhang, "Local Bifurcations of the Chen System," International. Journal of. Bifurcations and Chaos, vol. 12, no. 10, pp. 2257–2270, 2002

[63] P Cvitanovi and M. J. Feigenbaum, "Recycling Fourier Spectra of Chaotic Systems," Pennsylvania University, pp. 1–21, 2002

[64] L V Vela-Arevalo, "Time-Frequency Analysis Based on Wavelets for Hamiltonian Systems", Ph.D Thesis, California Institute of technology, 2002

[65] S Azad and S K. Sett, “Wavelets Detecting Chaos in logistic Map” National Conference on non-linear systems and dynamics, pp. 301–304, 2003.

[66] S K Solanki, “ Sunspots: An overview”, The Astronomy and Astrophysics Review, springer Verlag, vol.11, pp.153-286, 2003

[67] M Ataei, A Khaki-Sedigh, B Lohman,C Lucas, "Estimating the Lyapunov exponents of chaotic time series: a model based method." European Control Conference. 2003.

[68] Torma, Péter, and Csaba Szepesvári, "Combining local search, neural networks and particle filters to achieve fast and reliable contour tracking." Proceedings of the IEEE International Symposium on Intelligent Signal Processing. 2003.

[69] K. Zliu, “Orthogonal Wavelet Analysis of Lorenz,”IEEE ICSP Proceedings, vol.3, pp. 252–255, 2004.

[70] Rajesh Cherian Roy and R Gopikakumari and, "A new transform for 2-d signal representation (MRT) and some of its properties," Proceedings of the International Conference on Signal Processing and Communications, (SPCOM '04), pp. 363 - 367,2004

[71] Branko Ristic, SanjeevArulambalam, Neil Gordon “Beyond the Kalman Filter-Particle filters for tracking Applications” artech house.2004

[72] E.Solak, “Partial Identification of Lorenz System and Its Application to Key Space Reduction of Chaotic Cryptosystems,” IEEE Tranactions on Circuits and Syst.ems- II Express Briefs, vol. 51, no. 10, pp. 557–560, 2004

[73] Collette, Christophe, M. Ausloos. "Scaling analysis and evolution equation of the North Atlantic oscillation index

fluctuations." International journal of modern physics C 15.10 , pp. 1353-1366, 2004

[74] V. Venkatasubramanian and H. Leung, “An EM based method for semi blind identification of linear systems driven by chaotic signals,” *IEEE Conference on Cybernetics and Intelligent Systems* vol. 1, pp. 554–557, 2004.

[75] H. Leung, “Blind identification of autoregressive system using chaos,” IEEE Transactions on Circuits and Systems- I Regular. Papers, vol. 52, no. 9, pp. 1953–1964, 2005

[76] D. Batenkov, “Fast Fourier Transform - Overview”, Key papers on Computer Science Seminar, 2005.

[77] Trebatický, Peter, "Recurrent neural network training with the extended Kalman filter." IIT- Student Research Conference. Pp. 57-64, 2005.

[78] C. Chandré and T. Uzer, “Instantaneous frequencies of a chaotic system,” Pramana, vol. 64, no. 3, pp. 371–379, Mar. 2005

[79] Schon, Thomas, Fredrik Gustafson, and P-J. Nordlund. "Marginalized particle filters for mixed linear/non-linear state-space models." , IEEE Transactions on Signal Processing, 53.7 pp. 2279-2289, 2005

[80] J. G. Lu, “Chaotic dynamics of the fractional-order Lü system and its synchronization,” Physics Letters A, vol. 354, no. 4, pp. 305–311, 2006.

[81] Z. Qiao and J. Cheng, “A Novel Linear Feedback Control Approach of Lorenz Chaotic System,” 2006 International. Conference on. Computational. Intelligence for Modeling Control and Automation. pp. 67–69, 2006.

[82] H. Ma and C. Han, “Selection of Embedding Dimension and Delay Time in Phase Space Reconstruction,” Frontiers of Electrical and. Electronics Engineering in China, vol. 1, no. 1, pp. 111–114, Jan. 2006

[83] P. Han, S. Zhou, and D. Wang, “A Multi-objective Genetic Programming/ NARMAX Approach to Chaotic Systems Identification,” 26th World Congress on Intelligent Control and Automation., vol. 1, no. 6, pp. 1735–1739, 2006

[84] Q. Wen and P. Qicoiig, “An improved particle filter algorithm based on neural network,”IFIP International Federation for Information Processing, vol. 228, pp. 297–305, 2006

[85] E. J. Doedel, B. Krauskopf, and H. M. Osinga, “Global bifurcations of the Lorenz manifold,” Non-linearity, vol. 19, no. 12, pp. 2947–2972, 2006

[86] J. G. Lu, “Chaotic dynamics of the fractional-order Lü system and its synchronization,” Physics. Letters. A, vol. 354, no. 4, pp. 305–311, 2006

[87] B. Shanker and A. B. Babu, “Convection due to oblique magnetic field in the penumbral region of sunspot,”, Indian Journal for Radio and Space physics, vol. 35, pp. 84–89, 2006

[88] E. P. Gerber, “A Dynamical and Statistical Understanding of the North Atlantic Oscillation and Annular Modes,” Ph.D Thesis, Princeton University, 2006

[89] J. S. Murgu, “Wavelet analysis of chaotic time series,”, Revista Mexican,de Fisica vol. 52, no. 2, pp. 155–162, 2006

[90] Cattani, Carlo, and Ivana Bochicchio. "Wavelet analysis of chaotic systems."Journal of Interdisciplinary Mathematics 9.3 pp. 445-458, 2006

[91] E. Araujo and L. dos Santos Coelho, “Fuzzy Model and Particle Swarm Optimization for Non-linear Identification of a Chua’s Oscillator,” 2007 IEEE International Fuzzy Systems Conerence., pp. 1–6, Jun. 2007

[92] S.-M. Chow, E. Ferrer, and J. R. Nesselroade, “An Unscented Kalman Filter Approach to the Estimation of Non-linear Dynamical Systems Models,” Journal of Multivariate Behaviou Research., vol. 42, no. 2, pp. 283–321, 2007

[93] Wu Xue-Dong and Song Zhi-Hua “GEKF , GUKF and GGPF based prediction of chaotic time-series with additive white noise,”Chinese PhysicsB, vol. 17, no. 9, pp. 3241–3246, 2008

[94] C. Yong, “Chaos System Filter on State-space Model and EKF ,” Proceedings of the IEEE International conference on Automation and Logistics,Shenyang,China pp. 1259–1263, 2009

[95] C. Yin, “Applications of chaos theory on Partial Discharge detection and character analysis,” 2008 IEEE International. Conference on Industrial Technology pp. 1–4, 2008

[96] G. Qi, M. A. van Wyk, B. J. van Wyk, and G. Chen, “On a new hyperchaotic system,” Physics. Letters. A, vol. 372, no. 2, pp. 124–136, 2008

[97] A. Doucet, A. M. Johansen, “A Tutorial on Particle Filtering and Smoothing : Fifteen years later,” Version 1.1, 2008.

[98] Afonso, Manya. "Particle filter and extended kalman filter for non-linear estimation: a comparative study." IEEE Transactions on Signal Processing,pp1- 10, 2008.

[99] H. Ding, D. S. Yeung, Q. Ma, W. W. Y. Ng, D. Wu, and J. Li, “Prediction of chaotic time series using l-gem based rbfnn,”

Proceedings of the eighth international conference on machine learning and cybernetics, Baoding, pp. 12–15, 2009.

[100] Q. Yao and G. Liu, "Simulation and analysis of Lorenz system's dynamics characteristics,"International Conference on Image Analysis and Signal Processing, pp. 427–429, 2009.

[101] Z. Xiaohong, L. Honghui, and C. Zhiyong, "Parameter identification and self-adaptive synchronization of an uncertain time-delayed chaotic system," 2009 ISECS International. Colloquium on Computing, Communications, Control and Management., pp. 42–45, 2009.

[102] H. Jia, Z. Chen, and W. Wu, "A New Hyper-Chaotic Lü Attractor and Its Local Bifurcation Analysis," Int. Work. Chaos-Fractals Theory and. Applications., vol. 70, pp. 231–235, 2009.

[103] Rajesh Cherian Roy, " Development of a new transform MRT", ,Ph.D Dissertation, Cochin University of Science and Technology, Kochi, 2009.

[104] Bhadran.V, "Development and implementation of visual approach and parallel distributed architecture for 2D-DFT and UMRT computation". Ph.D Dissertation, Cochin University of Science and Technology, Kochi, 2009.

[105] S. Grillo, S. Massucco, A. Morini, A. Pitto, and F. Silvestro, "Bifurcation Analysis and Chaos Detection in Power Systems," International Journal of Innovations in Energy Systems and Power, vol. 5, no. 1, pp. 1–7, 2010.

[106] D. Kugiumtzis and A. Tsimpiris, "Measures of Analysis of Time Series (MATS)", Journal of Statistical software, vol. 33, no. 5, 2010.

[107] X. Jiang and S. Mahadevan, "Wavelet spectrum analysis approach to model validation of dynamic systems," Mechanical. Systems and Signal Processing., vol. 25, no. 2, pp. 575–590, 2011

[108] D. H. Hathaway, "A Standard Law for the Equatorward Drift of the Sunspot Zones," springer Journal of Solar Physics, vol. 273, no. 1, pp. 221–230,2011.

[109] S. M. Osprey, U. Kingdom, M. H. P. Ambaum, and U. King-, "Evidence for the Chaotic Origin of Northern Annular Mode Variability", Geophysical Research letters, 2011.

[110] C. E. Meador, "Numerical Calculation of Lyapunov Exponents for Three-Dimensional Systems of Ordinary Differential Equations,",Ph.D Thesis, Marshall University, 2011.

[111] Preetha Basu, Bhadran.V, R. Gopikakumari, " A New Algorithm to compute forward and inverse 2-D UMRT for N - a power of 2".Second international conference on power, signals, control and computation (EPSICON-2012), Jan 2-6, 2012, Thrissur.

[112] V. L. Jaya, P. Basu, and R. Gopikakumari, "SMRT: A new placement approach of 2-D unique MRT coefficients for N a power of 2," 2012 Annual. IEEE India Conference, no. 4, pp. 233–237, Dec. 2012.Chilean Journal of Statistics, vol. 4, no. 1, pp. 35–54, 2013.

[113] Sunspot index and Long term solar observations, Royal Observatory of Belgium, Brussels, http://www.sidc.be/silso/datafiles

[114] NAO data: Climatic Research Unit, University of East Anglia, http://www.cru.uea.ac.uk/cru/data/nao/nao.dat

[115] National Oceanic and Atmospheric Administration(NOAA), United State Department of Commerce, http://oceanservice.noaa.gov

[116] National Aeronautics and Space Administration (NASA), United States of America,
htttp://solarscience.msfc.nasa.gov/SunspotCycle.html
[117] Venice Lagoon water level: A. Tomasin, CNR-ISDMG Universita Ca'Foscari,Venice,
http://tracer.uc3m.es/tws/TimeSeriesWeb/data/level80.txt

List of Papers Published

International journals

1. Archana R, A Unnikrishnan, R Gopikakumari "Modeling of Venice Lagoon time series with improved Kalman Filter based neural networks" Special issue of international journal of computer application, June 2012

2. Archana R, A Unnikrishnan, R Gopikakumari "Computation of state space evolution of chaotic systems from time series of output, based on neural network models". International Journal for Engineering research and development vol. 2, Issue 2, pp. 49-56, July 2012

3. Archana R, A Unnikrishnan, R Gopikakumari "Modeling of Venice Lagoon time series with improved Kalman Filter based neural networks" Special issue of international journal of computer application , January 2015 (Paper accepted)

International/National Conferences &Seminars

1. Archana R1, R. Gopikakumari2 ,A Unnikrishnan3 ,M.V Rajesh4, "Reconstruction of Chaotic Systems based on Artificial Neural Network with Extended Kalman Filter algorithm". Presented in International Seminar on New Trends in Applications of Mathematics. Sponsored by Central Statistics Office of Government

of India, Bharath Matha College, Thrikkakara January 31, February 1-2, 2011.

2. Archana.R, A Unnikrishnan, R Gopikakumari, M.V Rajesh "Time series modeling of non-linear systems: a dynamic neural network approach". Presented and published in the proceedings of the National Conference on Information, Communication & Intelligent Systems", organized jointly by the Institution of Electronics & Telecommunication Engineers India (IETE) and KMEA Engineering College 25 -26 Feb 2011.

3. Archana R, A Unnikrishnan, R Gopikakumari "An Intelligent Computational Algorithm based on Neural Networks for the Identification of Chaotic systems", proceedings of IEEE international conference on recent advances in intelligent computational systems, jointly organized by IEEE Kerala chapter ,CET& SET,pp.605-609, Sep 22-24 2011

4. Archana R, A Unnikrishnan, R Gopikakumari, "An improved EKF based neural network training algorithm for identification of chaotic systems driven by time series, proceedings of IEEE international conference on power, signals, controls and computation, pp. 1-6, 3-6 January, 2012

5. Archana R, A Unnikrishnan, R Gopikakumari "Bifurcation analysis of chaotic systems using a model built on Artificial Neural Networks" Second International Conference on Computational

techniques and Artificial Intelligence Organized by PSRC, Dubai, UAE, March 2013

6. Archana R, A Unnikrishnan, R Gopikakumari, "Analysis and modeling of chaotic systems in nature with a neural network based training algorithm", 24th Swadeshi Science Congress November 6-8, 2014 at Thunchath Ezhuthachan Malayalam University.Organised by Swadeshi science movement (A unit of Vijnan Bharathi)